

**ARTEMIN REGULATES NOCICEPTOR RESPONSES
TO THERMAL AND CHEMICAL STIMULI**

by

Christopher Michael Elitt

Sc.B., Neuroscience, Brown University, 2000

Submitted to the Graduate Faculty of
the University of Pittsburgh School of Medicine in partial fulfillment
of the requirements for the degree of
Doctor of Philosophy

University of Pittsburgh

2006

UNIVERSITY OF PITTSBURGH

School of Medicine

This dissertation was presented

by

Christopher Michael Elitt

It was defended on

August 24, 2006

and approved by

Kathryn M. Albers, Ph.D.
Associate Professor of Medicine and Neurobiology

H. Richard Koerber, Ph.D.
Associate Professor of Neurobiology

J. Patrick Card, Ph.D.
Associate Professor of Neuroscience and Psychiatry

Carl F. Lagenaur, Ph.D.
Associate Professor of Neurobiology

Douglas E. Wright, Ph.D.
Associate Professor of Anatomy and Cell Biology, University of Kansas Medical Center

Brian M. Davis, Ph.D.
Dissertation Advisor
Associate Professor of Medicine and Neurobiology

Copyright © by Christopher Michael Elitt

2006

ARTEMIN REGULATES NOCICEPTOR RESPONSES TO THERMAL AND CHEMICAL STIMULI

Christopher Michael Elitt, PhD

University of Pittsburgh, 2006

Chronic pain is a major clinical problem. Target-derived growth factors have been implicated in the initiation and maintenance of persistent pain states. Artemin, a member of the glial cell line-derived neurotrophic factor (GDNF) family, binds to its GPI-anchored receptor, GFR α 3, and initiates intracellular signaling via the tyrosine kinase, Ret. Expression of the GFR α 3 receptor is largely restricted to the peripheral nervous system and is found in a subpopulation of nociceptive sensory neurons of the dorsal root and trigeminal ganglia (DRG & TG) that coexpress the Ret and TrkA receptor tyrosine kinases and the thermosensitive channel TRPV1. To investigate the role of artemin in regulating nociceptor properties and function, we isolated transgenic mice that overexpress artemin in keratinized tissues (ART-OE). Expression of artemin increased DRG neuron number, confirming the survival promoting effects of artemin. In addition, ART-OE mice had increased mRNA encoding GFR α 3, TrkA, TRPV1 and the putative noxious cold and mustard oil detecting channel, TRPA1. Immunolabeling showed that nearly all GFR α 3-positive neurons expressed TRPV1 and most of these neurons were also TRPA1-positive. Somas of GFR α 3/TRPV1-positive neurons in the ART-OE mice were hypertrophied and there was increased staining for these proteins in the periphery. Interestingly, increases in TRPV1 and TRPA1 mRNA were more robust in TG than DRG. Because of these differential effects, lingual afferents innervating the heavily keratinized tongue were also examined. Retrogradely-labeled

lingual afferents from ART-OE tongues showed an increased percentage of GFR α 3- and TRPV1-positive neurons. Behavior analysis showed that these anatomical changes were correlated with increased sensitivity to noxious heat, noxious cold, capsaicin and mustard oil applied to the hindpaw, as well as oral sensitivity to capsaicin and mustard oil placed in the drinking water of these mice. Functional analysis of dissociated sensory neurons using calcium imaging showed hypersensitivity to capsaicin and mustard oil in trigeminal neurons isolated from ART-OE mice, and even greater sensitivity in the lingual subpopulation. Taken together, these results indicate that artemin promotes the survival and modulates functional properties of a select population of TRPV1- and TRPA1-positive nociceptors critical for the detection of noxious thermal and chemical stimuli in both cutaneous and lingual systems.

TABLE OF CONTENTS

ACKNOWLEDGEMENTS	XIV
1.0 INTRODUCTION.....	1
1.1 THE PAIN PATHWAY AND TYPES OF CHRONIC PAIN.....	1
1.2 SENSORY NEURON DEVELOPMENT.....	4
1.3 GLIAL CELL LINED-DERIVED NEUROTROPHIC FACTOR (GDNF) FAMILY MEMBERS	5
1.3.1 GDNF	5
1.3.2 Neurturin	7
1.3.3 Artemin	7
1.4 TRP CHANNELS	10
1.4.1 TRPV1.....	13
1.4.2 TRPA1.....	14
1.5 LINGUAL AFFERENTS.....	17
1.5.1 Tongue Anatomy and Innervation	18
1.5.2 Previous studies on lingual afferents.....	18
1.5.3 Clinical Relevance of Lingual Afferents	19
1.6 GOALS OF THE DISSERATION.....	20
2.0 METHODS	22
2.1 CONSTRUCTION OF TRANSGENIC MICE.....	22
2.2 TOTAL CELL COUNTS.....	23
2.3 TISSUE IMMUNOLABELING	23

2.4	CONFOCAL ANALYSIS OF DRG NEURONS	24
2.5	SURGICAL PROCEDURE FOR RETROGRADE LABELING OF LINGUAL AFFERENTS.....	25
2.6	TISSUE PREPARATION.....	25
2.7	CONFOCAL ANALYSIS OF WGA-BACKLABELED IMMUNOPosITIVE TRIGEMINAL NEURONS.....	26
2.8	LINGUAL NERVE ANALYSIS	26
2.9	REAL TIME PCR ANALYSIS OF NOCICEPTOR-RELATED GENES ..	27
2.10	HARGREAVES' TEST (HEAT).....	27
2.11	COLD TAIL WITHDRAWAL ASSAY	29
2.12	NOXIOUS COLD ASSAY	29
2.13	PLACE PREFERENCE ASSAY.....	30
2.14	DRINKING BEHAVIOR.....	30
2.15	MUSTARD OIL NOCIFENSIVE BEHAVIOR.....	31
2.16	CAPSAICIN NOCIFENSIVE BEHAVIOR.....	31
2.17	COMPLETE FREUND'S ADJUVANT (CFA) INJECTION AND BEHAVIOR	32
2.18	MECHANICAL SENSITIVITY BEHAVIOR	32
2.19	CELL PREPARATION FOR CALCIUM IMAGING OF TRIGEMINAL NEURONS AND IDENTIFIED LINGUAL AFFERENTS.....	33
2.20	IMAGING PROTOCOL.....	33
3.0	ANATOMY RESULTS	36

3.1	HUMAN K14 KERATIN PROMOTER DRIVES ARTEMIN TRANSGENE EXPRESSION IN THE SKIN AND TONGUE	36
3.2	ARTEMIN OVEREXPRESSION INCREASES NEURON NUMBER IN SENSORY GANGLIA	36
3.3	ARTEMIN OVEREXPRESSION MODULATES GFR α 3 EXPRESSION.	38
3.4	ARTEMIN INCREASES TRPV1 MRNA IN SENSORY GANGLIA	42
3.5	ARTEMIN CAUSES HYPERTROPHY OF TRPV1-POSITIVE AFFERENTS	42
3.6	THE TRPA1 CHANNEL PROTEIN IS A MARKER FOR GFR α 3 NEURONS AND IS MODULATED BY ARTEMIN LEVEL	43
3.7	TONGUES OF ART-OE MICE ARE HYPERINNERVATED BY GFR α 3, TRPV1 AND PRESUMPTIVE TRPA1-POSITIVE LINGUAL AFFERENTS.....	48
3.8	LINGUAL NERVES FROM ART-OE MICE ARE HYPERTROPHIED ..	50
4.0	BEHAVIOR RESULTS.....	52
4.1	ART-OE MICE ARE HYPERSENSITIVE TO NOXIOUS HEAT	52
4.2	ART-OE MICE ARE HYPERSENSITIVE TO NOXIOUS COLD STIMULI 54	
4.3	ART-OE MICE ARE NOT SENSITIZED TO MECHANICAL STIMULI	57
4.4	ART-OE MICE ARE HYPERSENSITIVE TO MUSTARD OIL APPLIED TO THE HINDPAW	59
4.5	ART-OE MICE ARE HYPERSENSITIVE TO CAPSAICIN INJECTED INTO THE HINDPAW	61

4.6	IN A MODEL OF INFLAMMATORY PAIN, ART-OE MICE DISPLAY SIMILAR SENSITIVITY TO NOXIOUS HEAT AS WT MICE BUT RECOVER TO THRESHOLDS ABOVE BASELINE	64
4.7	ART-OE MICE DISPLAY ORAL SENSITIVITY TO CAPSAICIN AND MUSTARD OIL IN THEIR DRINKING WATER	66
5.0	CALCIUM IMAGING RESULTS	69
5.1	MUSTARD OIL RESPONSES IN TRIGEMINAL NEURONS (NON-BACK-LABELED NEURONS)	69
5.2	CAPSAICIN RESPONSES IN TRIGEMINAL NEURONS (NON-BACK-LABELED NEURONS)	72
5.3	LINGUAL AFFERENTS FROM ART-OE MICE APPEAR TO BE SENSITIZED TO CAPSAICIN AND MUSTARD OIL	72
6.0	DISCUSSION	74
6.1	ANATOMY: SURVIVAL EFFECTS OF ARTEMIN	74
6.2	ANATOMY: GFR α 3 AND TRPV1 IMMUNOLABELING.....	75
6.3	ANATOMY: LINGUAL AFFERENTS	76
6.4	ANATOMY: ARTEMIN REGULATION OF TRPA1	77
6.5	BEHAVIORAL RESPONSES TO HEAT.....	78
6.6	MUSTARD OIL BEHAVIOR.....	79
6.7	ROLE OF TRPA1 IN COLD BEHAVIOR.....	80
6.8	ORAL BEHAVIOR.....	82
6.9	CALCIUM IMAGING STUDIES.....	83
6.10	BROADER ISSUES AND FUTURE EXPERIMENTS.....	85

BIBLIOGRAPHY..... 87

LIST OF TABLES

Table 1. Primer Sequences used for real time PCR assays.....	28
Table 2. Change in expression of receptor and TRP channel genes in lumbar DRG (L3, L4 and L5) and TG of WT and ART-OE mice.....	41

LIST OF FIGURES

Figure 1. Diagram of the pain pathway.	2
Figure 2. GDNF family members and their GFR α receptors.	6
Figure 3. Thermosensitive TRP Channels.	12
Figure 4. K14 keratin promoter drives artemin transgene expression in skin and tongue keratinocytes.	37
Figure 5. Artemin overexpression in the skin increases sensory ganglia size and neuronal number.	39
Figure 6. Sensory neurons responsive to artemin are hypertrophied and express TRPV1.....	40
Figure 7. Skin-derived artemin increases cutaneous GFR α 3-positive afferents and intensity of TRPV1 labeling.	44
Figure 8. Artemin increases the intensity of TRPV1 expression in GFR α 3 epidermal afferents.	45
Figure 9. Tongue epithelium from ART-OE mice are hyperinnervated and have increased GFR α 3-positive fibers.....	46
Figure 10. GFR α 3-positive afferents express the TRPA1 channel.....	47
Figure 11. WGA-Positive Lingual Afferents from ART-OE mice have increased GFR α 3, TRPV1 and IB4.....	49
Figure 12. Lingual Nerves from ART-OE mice are hypertrophied.....	51
Figure 13. ART-OE mice are hypersensitive to noxious heat.	53
Figure 14. ART-OE mice display hypersensitivity to cold in tail flick assays.....	55
Figure 15. ART-OE mice display behavioral hypersensitivity to noxious cold (-10°C).....	56

Figure 16. ART-OE mice are hypersensitive to noxious cold (4°C).	58
Figure 17. ART-OE mice are hypersensitive to mustard oil.	60
Figure 18. ART-OE mice are hypersensitive to capsaicin injected into the hindpaw.	62
Figure 19. ART-OE mice display sensitivity to heat following capsaicin injection.	63
Figure 20. ART-OE mice display similar heat sensitivity to CFA injection	65
Figure 21. ART-OE mice display oral sensitivity to capsaicin and mustard oil.....	68
Figure 22. Trigeminal and Lingual Afferent Calcium Responses to Mustard Oil and Capsaicin	70
Figure 23. Magnitude of Calcium Responses to Mustard Oil and Capsaicin in Trigeminal and Lingual Afferents	71

ACKNOWLEDGEMENTS

The work presented in this dissertation would not have been possible without the tremendous support of my advisor, Brian Davis. From the first day that I joined Brian's lab, he did everything possible to ensure my success as a graduate student. His enthusiasm and energy for science were infectious. I can only hope to be half as good of a mentor in the future. Thank you, Brian.

I also want to thank Kathryn Albers who created the transgenic mice used in my studies and always was very encouraging and helpful. As chair of my dissertation committee, she helped guide my project in an efficient and productive manner. The other members of my committee Rick Koerber, Pat Card, Carl Lagenaur and Doug Wright also deserve recognition for their insightful suggestions about my project.

I want to sincerely thank Sacha Malin, PhD. At a time when she was very busy with her own experiments, she devoted quite a number of days to teach me how to perform calcium imaging and helped me with the behavioral experiments in my studies. Our informal scientific exchanges were always very productive for me. She is one of the most brilliant young scientists I have had the pleasure of working with and I will always be grateful to her for being so generous with her time. She's also a pleasure to hang out with outside the lab (and makes amazing sangria).

I want to thank all the other members of the Davis Lab who were extremely helpful during my time in the lab. Derek Molliver and Julie Christianson, who first welcomed me into the lab, were always available to answer my questions and occasionally have a drink or two after

a challenging day. Thanks also to the newer members of the laboratory, Ting Wang and Savanh Chanthaphavong, as well as the technicians, Chris Sullivan, Mela Poonacha and Jessica Lindsey.

I also would like to thank my parents, Don & Sharon, and my brothers, Mike, Mark and Matt, for their encouragement and understanding during my time in the laboratory. I also need to thank my friends for their advice and support during these challenging three years. Maggie Rosenberg, in particular, deserves special recognition for her unbelievable support in the final days of my dissertation writing. She did all the little things to keep me functioning during those dark hours. Finally, I want to acknowledge my good friend Ron Tribble who helped me navigate the software to upload this dissertation and undoubtedly saved me hours of frustration.

1.0 INTRODUCTION

1.1 THE PAIN PATHWAY AND TYPES OF CHRONIC PAIN

Chronic pain is a major clinical problem that has significant physical, emotional and economic costs. According to estimates by the American Pain Society, nearly 50 million people are partially or totally disabled by pain and 45% of all Americans seek care for persistent pain at some point in their lives. Current therapies for chronic pain consist primarily of non steroidal anti-inflammatory drugs (NSAIDS) or opioids, both of which are relatively non-specific drugs for the diverse types of persistent pain and have many unpleasant side effects. It is not surprising, therefore, that nearly two-thirds of chronic pain patients report inadequate pain control (<http://www.painineurope.com>). Developing new treatments for chronic pain requires understanding nociceptive sensory neurons and determining molecular changes in these neurons that may contribute to persistent pain states.

Pain sensations from the body and head are transmitted from the periphery by neurons located in dorsal root (DRG) and trigeminal ganglia (TG), respectively. These pseudounipolar neurons contain a peripheral process that innervates the target (skin, tongue, face, etc.) and a central process that synapses on second order neurons in the superficial dorsal horn of the spinal cord (or analogous area in the brainstem for TG neurons) (Figure 1). Dorsal horn neurons project to the thalamus or brainstem where third order neurons relay pain signals to the cortex. Our experiments focus on the first neuron in this pathway, the primary afferent.

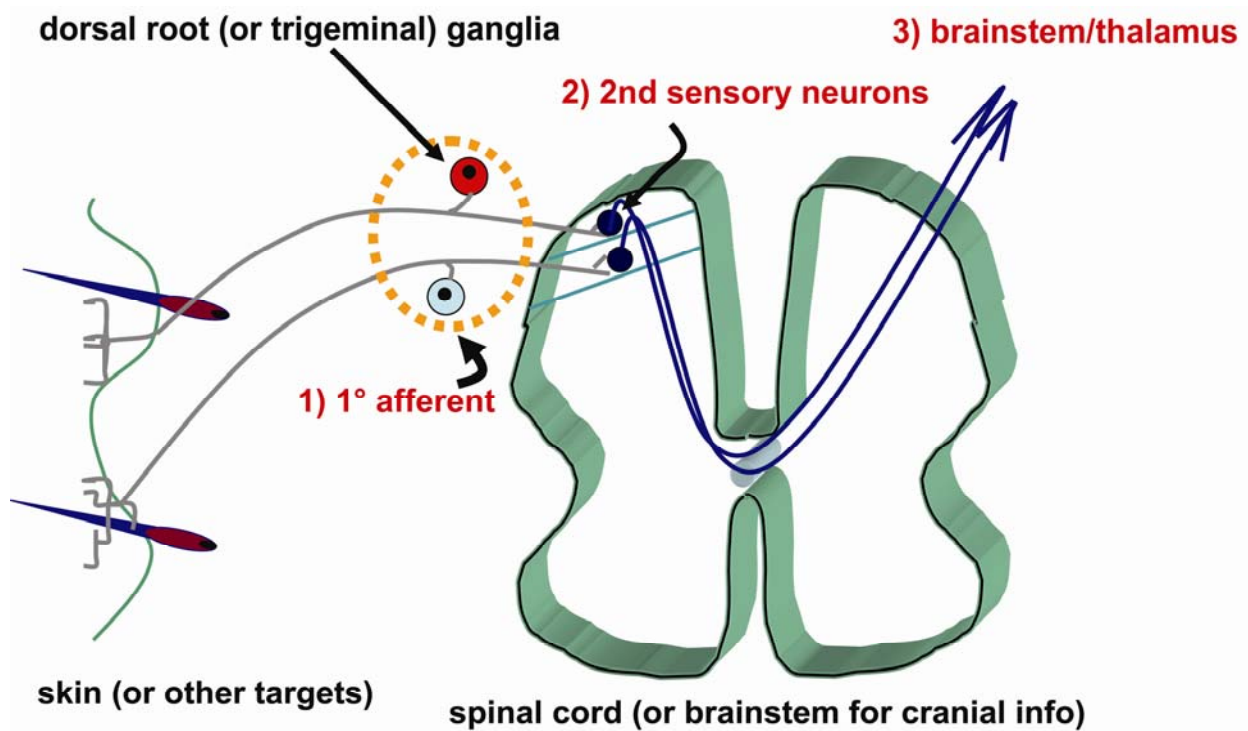


Figure 1. Diagram of the pain pathway.

It takes three neurons to convey pain signals from the periphery to the cerebral cortex. Primary afferents relay nociceptive information to the central nervous system by synapsing on second order neurons of the superficial dorsal horn in the spinal cord (or equivalent medullary dorsal horn of the brainstem). These second order neurons project to third order neurons in the thalamus which ultimately convey the signals to the cerebral cortex.

Primary afferents that detect damaging or potentially damaging tissue stimuli are called nociceptors. These neurons are primarily small diameter unmyelinated C-fibers and lightly myelinated A δ fibers, although some A β fibers also function as nociceptors (Djouhri and Lawson, 2004). Most of the time these specialized sensory neurons serve a protective function to prevent tissue injury when noxious stimuli are encountered (e.g. when tissue is being burned by accidentally touching a scalding hot stove or when frostbite is imminent after throwing snowballs with bare hands). Many plants have also evolved to contain pungent chemicals that can activate these same nociceptors, producing acute pain in the oral cavities of plant consuming animals. Some of these chemicals include: capsaicin, found in chili peppers; allyl isothiocyanate, found in mustard oil; allicin, found in garlic; and cinnamaldehyde, found in cinnamon. All of these examples illustrate potential adequate stimuli for nociceptors during acute pain states.

Chronic pain, on the other hand, is pathologic and serves no obvious protective purpose. Frequently, chronic pain is divided into inflammatory pain, triggered by increased nociceptive input from inflamed or injured tissue, and neuropathic pain, triggered by changes in injured nerves or adjacent uninjured fibers. In both types of pain, pain sensations are initiated peripherally, by the primary afferent. However, central mechanisms also play a role in the maintenance of chronic pain conditions as indicated by the contribution of descending input from the rostral ventral medulla to the maintenance of both inflammatory and neuropathic pain (reviewed in (Porreca et al., 2002)).

While the relative contributions of peripheral vs. central mechanisms leading to sensitized pain circuits is complex, without primary afferent input persistent pain states are rarely

initiated (an exception is stroke-induced pain). Thus, in recent years many studies have examined molecular changes in the primary afferent that initiate peripheral sensitization in primary afferents. Target-derived growth factors such as nerve growth factor (NGF) and glial cell line-derived neurotrophic factor (GDNF) have been implicated in this sensitization process.

1.2 SENSORY NEURON DEVELOPMENT

During development, sensory neurons innervating target tissues depend on limited quantities of target-derived growth factors for survival (The Neurotrophic Hypothesis) (reviewed in (Davies, 1996)). This competition leads to programmed cell death such that nearly 50% of sensory neurons die via apoptosis during development. Thus, according to the neurotrophic hypothesis, artificially increasing the concentration of a target-derived growth factor at critical times during development could selectively rescue neurons from apoptotic cell death. Our laboratories have previously validated this theory using the K14 keratin promoter to drive transgene expression of numerous growth factors, such as NGF (Albers et al., 1994), selectively in keratinized targets. This approach has been extended to a member of the GDNF family, artemin, in this study.

Like all sensory neurons, early in embryonic development (E11-E16) nociceptors are dependent on the neurotrophin NGF. This dependency is highlighted by the complete absence of nociceptors in mice lacking NGF or its receptor tyrosine kinase, TrkA (Crowley et al., 1994; Smeyne et al., 1994; Silos-Santiago et al., 1995). However, this dependency switches late in development such that approximately 50% of nociceptors begin to express the receptor tyrosine kinase, Ret, and become responsive to members of the GDNF family (Molliver and Snider, 1997).

1.3 GLIAL CELL LINED-DERIVED NEUROTROPHIC FACTOR (GDNF) FAMILY MEMBERS

The GDNF family ligands (GFLs) consist of GDNF, neurturin, artemin and persephin. Each of the GFLs binds a preferred GDNF-family receptor- α (GFR α) that is coupled to the plasma membrane via a glycosyl phosphatidylinositol (GPI) anchor (reviewed in (Airaksinen and Saarma, 2002)). GDNF preferentially binds GFR α 1, neurturin preferentially binds GFR α 2, artemin preferentially binds GFR α 3 and persephin preferentially binds GFR α 4 (Figure 2). Persephin does not act as a neurotrophic factor in the PNS (Milbrandt et al., 1998) and will not be discussed further. While GDNF and neurturin can also bind GFR α 2 and GFR α 1 (Jing et al., 1997), respectively, only artemin can activate GFR α 3 (Baloh et al., 1998b). Upon GFL binding, the GFL/GFR α complex binds to the extracellular domain of the receptor tyrosine kinase (Ret). This binding triggers autophosphorylation of the intracellular tyrosine residues which initiate a host of downstream intracellular signaling cascades. The phosphotyrosine residues can activate various signaling pathways including RAS/ERK, PI3K/AKT, p38MAPK and JNK (reviewed in (Takahashi, 2001)), important for a variety of cell processes including survival, proliferation, and neurite outgrowth. In addition, the GPI-linked proteins cluster into lipid rafts in the plasma membrane and this location is critical for Ret signaling (Tansey et al., 2000).

1.3.1 GDNF

GDNF was purified from a rat glial cell line and shown to support embryonic dopaminergic midbrain neurons *in vitro* (Lin et al., 1993), creating great excitement that it might be used to treat neurodegenerative diseases, like Parkinson's Disease. In the peripheral nervous system, GFR α 1-positive sensory neurons bind the lectin IB4, are peptide poor, and some appear

GDNF Family

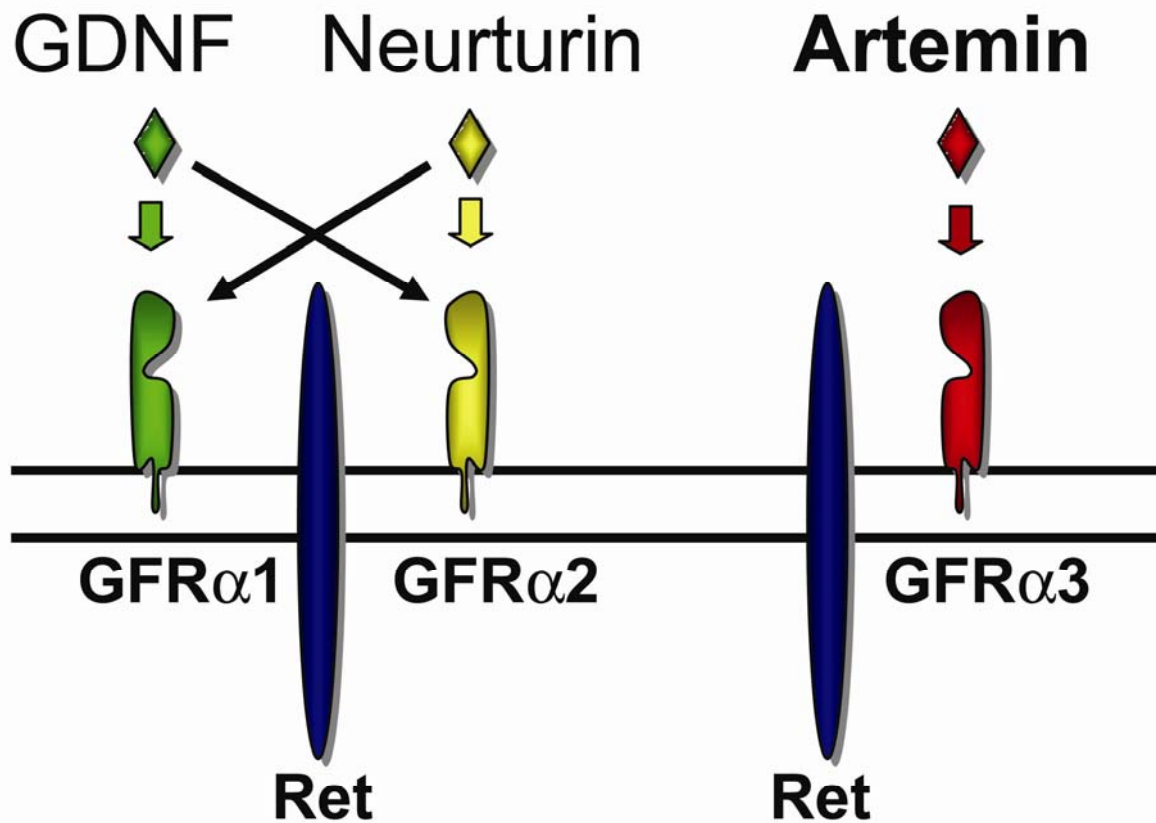


Figure 2. GDNF family members and their GFR α receptors.

The GDNF family members consist of GDNF, neurturin and artemin (persephin, not shown, is also a member of the GDNF family and bind GFR α 4). Each GDNF family ligand (GFL) binds a preferred GFR α co-receptor that is coupled to the plasma membrane by a glycosyl-phosphatidyl inositol(GPI)-linked anchor. The GFR α s are coupled to the receptor tyrosine kinase, RET, which via phosphorylation, initiates intracellular signaling. There is some cross talk between receptors as indicated for GDNF and neurturin, although GFR α 3 appears to be specific for artemin.

to be mechanoreceptors (Silverman and Kruger, 1988; Molliver and Snider, 1997; Bennett et al., 1998; Albers et al., 2006). Mice lacking GDNF have a 23% loss of DRG neurons at postnatal day 0, fail to develop kidneys and have deficits in the enteric nervous system (Moore et al., 1996). In addition, mice overexpressing GDNF in the skin have a 27% increase in Ret-positive, IB4-binding DRG neurons (Zwick et al., 2002).

1.3.2 Neurturin

Neurturin was initially purified and cloned from the conditioned media of CHO cells as a factor which supported the long term survival of superior cervical ganglion sympathetic neurons, nodose ganglia sensory neurons and a small population of dorsal root ganglia sensory neurons in culture (Kotzbauer et al., 1996). Mice lacking neurturin have fewer GFR α 2-positive neurons and mice lacking neurturin (Heuckeroth et al., 1999) or GFR α 2 have defects in innervation to the skin, enteric nervous system and parasympathetic innervation of glands (Heuckeroth et al., 1999; Rossi et al., 1999; Lindfors et al., 2006). In addition, mice lacking GFR α 2 exhibit reduced heat currents in IB4-positive neurons, but do not lose myelinated or unmyelinated fibers in the saphenous nerve, suggesting that no cutaneous GFR α 2-positive neurons were lost in these mice (Stucky et al., 2002).

1.3.3 Artemin

Following the discovery of neurturin and the cloning of its preferred receptor, GFR α 2, a third member of the GFR α family, GFR α 3, was cloned based on sequence homology to the other GFR α s (Jing et al., 1997; Widenfalk et al., 1998; Worby et al., 1998). In situ hybridization signals for GFR α 3 are found in developing (E14 to P7) dorsal root, trigeminal and sympathetic ganglia, as well as in developing nerves and Schwann cells (Widenfalk et al., 1998). In contrast

to GFR α 1 and GFR α 2, most studies indicate that GFR α 3 is not expressed in the central nervous system in developing or adult mice (Baloh et al., 1998a; Widenfalk et al., 1998). However, one group reported detectable expression of GFR α 3 in mouse brain at E12 and E15 using RNA protection assays, but expression was quickly downregulated to undetectable levels by P3 (Naveilhan et al., 1998). GFR α 3 is, however, expressed in the developing digestive tract and the urogenital system (Baloh et al., 1998a; Worby et al., 1998).

In the adult mouse, GFR α 3 expression becomes restricted primarily to neuronal tissues (dorsal root and cranial ganglia), although one group showed small amounts of GFR α 3 mRNA (relative to trigeminal ganglia) in pituitary gland, thymus, lung and duodenum (Naveilhan et al., 1998). All studies indicate that, by far, the highest level of expression of GFR α 3 mRNA is in cranial and dorsal root ganglia (Baloh et al., 1998a; Naveilhan et al., 1998). Moreover, in the adult, only a subpopulation of dorsal root and trigeminal neurons express GFR α 3 (Baloh et al., 1998a), and this subpopulation appears to be distinct from the GFR α 1 and GFR α 2 populations (Naveilhan et al., 1998). From these studies characterizing the expression patterns of GFR α 3 mRNA, it also became apparent that none of the known ligands in the GDNF family could initiate Ret signaling via this receptor (Jing et al., 1997; Baloh et al., 1998a), leading to the search for the ligand for GFR α 3.

Artemin was cloned shortly after the discovery of GFR α 3 based on homology to the other members of the GDNF family (Baloh et al., 1998b). In this initial report, artemin mRNA was found to be expressed at low levels in many adult peripheral tissues, the highest being in the pituitary gland, placenta and trachea. In addition, fetal lung and fetal kidney expressed artemin mRNA and very low levels of expression were detected in the fetal and adult brain. In E14 rats, the developing DRG nerve roots robustly expressed artemin mRNA, but expression was absent

in the cell bodies of DRG neurons, suggesting that Schwann cells of the developing nerve were the source of artemin mRNA (Baloh et al., 1998b). More recent studies indicate that artemin is expressed in the smooth muscle of the vasculature (Honma et al., 2002), hippocampal neurons (Quartu et al., 2005), carotid body cells (Leitner et al., 2005) and gut tissues (Lucini et al., 2005). There are at least 5 differently spliced mRNA variants of artemin, only two of which produce functional artemin protein (Masure et al., 1999). Therefore, it is not surprising that mRNA expression pattern do not perfectly match artemin protein studies. However, it is clear that artemin protein is expressed by a variety of target tissues and therefore could act a survival factor for neurons innervating these structures and/or contribute to the homeostasis of adult neurons in these targets.

Artemin supports the survival of a subset of postnatal dorsal root and trigeminal ganglia sensory neurons (Baloh et al., 1998b; Baudet et al., 2000) and is required for migration of sympathetic precursors (Nishino et al., 1999). In the DRG, artemin promotes the *in vitro* survival of as many or more neurons than GDNF or neurturin and increasing doses of artemin increases the survival of DRG neurons (Baloh et al., 1998b). Interestingly, in the P1 trigeminal ganglia, recombinant artemin promotes significantly greater survival of neurons compared to GDNF, neurturin or NGF (Baloh et al., 1998b), suggesting that trigeminal neurons may be particularly sensitive to artemin concentrations during development. Similarly, conditioned media from mouse cells transfected with artemin cDNA only promoted the survival of 5% of embryonic DRG neurons from E12 and E16 embryos but promoted survival of 20% and 72% of P0 and P15 neurons, respectively (Baudet et al., 2000). Therefore, artemin appears to support the survival of a subpopulation of postnatal sensory neurons.

Until very recently, few studies have examined GFR α 3 or artemin protein expression, due to the absence of antibodies for these ligands. Orozco et al. produced an anti-mouse GFR α 3 antibody and examined co-localization with various markers of nociceptors (Orozco et al., 2001). In adult mouse L5 DRG nearly 20% of neurons are positive for GFR α 3 and nearly all of those cells (97.5%) co-localize with peripherin, a marker of small diameter neurons that primarily give rise to unmyelinated fibers. The majority of the GFR α 3-positive neurons also express calcitonin gene related peptide (CGRP) (70%), Ret (82%) and TrkA (80%), while a smaller percentage bind the lectin IB4 (30%). This suggests that most artemin responsive cells are IB4-negative neurons and respond to NGF. This is in contrast to GDNF and neurturin which primarily support non-peptidergic, IB4-binding neurons (Baloh et al., 1997). However, the most striking finding from this immunocytochemical characterization was that virtually all (99%) of GFR α 3-positive neurons also express the capsaicin receptor, TRPV1, suggesting that the artemin responsive population of neurons were of great importance for pain signaling. Thus, there is considerable evidence that GFR α 3-positive neurons are a unique subpopulation of sensory neurons with many nociceptive characteristics.

1.4 TRP CHANNELS

For many years, neurons that responded to noxious thermal, chemical or mechanical stimuli (nociceptors) were identified in part by their sensitivity to the “hot” or “spicy” ingredient in chili peppers, capsaicin. Application of capsaicin to the skin leads to a psychophysical sensation of burning pain (LaMotte et al., 1991). This sensation results from excitation of nociceptive neuron terminals and their local release of inflammatory mediators (CGRP and Substance P). High doses of capsaicin in the neonatal period can ablate nociceptive neurons (Jancso et al., 1977) and repeated applications of capsaicin in the adult produce desensitization of

nociceptors (Jancso et al., 1967; Jancso, 1992). This desensitization is the basis for over the counter capsaicin creams used to treat a variety of pain disorders (back pain, diabetic neuropathy, rheumatoid arthritis, etc).

The molecular transducer in nociceptors that produces these effects upon capsaicin application was unknown until Caterina et al. cloned the capsaicin receptor (Caterina et al., 1997). They used a functional screening strategy by isolating candidate cDNA clones from DRG mRNA, injecting them into HEK293 cells and then assaying for capsaicin sensitivity using Fura-2 calcium imaging. The newly cloned cDNA was initially named vanilloid receptor subtype 1, based on its responsiveness to members of the vanilloid family, capsaicin and resiniferatoxin. TRPV1 (formerly named VR1) contains six transmembrane domains with a short hydrophobic stretch between transmembrane regions 5 and 6 as well as three ankyrin repeat domains on the amino terminus (Figure 3). It is also a distant relative of *Drosophila* transient receptor potential (TRP) ion channels, which mediate depolarization of photoreceptors in the fly (Montell and Rubin, 1989). Initial characterization showed that in addition to capsaicin, TRPV1 also responds to noxious heat (<42°) and acid (protons). A variety of related channels have since been cloned and are hypothesized to play important roles in thermosensation (reviewed in (Jordt et al., 2003; Dhaka et al., 2006)). TRPV2 has been identified as an additional noxious heat channel, responding to temperatures >52°C in heterologous systems, whereas TRPV3 and TRPV4 respond to warmer temperatures (in the range of 27-39°C). In addition, two TRP channels that detect cold stimuli have also been identified. TRPM8 responds to innocuous cool temperatures (~8-28°C) and menthol whereas TRPA1 is activated by noxious cold temperatures <17°C as well as mustard oil, cinnamon oil and bradykinin (Figure 3). Thus, at least in heterologous systems

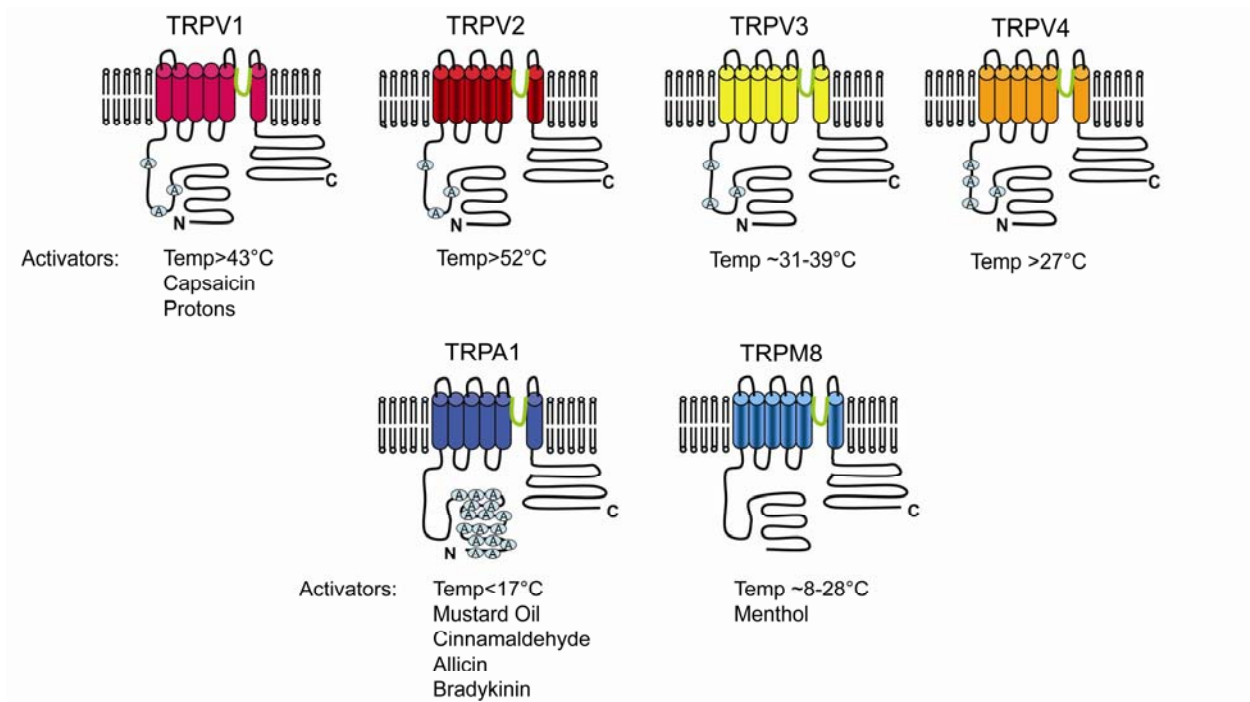


Figure 3. Thermosensitive TRP Channels.

The TRP family of cation channels contain six transmembrane domains with a hydrophobic region between domains 5 and 6. Different members of this family have been proposed to mediate flux of cations in response to different thermal stimuli such as noxious cold (TRPA1), innocuous cooling (TRPM8), warming (TRPV3, TRPV1) and noxious heat (TRPV1, TRPV2). In addition, some members of TRP family respond to chemicals that elicit burning or cooling/cold sensation in humans and animals. Adapted from Jordt et al., 2003.

TRPV1, TRPV2 and TRPA1 respond to *noxious* temperatures and/or chemicals, whereas TRPV3, TRPV4 and TRPM8 can respond to non-noxious thermal stimuli.

1.4.1 TRPV1

TRPV1 is a nonselective cation channel that is gated by noxious heat (>43°C), protons, and vanilloid compounds (capsaicin, resiniferatoxin) (Caterina and Julius, 2001). TRPV1 is localized to a subset of small diameter nociceptors in trigeminal and dorsal root ganglia (Caterina et al., 1997). In mouse, TRPV1 is mainly expressed in IB4-negative, peptidergic neurons (Zwick et al., 2002). In behavioral testing, TRPV1^{-/-} mice have normal mechanical thresholds and relatively normal thermal thresholds (Caterina et al., 2000; Davis et al., 2000). In contrast, in cultured DRG neurons from the TRPV1^{-/-} knockout animals, the electrophysiologic response to noxious heat is absent (Caterina et al., 2000; Davis et al., 2000). However, in an *ex vivo* physiological preparation where skin, DRG and spinal cord are maintained intact in artificial CSF, the response to noxious heat in TRPV1^{-/-} mice does not differ from wildtype mice (Woodbury et al., 2004). Therefore, in contrast to initial reports, TRPV1 does not appear to be necessary for the detection of noxious heat in normal animals.

However, there is considerable evidence that TRPV1 is required for inflammation-induced heat hyperalgesia. Wildtype mice injected with carrageenan or CFA (Complete Freund's Adjuvant) become inflamed and develop robust thermal and mechanical hyperalgesia whereas TRPV1 knockout mice do not experience thermal hyperalgesia following induction of inflammation (Caterina et al., 2000; Davis et al., 2000). Various laboratories have shown that inflammation or injury increases TRPV1 protein or mRNA (Tohda et al., 2001; Ji et al., 2002; Amaya et al., 2003; Molliver et al., 2005). In addition to increased synthesis of TRPV1, specific inflammatory mediators can sensitize TRPV1. For example pro-algesic substances released

during inflammation such as ATP (Moriyama et al., 2003) and bradykinin (Chuang et al., 2001; Sugiura et al., 2002) have been shown to sensitize TRPV1 and this sensitization is absent in TRPV1^{-/-} knockouts. In addition, neurotrophic factors such as NGF are increased following inflammation (Donnerer et al., 1992) and can sensitize nociceptors by modulating TRPV1 (Chuang et al., 2001; Galoyan et al., 2003). Taken together, these studies indicate that TRPV1 is part of a common signaling pathway used by different inflammatory modulators to produce hypersensitivity.

1.4.2 TRPA1

The role of TRPA1 in sensory neuron thermal and chemical detection remains controversial. The initial paper identifying TRPA1 (ANKTM1) showed that TRPA1 mRNA is expressed in a small subpopulation of DRG (3.6%) and trigeminal neurons, and almost all of these neurons contain TRPV1 (97%) and CGRP (97%) (Story et al., 2003). These authors propose that this population of afferents is distinct from those expressing the “cooling” receptor TRPM8. Specifically, TRPA1 expressing CHO or HEK cells have large calcium transients in response to low temperature (10°C), respond at lower temperatures than cells expressing TRPM8, and do not respond to heat, menthol, or hypotonic solutions. Analysis of adult DRG neurons (without NGF in the media) indicated that there are two populations of cold sensitive neurons, one that responds to menthol and cool temperatures with a threshold of activation of 24°C, and another group that responds to colder temperatures with a threshold of activation of 15°C but does not respond to menthol (Story et al., 2003). These findings support the hypothesis that TRPM8-expressing neurons respond to cool temperatures while TRPA1-expressing neurons respond to noxious cold temperatures.

A more general role for TRPA1 in pain detection has come from studies showing that plant-derived compounds (allyl isothiocyanates from mustard oil, cinnamaldehyde from cinnamon, allicin from garlic and Δ^9 -tetrahydrocannabinol (THC) from marijuana) can also activate the channel (Bandell et al., 2004; Jordt et al., 2004; Macpherson et al., 2006). In addition, bradykinin, an endogenous inflammatory peptide acting via a G-protein coupled receptor, activates TRPA1 (Bandell et al., 2004), suggesting a role for TRPA1 in tissue injury and inflammation. Interestingly, recent evidence shows that the fly homolog of mammalian TRPA1, *painless*, is essential for isothiocyanate avoidance in *Drosophila* (Al-Anzi et al., 2006), indicating that TRPA1 is an evolutionally conserved pathway for detecting and avoiding noxious chemicals.

Many of the studies characterizing TRPA1 activation in response to pungent chemicals also re-examined the expression patterns of TRPA1 and cold responses in dissociated cells, with variable results. In newborn rats, Jordt et al. detected TRPA1 mRNA in 20% of trigeminal neurons and found calcium responses to 20 μ M mustard oil in 35% of cells (all of which are also responsive to 1 μ M capsaicin) (Jordt et al., 2004). However, almost none (4%) of the mustard oil sensitive cells responded to noxious cold (5°C) and those that did also responded to menthol (Jordt et al., 2004). Other laboratories report much wider distributions of TRPA1 mRNA in mouse TG (37%) and DRG (57%) and have not found cold responses (27°C \rightarrow 15°C) in HEK cells transfected with TRPA1 (Nagata et al., 2005).

In addition to the first report of noxious cold activation of TRPA1 (Story et al., 2003), four other laboratories have confirmed this finding in heterologous systems (reviewed in (Dhaka et al., 2006)). Reid and colleagues contend that the difficulty in finding TRPA1-like responses in DRG neurons (Babes et al., 2004; Jordt et al., 2004), may reflect differences in the activation rate

of the channel in native and heterologous systems (Reid, 2005). They found that human and mouse clones are activated rapidly and strongly by cold (12°C), but native rat DRG neurons are activated very slowly in response to cold, with a delay of up to a 1 min, suggesting the possibility that cold activation of TRPA1 in native neurons is actively inhibited. They contend that release of this inhibition by an endogenous mediator such as bradykinin (Bandell et al., 2004) might permit TRPA1 to respond to cold only in damaged or inflamed tissue (Reid, 2005).

Recent work in inflammatory and neuropathic pain models supports this hypothesis. Following CFA injection in rats, TRPA1 mRNA expression increases from 32% of DRG neurons prior to injection to 44% 1 day post-CFA, 42% 3 days post-CFA and gradually returns to normal by day 7 (Obata et al., 2005). These changes parallel the time course of cold hyperalgesia observed in behavioral testing of these rats. This upregulation can be inhibited by anti-NGF antibody injection or by a p38 MAPK inhibitor and can be induced by intrathecal injection of NGF, but not GDNF. Similar increases in TRPA1 mRNA were seen following L5 spinal nerve ligation (SNL) in the spared L4 DRG (Obata et al., 2005; Katsura et al., 2006b). In both the inflammatory (CFA) and neuropathic (SNL) pain models, both TRPA1 induction and cold hyperalgesia could be prevented by treatment with TRPA1 antisense oligodeoxynucleotides (Obata et al., 2005; Katsura et al., 2006b). These results provide further support for the hypothesis that TRPA1 is essential for cold hyperalgesia seen following inflammation or injury, remarkably similar to the role of TRPV1 in heat hyperalgesia after inflammation.

Two groups recently disrupted the TRPA1 gene by deleting the pore region of the channel (Bautista et al., 2006; Kwan et al., 2006) and tested sensitivity to thermal, mechanical and chemical stimuli. Whereas Kwan et al. showed a substantially reduced number of mustard oil-responsive cells using calcium imaging and reduced behavioral sensitivity to oral or injected

mustard oil, Bautista et al. showed the complete absence of mustard oil responses behaviorally or in dissociated cells. Curiously, the remaining mustard oil responsive cells seen in Kwan study were in capsaicin insensitive cells, suggesting that there may be another mustard oil receptor in a small population of afferents. Most interesting, however, were the conflicting results regarding the behavioral responses to noxious cold. Bautista et al. found no difference in latency to hindpaw lift on a cold plate (0°C) and no difference in flinches/min in the acetone test (another measure of cold responsiveness where chilled acetone is dripped onto the skin) between wildtype and TRPA1^{-/-} mice. However, Kwan et al. found decreases in the number of hindpaw lifts over five minutes in the cold plate test (0°C) (particularly in female mice) and decreased duration of paw shake in the acetone test. Thus, the method of measuring responses and the gender of the mice used may have contributed to the conflicting results in these two papers. Further study regarding the role of TRPA1 in the detection of noxious cold is clearly necessary.

Taken together, these studies suggest that TRPA1 is a polymodal sensor for noxious stimuli and afferents containing both TRPV1 and TRPA1 may be critically important in pain signaling, particularly during inflammation or injury.

1.5 LINGUAL AFFERENTS

Most work on the role of growth factors in regulating survival and maintenance of nociceptors has been done in DRG neurons. However, for reasons that are not clear, the effects of alterations in epithelial-derived growth factors on trigeminal afferents are often more dramatic, perhaps reflecting the dense innervation of the whisker pad and oral cavity regions. In addition, persistent pain involving cranial structures is of major clinical significance and is understudied. Therefore, our study examined trigeminal neurons in parallel with our studies of

cutaneous DRG neurons, specifically focusing on lingual afferents that innervate the tongue, a structure that routinely contacts noxious thermal and chemical stimuli.

1.5.1 Tongue Anatomy and Innervation

The tongue epithelium is a highly innervated structure containing both special sensory (taste) and general sensory (somatic) afferents. For the anterior 2/3 of the tongue, taste information is conveyed through the chorda tympani (cranial nerve VII) to the geniculate ganglion and general sensory information is conveyed through the lingual nerve (cranial nerve V) to the trigeminal ganglion. Analogous to the cutaneous system where DRG neurons have both a peripheral and a central process, trigeminal neurons which innervate the tongue also have central projections to the brain stem trigeminal subnuclei caudalis (Vc) (medullary dorsal horn) (Carstens et al., 1995).

1.5.2 Previous studies on lingual afferents

Anatomical studies of cat lingual nerve fibers using electron microscopy showed that nearly 44% of fibers are unmyelinated (Holland and Robinson, 1992). This is in contrast to mouse cutaneous nerves (e.g. saphenous) in which 83% are unmyelinated (Stucky et al., 1999). There are very few studies on the response properties of lingual afferents to thermal and chemical stimuli. The most extensive study (Wang et al., 1993) showed that similar to the innervation of cutaneous structures, the tongue is innervated by a combination of myelinated (A β and A δ) and unmyelinated afferents. The A β fibers were all mechanoreceptive and did not respond to thermal or chemical stimuli. The A δ fibers were heterogeneous in their response properties with some being responsive to mechanical and chemical stimuli whereas others responded only to thermal stimuli or to both mechanical and thermal stimuli. The C-fibers were

rare and were either high threshold mechanoreceptors or polymodal nociceptors (Wang et al., 1993). Other studies have classified whole lingual nerve responses to non-noxious thermal stimuli (Lundy and Contreras, 1995; Pittman and Contreras, 1998). Almost no data is available regarding the response of lingual afferents to capsaicin and mustard oil.

Both mustard oil and capsaicin elicit burning sensation when either is applied to the tongue of human subjects (Simons et al., 2003). In addition, this study also showed that mustard oil exhibits self-desensitization and reciprocal cross desensitization with capsaicin (i.e. either ligand desensitizes responses to the other ligand). These studies support the hypothesis that the tongue contains nociceptors uniquely designed to detect noxious chemical stimuli. In addition, the cross desensitization raises the question as to whether the same primary afferents in the tongue have both TRPA1 and TRPV1 or if the two signals converge at higher levels of the pain pathway.

1.5.3 Clinical Relevance of Lingual Afferents

Dysfunction of lingual afferents leads to a variety of chronic oral pain disorders. One particularly disabling oral pain disorder is Burning Mouth Syndrome (BMS), characterized by spontaneous burning pain typically in the tip and anterior two-thirds of the tongue. BMS may affect up to 40% of post-menopausal women. Recent evidence suggests that patients with BMS have small fiber sensory neuropathy (Lauria et al., 2005) which might induce sensitization of remaining lingual afferents and contribute to this disorder. Although few treatments are available for BMS, topical (Epstein and Marcoe, 1994) and systemic capsaicin (Petrucci et al., 2004) provide symptomatic relief. Despite the prevalence of chronic oral pain disorders like BMS, there is a paucity of data regarding the afferents that innervate these important structures.

1.6 GOALS OF THE DISSERTATION

Prior to my studies, the role of artemin in regulating the phenotype and function of nociceptors was entirely unknown. Artemin was particularly interesting because all of the artemin-responsive neurons expressed TRPV1, a key molecular integrator of noxious stimuli. A few studies had also shown that artemin promoted the survival of postnatal sensory neurons *in vitro*, suggesting that like other growth factors, artemin might support a select population of nociceptors during development.

Just after I joined the Davis lab, Kathryn Albers' laboratory successfully created a novel line of transgenic mice that overexpressed artemin selectively in keratinized tissues. These mice seemed like an ideal starting point for investigating the developmental survival role of artemin and functional role of artemin in regulating adult responses to noxious heat. At this point, I hypothesized that the ART-OE mice would have increased survival of a population of nociceptors that were GFR α 3 and TRPV1-positive and functionally would be behaviorally hypersensitive to heat.

During the initial anatomical characterization of the ART-OE mice (Chapter 3), two striking findings broadened my goals from simply investigating the role of artemin in modulating heat sensitivity (via TRPV1) in the cutaneous system. First, in addition to increases in TRPV1, ART-OE mice displayed a dramatic upregulation in TRPA1, leading to the hypothesis that artemin might regulate responses to noxious cold and pungent chemical stimuli. The TRPA1 finding led to a battery of behavioral assays on cold and chemical detection (Chapter 4). Second, all of the changes in gene expression in the DRG were much larger in the TG, suggesting that artemin might differentially affect TG neurons. While the TG projects to many regions, I decided to characterize lingual afferents, as the tongue is heavily keratinized, routinely contacts

pungent chemicals and noxious temperatures, and is understudied. This led to anatomical characterization of lingual afferents in WT and ART-OE mice (Chapter 3) and additional oral behavioral experiments (Chapter 4).

Finally, to examine the functional responses of nociceptors to increased concentration of artemin at the single cell level, I performed calcium imaging on dissociated TG neurons that were retrogradely labeled from the tongue. Lingual and trigeminal afferent sensitivity to the ligands for TRPV1 and TRPA1 are discussed in Chapter 5.

2.0 METHODS

2.1 CONSTRUCTION OF TRANSGENIC MICE

We isolated transgenic mice that overexpress the coding portion of the artemin gene in basal keratinocytes of the epidermis and tongue. Mice were generated and screened as previously described for other growth factor genes (Albers et al., 1994; Albers et al., 1996; Zwick et al., 2002). A 1100 bp fragment was PCR cloned from genomic DNA isolated from mouse liver using primers (5'CGAAAGCTATGGAACTGGGA3'; 5'GATCATCCTCAGCCCAGACA3') that encompass nucleotides of the artemin gene (Accession #NT039264) (Honma et al., 2002). The amplified fragment, which contains two intronic sequences within the artemin coding region (see Fig. 1A), was cloned into the pCR4-TOPO vector (Invitrogen, San Jose, CA) and sequence fidelity verified by DNA sequencing in the University of Pittsburgh Genomics and Proteomics Core Laboratory. A purified fragment containing 2.3 Kb of the human K14 keratin promoter sequence, 1.1 Kb of mouse artemin DNA and 1.7 Kb of the human growth hormone gene containing intron/exon and polyA signal sequences was injected into C57Bl6J/C3H F1 hybrid fertilized oocytes. Founder lines were screened using slot blot assays done on DNA from tail skin using transgene specific and artemin specific random primed 32P-dCTP-labeled probes. Reverse transcriptase-PCR analysis of RNA from founder offspring backskin was used to assay the relative level of transgene expression. Detailed analysis was focused on the transgenic line that exhibited the highest transgene copy number. Primers to detect endogenous and transgenic artemin (5'CTCAGTCTCCTCAGCCCG3' and 5'TCCACGGTCCTCCAGGTG3') and transgene

specific primers (5'CGAGCTGATACGTTTCCCGCTTC3' and 5'AAGAGGGCAGCCAGTGTTTCTC3') were used. Analyses were performed on male and female transgenic and wildtype mice between 2 and 6 months old kept under AAALAC conditions in the animal facility of the University of Pittsburgh. Animals were cared for and used in accordance with guidelines of the *U.S. Public Health Service Policy on Humane Care and Use of Laboratory Animals* and the *NIH Guide for the Care and Use of Laboratory Animals*.

2.2 TOTAL CELL COUNTS

The number of L4 DRG neurons and TG neurons was estimated using previously described methodology (Harrison et al., 2004). Wildtype (n=4) and ART-OE (n=3) mice were deeply anesthetized, perfused with 0.9% NaCl and ganglia collected. Ganglia were postfixed in 4% paraformaldehyde for 30 min. Serial 8 μ M sections stained with cresyl violet were analyzed by counting neurons with visible nucleoli from at least ten equally spaced sections. Final estimates of cell number were obtained from raw counts that were adjusted using a correction factor to account for neurons with multiple nucleoli, which theoretically could be counted more than once.

2.3 TISSUE IMMUNOLABELING

Skin, ganglia and spinal cord collected from animals perfused with saline were placed in 30% sucrose, embedded in OCT and cut on a cryostat at 20 μ m thickness. Sections were fixed either for 10 min in -20°C acetone (GFR α 3 and TRPA1 labeling) or 10 min in 4°C 4% paraformaldehyde (TRPV1, CGRP and IB4). The percent of neurons labeled was determined by comparing the number of GFR α 3-positive, TRPV1-positive or both TRPV1 and GFR α 3-positive neurons with the total number of neurons labeled with antibodies to peripherin and neurofilament

200, which represents nearly all neurons in the ganglia. At least 3 40X fields from a minimum of four nonadjacent sections were counted. Only neurons with visible nuclei were counted to avoid counting errors that could result from ART-OE neuron hypertrophy. A minimum of 1000 neurons/animal were counted in at least 3 WT and 3 ART-OE mice. Somal size was measured using NIH Image J software using at least 150 profiles with nuclei per animal. Significance differences were determined using a Student's t-test. Antibodies used were rabbit anti-artemin (5Mg/ml; R&D systems, Minneapolis, MN), anti-TRPV1 (1:250 skin, 1:500 ganglia; Oncogene Research, San Diego, CA), goat anti-GFR α 3 (1:80; R&D Systems, Minneapolis, MN), mouse anti-peripherin (1:400; Chemicon, Temecula, CA), mouse anti-neurofilament 200 (1:400; Sigma, St. Louis, MO), rabbit anti-calcitonin gene related peptide (CGRP, 1:1000, Sigma), rabbit anti-TRPA1 (10 Mg/ml; a generous gift from D. Corey, Harvard University)(Corey et al., 2004). Isolectin B4 (IB4) conjugated to Cy3 was purchased from Molecular Probes and used at 1:200. Donkey anti-rabbit and donkey anti-goat secondary antibodies (Jackson ImmunoResearch Laboratories, West Grove, PA) were used at 1:200.

2.4 CONFOCAL ANALYSIS OF DRG NEURONS

Immunolabeled DRG (L3, L4, L5) sections were visualized with a Leica confocal microscope (Leica Microsystems; Wetzlar, Germany). To avoid selection bias, fields for analysis were chosen using NF200/Peripherin immunolabeling. The total number of neurons (Peripherin/NF200-positive) and the number of GFR α 3-positive, TRPV1-positive or both TRPV1 and GFR α 3-positive neurons was determined in at least three 40x fields from a minimum of four nonadjacent sections. Only neurons with a visible nucleus were counted because the neurons from ART-OE mice are hypertrophied and therefore would be

overrepresented if neuronal profiles were counted. A minimum of 1000 neurons/animal were counted in 3 WT and 3 ART-OE mice. Soma size was also measured using NIH Image J software. A minimum of 150 profiles with nuclei were measured for each animal.

2.5 SURGICAL PROCEDURE FOR RETROGRADE LABELING OF LINGUAL AFFERENTS

Animals were lightly anesthetized with inhaled isoflurane and then deeply anesthetized with an intraperitoneal injection of 2.5% avertin (2,2,2-tribromoethanol tert-amyl alcohol diluted in 0.9% saline; 20 μ l/g body weight). The tongue was extracted slightly from the mouth and approximately 1 μ l of 2% wheat germ agglutinin (WGA-488) in sterile saline was injected into the superficial dorsal epithelium of the tip of the tongue using a glass micropipette. Injections were performed bilaterally. The injection sites were carefully washed with saline and dried with a cotton swab to prevent leakage to surrounding tissues. Mice were allowed to recover for two days and then processed for immunocytochemistry.

2.6 TISSUE PREPARATION

Animals were anesthetized as described above and then transcardially perfused with ice cold 4% paraformaldehyde in 0.1M phosphate buffer (PB), pH 7.4. Trigeminal ganglia and tongues were collected by dissection. Trigeminal ganglia were embedded in 10% gelatin, post-fixed for 1hr in 4% paraformaldehyde and then cryoprotected in 25% sucrose at 4°C overnight. 35 μ m sections were cut using a sliding microtome. The tongues were cryoprotected in 25% sucrose overnight and then 20 μ m sections cut on a cryostat. Immunocytochemistry was

performed for TRPV1, GFR α 3, CGRP and IB4 using the primary and secondary antibody concentrations and methods described in the Tissue Immunolabeling section above.

2.7 CONFOCAL ANALYSIS OF WGA-BACKLABELED IMMUNOPOSITIVE TRIGEMINAL NEURONS

Retrogradely-labeled afferents were visualized using a Leica confocal microscope (Leica Microsystems; Wetzlar, Germany). WGA-positive neurons were counted at 40X in at least 4 non-overlapping fields from 4 sections (spaced at least 175 μ M apart). A minimum of 3 WT and 3 ART-OE mice were analyzed. Since some cell bodies in ART-OE mice are hypertrophied, we only analyzed cells with a visible nucleus to minimize bias from this hypertrophy. The number of WGA-positive neurons that were also TRPV1-positive, IB4-positive, CGRP-positive or GFR α 3-positive was determined.

2.8 LINGUAL NERVE ANALYSIS

Lingual nerve segments were removed, post-fixed 2 hr in 4% paraformaldehyde and 2% glutaraldehyde, washed in 0.1 M phosphate buffer, immersed in osmium tetroxide for 90 min at 4°C, dehydrated in graded ethanols, embedded in Spurr's resin (EM Corporation), and cut at 0.7–0.8 nm on an ultramicrotome (Reichert Ultracut E). Sections were stained with lead citrate and uranyl acetate and photographed on an electron microscope. The number of myelinated and unmyelinated axons was determined for three images (2900x) from three WT and three ART-OE mice. To determine axon diameters, axon profiles were measured in each group using NIH Image J software.

2.9 REAL TIME PCR ANALYSIS OF NOCICEPTOR-RELATED GENES

RNA was isolated from TG and DRG using Trizol purification (Invitrogen). RNA was DNased to remove genomic DNA and 1 µg reverse transcribed using Superscript (Invitrogen). SYBR Green PCR amplification was performed using an Applied Biosystems 5700 real-time thermal cycler. The thermal cycler measures the relative fluorescence of SYBR Green bound to double-stranded DNA compared to a passive reference for each cycle. Threshold cycle (C_t) values, the cycle number in which SYBR Green fluorescence rises above background, were recorded as a measure of initial template concentration. Relative fold changes in RNA levels were calculated by the ddCt method (Livak and Schmittgen, 2001) using GAPDH as a reference standard. Primers for GAPDH, TRPV1, TRPV2, TRPV3, TRPV4, TRPM8, TRPA1, GFR α 3, RET, and TrkA were designed using ABI software (Table 1). Statistical significance was determined using a Student's t-test.

2.10 HARGREAVES' TEST (HEAT)

Transgenic mice of mixed gender were tested for heat sensitivity using the Hargreaves' test (Hargreaves et al., 1988). Mice were placed on a 30°C heated glass surface in individual chambers (10.0 cm in length x 10.0 cm in width x 13.0cm in height) of a 16-chamber plexiglass container (IITC Inc., Woodland Hills, CA). Animals were acclimated to the apparatus for 1.5 h prior to testing. The apparatus was set at a laser intensity of 15% and testing done using repeated measures (2 measures per foot) of the left and right glabrous hindpaw skin. Four response times were averaged for each animal. Mean response times for each set of animals were determined and values expressed \pm the standard error of the mean (SEM). Significance was determined using Student's t test.

Gene	Forward Primer (5'→3')	Reverse Primer (5'→3')
GFR α 3	CTTGGTGACTACGAGTTGGATGTC	AGATTCATTTTCCAGGGTTTGC
C-RET	ACTCGGCTCTCTGAGATAGACA	AGACCTTGGTCCAGGTCAACAA
TrkA	AGAGTGGCCTCCGCTTTGT	CGCATTGGAGGACAGATTCA
TRPV1	TTCCTGCAGAAGAGCAAGAAGC	CCCATTGTGCAGATTGAGCAT
TRPV2	CCAGCCATTCCCTCATCAAAA	AAGTACCACAGCTGGCCCAGTA
TRPV3	TGAAAGAAGGCATTGCCATTT	GAAACCAGGCATCTGACAGGAT
TRPV4	TGGATTCCTTGTTGACTACGG	CACAATGTCAAAGAGGATGGGC
TRPA1	GCAGGTGGAACCTTCATACCAACT	CACTTTGCGTAAGTACCAGAGTGG
TRPM8	CGTGGGAGGGTGTCATGAAG	GTTGTCGTTGGCTTTCGTGTT
GAPDH	ATGTGTCCGTCGTGGATCTGA	ATGCCTGCTTCACCACCTTCTT

Table 1. Primer Sequences used for real time PCR assays.

2.11 COLD TAIL WITHDRAWAL ASSAY

For cold measures, individual mice (10 WT, 10 ART-OE) were restrained in an open-ended tube and the distal third of the tail immersed in an ethanol bath (Mogil and Adhikari, 1999). Assays were done at 0°C and -15°C on two different sets of mice. Temperature of the bath was maintained using a temperature controlled ethanol bath (NesLab RTE7). The time until a vigorous tail withdrawal response occurred was measured to 0.1 sec using a stopwatch.

2.12 NOXIOUS COLD ASSAY

Mice were placed on a block of ice covered by a plexiglass box (2" wide x 2" long x 12" high) and responses tested for 1 minute. The block of ice was kept frozen in a -20°C freezer and was removed from the freezer just prior to testing. To minimize changes in temperature, a fresh block of ice was used for every 5 mice. Since each mouse was tested for only 1 minute, there was very little melting of the ice block. While the exact temperature of the ice block is difficult to know for certain, there was no appreciable melting of the ice indicating that temperature was less than 0°C. Given the large number of nocifensive responses (10-20 in 1 minute) observed in our study in comparison to others (Kwan et al show less than 10 paw lifts in a 5 minute testing period in response to cold plate set at 0°C;(Kwan et al., 2006)), the temperature of the ice block was most likely in the range of -20°C to -10°C during our testing. The latency to first response and number of nocifensive events (paw lifts, paw biting, paw shaking, or jumps) were recorded. Because we found that cold responses desensitize with repeated testing, each mouse was tested only once.

2.13 PLACE PREFERENCE ASSAY

Mice were placed in a 2 inch by 4 inch plexiglass chamber where one side of the floor was room temperature (22°C) and the other side was 5°C. The cold side was connected to a temperature regulator (Physitemp BFS-30TC Controller, Physitemp Instruments, Clifton, NJ) and cool water was circulated through the cold block to dissipate heat (Physitemp PTU-3 Pump and Tank Unit). Mice were initially placed on the 5°C side. Mice were tested for 5 minutes and time spent on each side was recorded using a stopwatch. Because we found that cold responses desensitize with repeated testing, each mouse was tested only once.

2.14 DRINKING BEHAVIOR

Mice were tested for oral sensitivity to capsaicin or mustard oil using a drinking paradigm modified from previous studies (Simons et al., 2001; Furuse et al., 2002). A total of 40 mice were used for these experiments (10 WT males, 10 WT females, 10 ART-OE males, 10 ART-OE females). Mice were housed in cages individually and given food and water ad libitum. For the drinking aversion test, a two water bottle choice test was used. One bottle contained normal water plus vehicle and the other bottle contained 1 μ M capsaicin (Sigma-Aldrich) or 100 μ M mustard oil (Sigma-Aldrich). Mice were tested over 72 hrs. Mice were allowed to drink freely from the two bottles for 24hrs and then the volume consumed was measured. To ensure that there was not a place preference, the bottle positions were reversed at the end of each day. The average volume consumed over the three test days and the ratio of capsaicin or mustard oil intake versus total liquid intake (percentage) was calculated. To ensure that there was not a difference in the total volume of liquid consumed by the transgenic compared to the wildtype mice, mice were also tested using the same paradigm with both bottles filled with normal water.

All mice drank the same volume of water and did not display a bottle preference when both bottles contained normal water.

2.15 MUSTARD OIL NOCIFENSIVE BEHAVIOR

To test responses to mustard oil, we used a previously established protocol (Caterina et al., 2000). Briefly, 10% mustard oil (allyl isothiocyanate, Sigma-Aldrich CH-9471) in mineral oil was painted onto the plantar surface of one of the mouse hindpaws and then nocifensive behavior (licking, biting, foot lifts) was quantified. Both the number of events and the duration of nocifensive behavior were determined. Mice began to display nocifensive behavior almost immediately after mustard oil was painted on the paw. Duration of behavior was measured as the time from application of mustard oil to the time where 30 seconds had elapsed from the last nocifensive event. Mice were tested for a maximum of 5 minutes. To minimize spread of the mustard oil to the non-painted paw, mice were tested on an absorbent pad. Immediately following testing, mice were sacrificed using an overdose of inhaled isoflurane and the diameters of the painted and non-painted paws were measured using a caliper micrometer.

2.16 CAPSAICIN NOCIFENSIVE BEHAVIOR

Nocifensive behavior and thermal sensitivity to noxious heat were assayed following injection of the TRPV1 agonist, capsaicin, into the mouse hindpaw. These studies utilized a previously reported injection paradigm (Caterina et al., 2000). Briefly, following baseline testing for sensitivity to noxious heat using the Hargreave's test (see above), 10 μ l capsaicin solution (1 μ g in 10 μ l saline/10% ethanol/0.5% Tween 20) or 10 μ l saline with 0.5% Tween 20 was injected subcutaneously into the plantar surface of one of the hindpaws. Nocifensive behavior was then determined as described previously in the mustard oil behavior section. Following

testing, mice were tested for thermal sensitivity to noxious heat using the Hargreave's test at 10 min, 30 min and 60 min post-injection. In contrast to the mustard oil studies, capsaicin injection did not lead to any appreciable paw edema at 5 min and therefore paw diameter was not measured in these studies.

2.17 COMPLETE FREUND'S ADJUVANT (CFA) INJECTION AND BEHAVIOR

Detailed methods for this model of inflammatory pain have been previously described (Zwick et al., 2002). Briefly, 10 WT and 10 ART-OE male mice were anesthetized with isoflurane and 20 μ l of complete Freund's adjuvant (CFA) emulsion was injected into the plantar surface of both hindpaws. Hargreave's testing was performed 1, 3, 5, and 7 days post-CFA injection to evaluate withdrawal latencies to noxious radiant heat.

2.18 MECHANICAL SENSITIVITY BEHAVIOR

Mice were tested for mechanical sensitivity using von Frey filaments. Two groups of mice were tested. The first group contained mixed gender mice (WT: n=10, ART-OE: n=10) and were testing on the dorsal surface of the hindpaw using the "up/down" method. Briefly, von Frey filaments were applied 5 times to the dorsal hindpaw and response (lifting, biting, etc) to any of the 5 applications recorded as a response. High and low force filaments were alternated until a threshold of sensitivity was reached. The second group of mice contained only male mice (WT: n=10, ART-OE: n=10) and were tested on the plantar surface of the hindpaw. The number of responses to three separate trials of 5 applications of a 4.08 (1g) von Frey filament to each hindpaw were determined. The responses are represented as a percentage of total applications.

2.19 CELL PREPARATION FOR CALCIUM IMAGING OF TRIGEMINAL NEURONS AND IDENTIFIED LINGUAL AFFERENTS

Lingual Afferents were backlabeled as described above. Two days following injection, mice were perfused with ice cold $\text{Ca}^{+2}/\text{Mg}^{+2}$ -free Hanks' Balanced Salt Solution (HBSS) (Gibco 14170-112). Trigeminal ganglia were dissected, placed in ice cold HBSS and minced using iridectomy scissors to pieces approximately the size of a DRG. Trigeminal ganglia were then incubated in 60U of papain in a solution of cysteine (1mg/3ml HBSS) and saturated NaHCO_3 for 20 min at 37°C , the solution removed and 12mg collagenase Type II and 14mg dispase Type II in 3 ml HBSS added for 20 min at 37°C . Cells were spun at 500g for 4min and the collagenase/dispase solution was removed. Cells were resuspended in 500 μl L-15 (Gibco) plus 10% FBS (Gibco) and 1M HEPES and triturated. The resuspended cells were gently placed on the top of a 40/60 percoll gradient (Fisher) (4mls 40% percoll in L15 layered on 4mls 60% percoll) and spun at 1300g for 10min. The upper layer containing myelin debris was removed and washed with 4ml of fresh L15. Cells were spun at 1000g for 6min and the resultant pellet of cells was resuspended in 400 μl F12 media (Gibco) with 10% FBS and antibiotics (penicillin/streptomycin, 50 units/ml). No additional growth factors were added to the culture medium. Cells were plated onto laminin (0.1mg/mL) and poly-d-lysine (5mg) coated glass coverslips. Cells were incubated for 2 h at 37°C , fed with F12 media and incubated overnight. Calcium imaging was performed 12-24hrs after plating.

2.20 IMAGING PROTOCOL

Cells were loaded with calcium indicator by incubation with HBSS containing bovine serum albumin and 2 μM of the acetoxymethyl ester of fura-2 (Molecular Probes, Oregon) for 30

min at 37°C. Coverslips were mounted on an Olympus upright microscope stage with HBSS buffer flowing at 5 ml/minute. Perfusion rate was controlled with a gravity flow system (Warner VC66) and perfusate temperature was maintained at 30°C using a heated stage and an in-line heating system (Warner PH1, SHM-6, TC344B). Drugs were delivered with a rapid-switching local perfusion system. Firmly attached, WGA-backlabeled cells were identified using a 480nm filter and chosen as regions of interest in the software (Simple PCI; CImaging). Unlabeled, adjacent cells were also identified and imaged. All fields were first tested with brief application of 50mM K⁺ (high K⁺) and Ca⁺⁺ transients imaged to standardize pipette placement and to insure that cells were healthy and responsive. Responses were measured as the ratio of absorbance at 340nm to that obtained at 380nm (Sutter DG4; Retiga 1300; $\Delta F_{340/380}$); peak responses were > 0.08 $\Delta F_{340/380}$ and were easily distinguished from optical noise (< 0.02 $\Delta F_{340/380}$). Absorbance data at 340 and 380 nm were collected at one per second. Cells not responsive to high K⁺ application were not analyzed further. Calcium transients were examined in response to local application of either 1 μ M capsaicin (5-6sec) or 100 μ M mustard oil (15-20sec) using a rapid-switching perfusion system (Warner Instruments). These doses of capsaicin and mustard oil were chosen because previous studies in our laboratory indicated that they elicited responses >0.1 $\Delta F_{340/380}$ from the maximal number of cells and could be applied repeatedly without significant loss in the number of responding cells. These concentrations are also within the range reported in the literature for calcium imaging in mouse trigeminal neurons.

In the standard protocol, cells were first tested with mustard oil (100 μ M) allowed to return to baseline (typically 5 minutes), tested with application of capsaicin (1 μ M) and allowed to return to baseline (typically 10 minutes), and then tested a second time with mustard oil. A separate group of cells was only tested with capsaicin. However, there were no differences in

capsaicin responses between the cells only exposed to capsaicin and cells exposed first to mustard oil and then to capsaicin. Therefore, in our analysis of capsaicin responsive cells, these two sets of cells were pooled.

The number of capsaicin or mustard oil responsive cells was determined as a percentage of total healthy cells (cells that responded to high K⁺). Ca⁺⁺ response peak and area (F_{peak}, F_{area}) were calculated using Microsoft Excel for suprathreshold responses (peak response > 0.08 ΔF_{340/380}) as a measure of total Ca⁺⁺ influx. The portion of the calcium response used for this measurement included the entire curve from the initiation of the response until the point at which the calcium signal returned to the prestimulus baseline. Response parameters were compared for significance using Student's t test. 10mM capsaicin (Sigma-Aldrich) in 1-methyl-2-pyrrolidinone was used as a stock solution; 1.0 μM capsaicin was made fresh daily in HBSS. 100mM mustard oil (Sigma-Aldrich) in 1-methyl-2-pyrrolidinone was made fresh daily and diluted to 100μM using HBSS.

3.0 ANATOMY RESULTS

3.1 HUMAN K14 KERATIN PROMOTER DRIVES ARTEMIN TRANSGENE EXPRESSION IN THE SKIN AND TONGUE

The human K14 keratin promoter directed expression of artemin in basal keratinocytes of the epidermis and keratinized epithelium of the oral cavity (Figure 4A). K14 transgene expression begins at approximately embryonic day E11, continues into adulthood and has previously been shown to successfully express high levels of NGF, NT3, BDNF, NT4 and GDNF in the skin and oral cavity (Albers et al., 1994; Albers et al., 1996; Krimm et al., 2001; Zwick et al., 2002). Artemin transgene expression was confirmed using RT-PCR and an anti-artemin antibody. RT-PCR analysis showed a low level of artemin mRNA in skin from wildtype (WT) mice and an enhanced level in skin from artemin overexpresser (ART-OE) mice (Figure 4B). Immunoreactivity for artemin protein in the epithelium of WT skin and tongue was only slightly detectable but was significantly enhanced in the K14 keratin expressing keratinocytes of the ART-OE mouse (Figure 4C & 4D).

3.2 ARTEMIN OVEREXPRESSION INCREASES NEURON NUMBER IN SENSORY GANGLIA

On gross examination, both DRG and TG were enlarged in the ART-OE mice (Figure 5A), suggesting that artemin could be a neuronal survival factor. Artemin protein is retrogradely

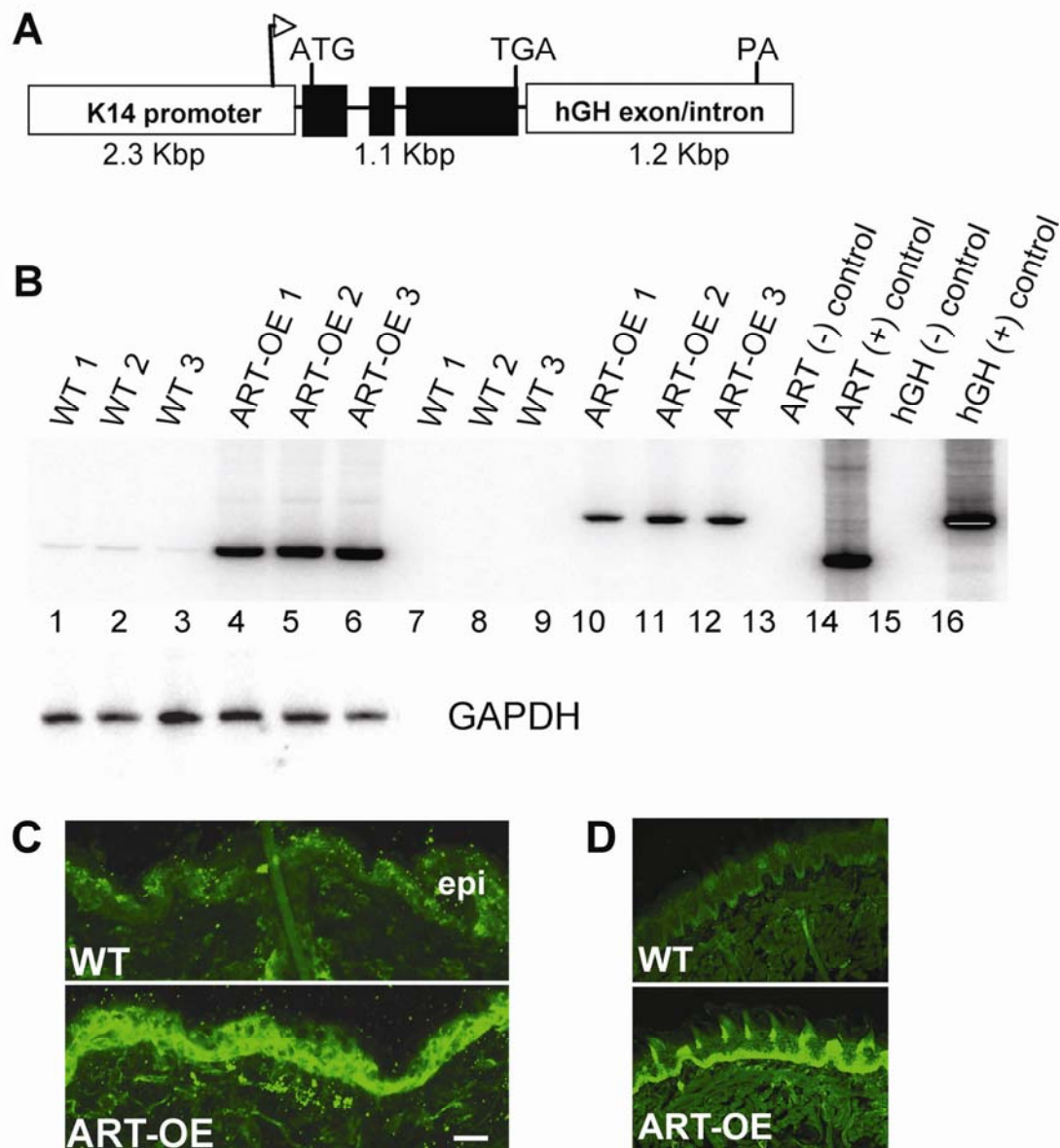


Figure 4. K14 keratin promoter drives artemin transgene expression in skin and tongue keratinocytes.

A) Diagram of transgene construct used for isolation of artemin overexpressor (ART-OE) mice. The keratin K14 promoter drives expression of the artemin sequence represented by black boxes. Lines connecting the boxes indicate two intronic sequences retained in the artemin sequence. The 3' hGH sequence provides splice sites and a poly A (PA) addition signal. Arrow indicates transcription start site, ATG and TGA are translation start and stop sites, respectively. **B)** RT-PCR analysis of RNA isolated from wildtype (WT, n=3) and transgenic (ART-OE, n=3) back skin showing increased expression of artemin mRNA in ART-OE skin. Lanes 1-6 show amplicons obtained using primers to the artemin gene sequence; lanes 7-12 show products using transgene specific PCR primers; lanes 13 and 15 are negative controls for the PCR reaction and lanes 14 and 16 are positive controls for the artemin and transgene sequences, respectively. Note significant enhancement in level of artemin mRNA and lack of transgene expression in transgenic skin samples. **C)** Immunolabeling of whisker pad skin from WT (top panel) and ART-OE (bottom) mice using an antibody to artemin. Artemin protein is significantly increased in basal keratinocytes of ART-OE mice. Bar in lower panel, 25Mm. **D)** Immunolabeling for artemin in tongue epithelium shows increased artemin expression in the keratinized epithelium of the ART-OE tongue (bottom panel) compared to WT tongue (upper panel).

transported from the skin and tongue to DRG and TG neurons as indicated by increased artemin immunoreactivity in the ART-OE ganglia (Figure 5B). Increased artemin protein produced a modest increase (20.5%) in cell number in the ART-OE mouse (DRG: WT 4800 ± 238 ; ART-OE 5788 ± 250 ; $p < 0.011$) (Figure 5C). These results support a role for artemin as a developmental survival factor for a subpopulation of sensory neurons.

3.3 ARTEMIN OVEREXPRESSION MODULATES GFRA3 EXPRESSION

Sensory ganglia were labeled with an anti-GFR α 3 antibody to determine if properties of GFR α 3-positive neurons changed in response to the increase in skin-derived artemin. The percent of GFR α 3-positive neurons was unchanged in ART-OE DRG (WT 19.64 ± 0.57 %; ART-OE 18.07 ± 1.47 %), but cell diameter measures showed these neurons to be hypertrophied (WT 20.03 ± 0.67 μ m; ART-OE 26.09 ± 0.99 μ m; $p < 0.05$) (Fig. 6A, D). GFR α 3 expression was also examined on the transcriptional level by assaying the relative abundance of GFR α 3 mRNA in WT and ART-OE ganglia (Table 2). Real time PCR analysis of lumbar DRG and TG showed GFR α 3 mRNA increased by 34% and 81% in the DRG and TG, respectively, of ART-OE animals ($p \leq 0.005$). Since the percent of GFR α 3-positive neurons was unchanged, this increase in GFR α 3 mRNA suggests its expression was elevated on a per cell level. Interestingly, transcripts encoding tyrosine kinases Ret and TrkA, which are coexpressed in ~80% of GFR α 3-positive neurons (Orozco et al., 2001), were differentially regulated in ART-OE ganglia (Table 2). Relative to WT ganglia, Ret transcript level was unchanged whereas TrkA mRNA levels were increased 37% and 56% in DRG and TG, respectively ($p < 0.005$).

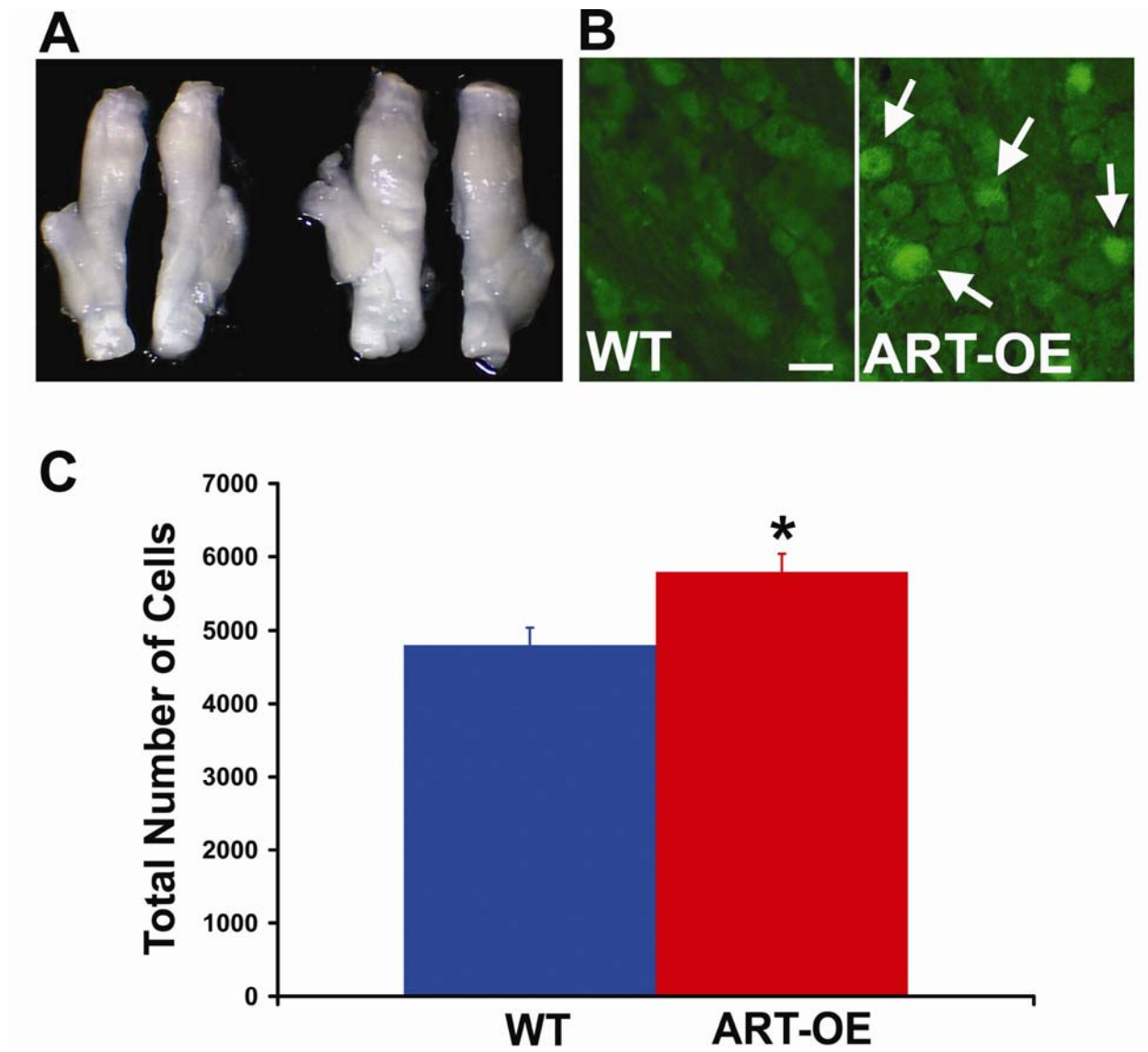


Figure 5. Artemin overexpression in the skin increases sensory ganglia size and neuronal number.
 A) Ganglia from ART-OE mice are larger relative to WT ganglia. DRG showed a similar enlargement (not shown).
 B) Artemin is retrogradely transported from the skin as indicated by artemin-immunoreactivity in trigeminal ganglia neurons of ART-OE (arrows) but not WT mice. C) Total cell counts showed that there was a modest increase in cell number (20.5%) in the L4 DRG from ART-OE mice. WT; n=3; ART-OE; n=4. Mean ± SEM, $P < 0.05$ vs. WT.

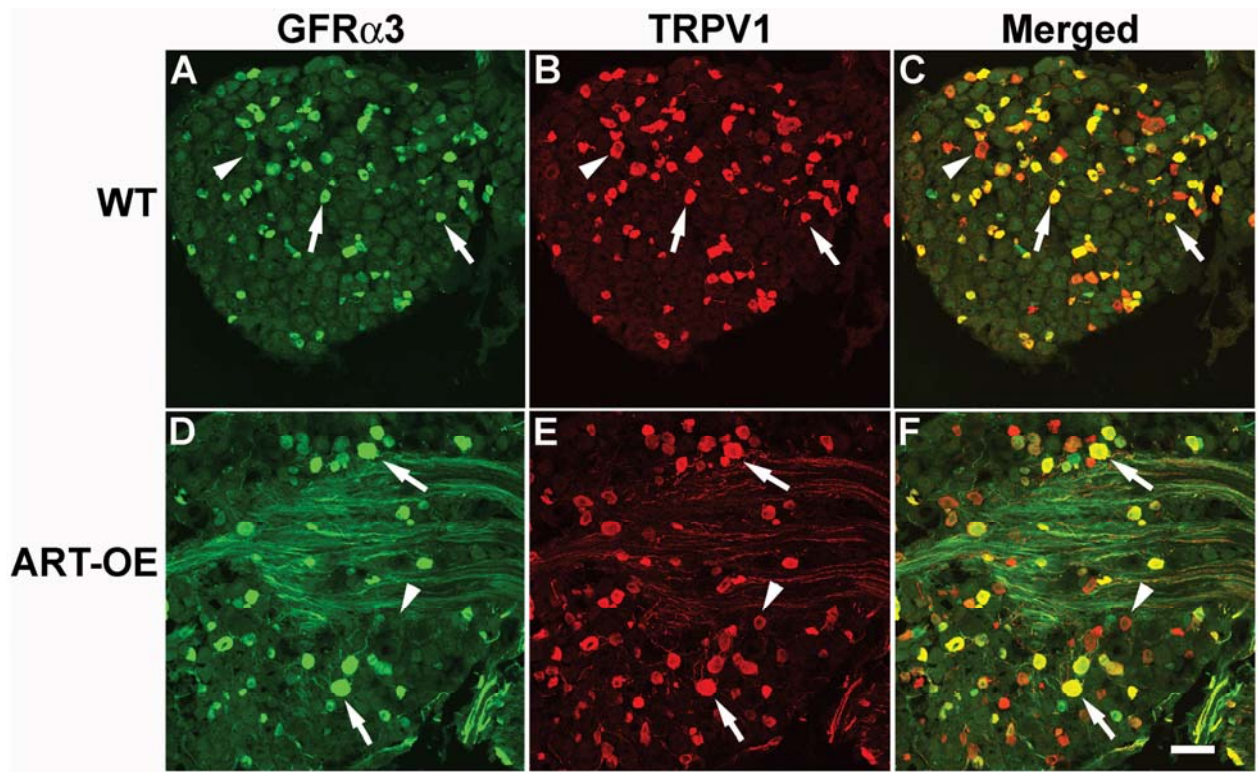


Figure 6. Sensory neurons responsive to artemin are hypertrophied and express TRPV1.

A) GFR α 3 immunolabeling (green) of WT (A, C) and ART-OE (D, F) DRG show GFR α 3-positive neurons are larger in size. Nearly all GFR α 3 neurons in WT (B) and ART-OE (E) ganglia express TRPV1 (red; arrows) though several TRPV1-labeled neurons do not express GFR α 3 (arrowheads; see merged images of WT (C) and ART-OE (F) ganglia). Trigeminal neurons showed a similar hypertrophy in TRPV1/GFR α 3 neuron size. Bar in C = 60 μ m and applies to all panels.

Gene Assayed	DRG Percent Change	TG Percent Change
GFR α 3	+34%*	+81%*
Ret	+6%	+1%
TrkA	+37%*	+56%*
TRPV1	+61%**	+190%**
TRPV2	+6%	+7%
TRPV3	-28%	+23%
TRPV4	+8%	+5%
TRPA1	+210%**	+403%**
TRPM8	not assessed	-70%*

Table 2. Change in expression of receptor and TRP channel genes in lumbar DRG (L3, L4 and L5) and TG of WT and ART-OE mice.

RT-PCR assays using RNA from DRG and TG were performed using 4-6 animals per group. **P<0.0005, *P<0.005.

3.4 ARTEMIN INCREASES TRPV1 MRNA IN SENSORY GANGLIA

Since all GFR α 3-positive afferents in mouse are also TRPV1-positive (Orozco et al., 2001), we tested whether transcriptional regulation of TRPV1 or other TRP channel genes was altered in ART-OE ganglia using SYBR RT-PCR (Table 2). TRPV1 transcript level was 61% and 190% higher in the DRG and TG of the ART-OE mice compared to WT mice. No change in TRPV2, TRPV3, or TRPV4 was observed.

3.5 ARTEMIN CAUSES HYPERTROPHY OF TRPV1-POSITIVE AFFERENTS

Immunolabeling of L4/L5 DRG with antibodies to TRPV1 and GFR α 3 (Figure 6B, 6E) showed most GFR α 3-positive neurons expressed TRPV1 in both WT ($94.25 \pm 0.88\%$) and ART-OE (96.55 ± 2.00) mice, although not all TRPV1 neurons were GFR α 3-positive (in either WT or ART-OE). The overall percentage of TRPV1 neurons in ART-OE mice was also unchanged compared to WT mice (WT $27.53 \pm 1.19 \%$; ART-OE $28.81 \pm 2.75 \%$). However, TRPV1 neurons in ART-OE ganglia showed hypertrophy in size (WT $20.42 \pm 3.90 \mu\text{M}$; ART-OE $24.43 \pm 1.39 \mu\text{M}$; $p < 0.05$) (Fig. 6B, E). Increases in somal size of GFR α 3/TRPV1-positive neurons were even larger in the TG of ART-OE mice compared to the differences observed between the WT and ART-OE DRG (see Figure 10 compared to Figure 6). These results in DRG and TG confirm that the GFR α 3/TRPV1 neuron population was responsive to artemin.

The increased diameter of TRPV1-positive neurons raised the possibility that increased levels of artemin alter peripheral projection patterns of GFR α 3-,TRPV1-positive neurons. Skin and tongue innervation were therefore examined by immunolabeling whisker pad, backskin, footpad skin and tongue epithelium. Using the general neuronal marker PGP-9.5, no major change in innervation density or projection pattern was found in the skin (not shown). Colabeling

of WT and ART-OE whisker pad and footpad skin using anti-GFR α 3 and anti-TRPV1 antibodies did, however, reveal a significant change in afferent innervation in ART-OE skin. Whisker pad (Figure 7, 8) and footpad skin (not shown) of ART-OE mice showed greater density of GFR α 3-labeled afferents compared to WT skin (compare Figure 7A and 7D; Fig. 8A and 8D). In addition, the number of TRPV1-positive afferents in ART-OE skin was significantly increased in dermal and epidermal compartments (compare Fig. 7B, 7E; Fig. 8B, 8E). In addition, the tongue epithelium showed increased PGP9.5 staining (Figure 9A) and increased GFR α 3-positive (and presumptive TRPV1-positive) fibers (Figure 9B). Thus, increased artemin in skin and tongue enhances projections of TRPV1- and GFR α 3-positive fibers. Whether this is due to an increase in the number of TRPV1/GFR α 3-positive afferents or increased branching of processes is unclear. However, the somal hypertrophy of these neurons and increase in TRPV1 and GFR α 3 mRNA expression is consistent with the presence and maintenance of more highly branched peripheral processes.

3.6 THE TRPA1 CHANNEL PROTEIN IS A MARKER FOR GFRA3 NEURONS AND IS MODULATED BY ARTEMIN LEVEL

In addition to TRPV1, increased skin expression of artemin led to enhanced expression of TRPA1, a channel protein reported to be activated by pungent compounds and noxious cold (Peier et al., 2002; Bandell et al., 2004; Bautista et al., 2005). TRPA1 mRNA was increased 210% in DRG and 403% in TG of ART-OE transgenic mice compared to WT (Table 2). In WT (Fig. 10A-10C) and ART-OE (Figure 10D-10F) TG and DRG (not shown) immunolabeled with antibodies to TRPA1 and GFR α 3, a large degree of overlap in TRPA1 and GFR α 3 expression occurred. Based on this overlap it appears that TRPA1 is expressed by nearly all sensory neurons that are GFR α 3-positive and therefore artemin-responsive and TRPV1-positive. In

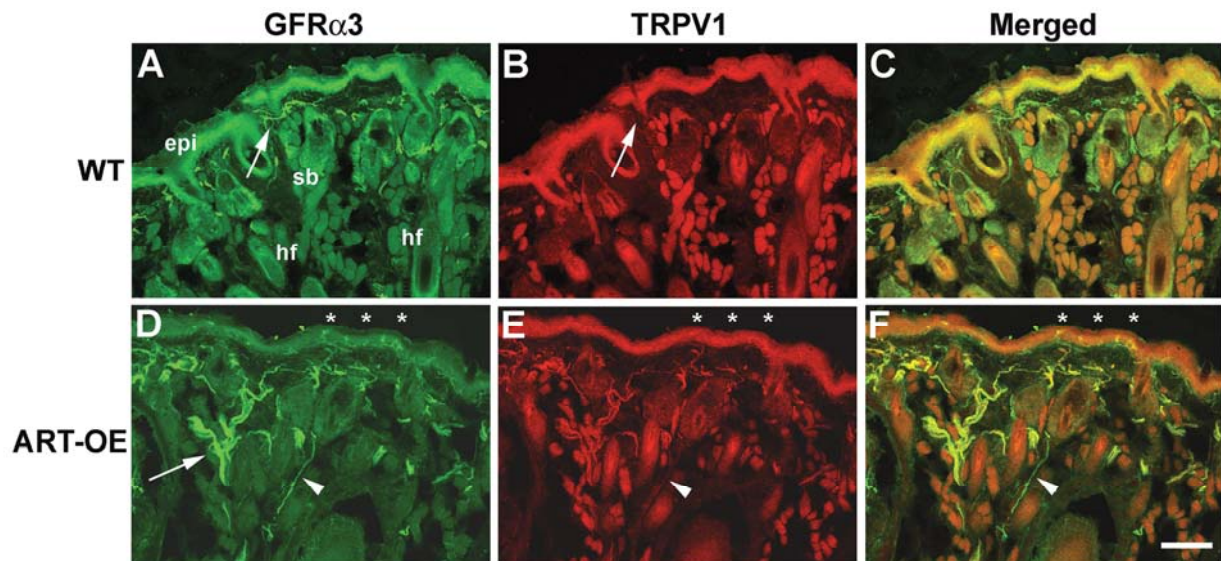


Figure 7. Skin-derived artemin increases cutaneous GFR α 3-positive afferents and intensity of TRPV1 labeling.

Low power view compares innervation of whisker pad skin of WT (A-C) and ART-OE (D-F) animals. An increase in GFR α 3-positive afferents (green, arrows) occurs in dermis of ART-OE skin. Immunolabeling with anti-TRPV1 (red, B, E) shows high expression in ART-OE afferents (E). Few TRPV1 fibers were seen in WT skin (B). TRPV1 labeling of GFR α 3 afferents of ART-OE skin was particularly evident in merged images (F) where overlap appears yellow. Overlap was rarely seen in WT skin (C). Asterisks (panels D, E and F) indicate appearance of GFR α 3 and TRPV1 afferents in epidermis of ART-OE skin (see Fig. 8). Arrowheads in D-F indicate a GFR α 3-positive fiber that is not TRPV1 positive and may represent sympathetic innervation. Bar in F = 100 μ m and applies to all panels. Epi, epidermis; sb, sebaceous gland; hf, hair follicle.

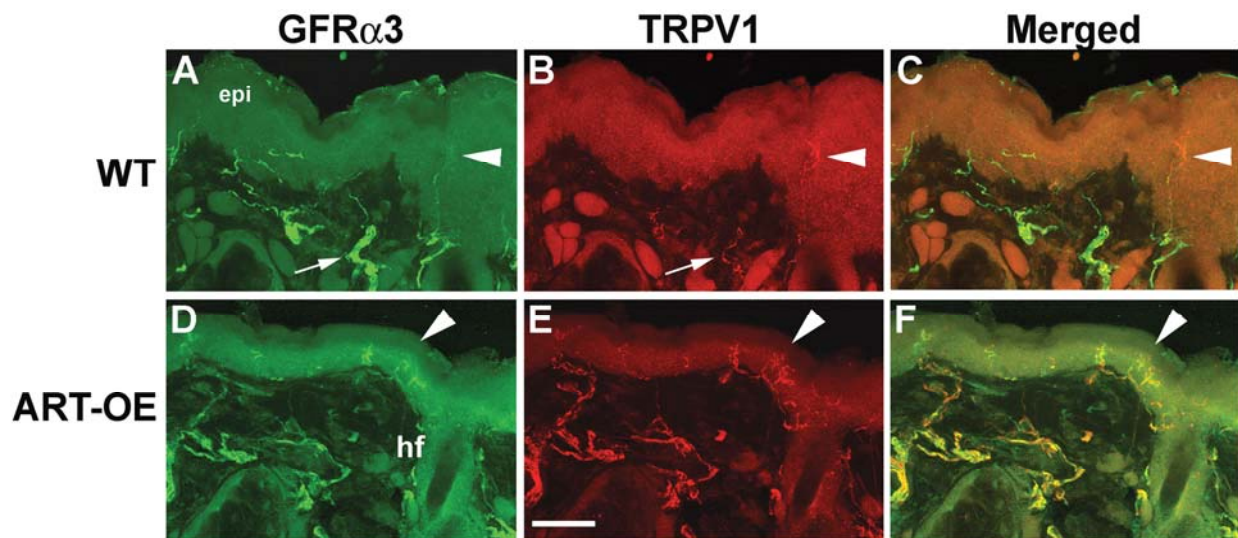


Figure 8. Artemin increases the intensity of TRPV1 expression in GFR α 3 epidermal afferents.

High magnification view of GFR α 3 (green, A,D) and TRPV1 (red, B,E) labeling in whisker pad epidermis of adult WT (A,B and C) and ART-OE (D,E and F) mice. In WT skin, few dermal (arrows) and epidermal (arrowheads) GFR α 3-positive fibers express TRPV1. In contrast, ART-OE skin has many TRPV1-positive fibers that appear to sprout in the epidermal layer (panels E, F). Bar in E = 40 μ m and applies to all panels. Epi, epidermis; hf, hair follicle.

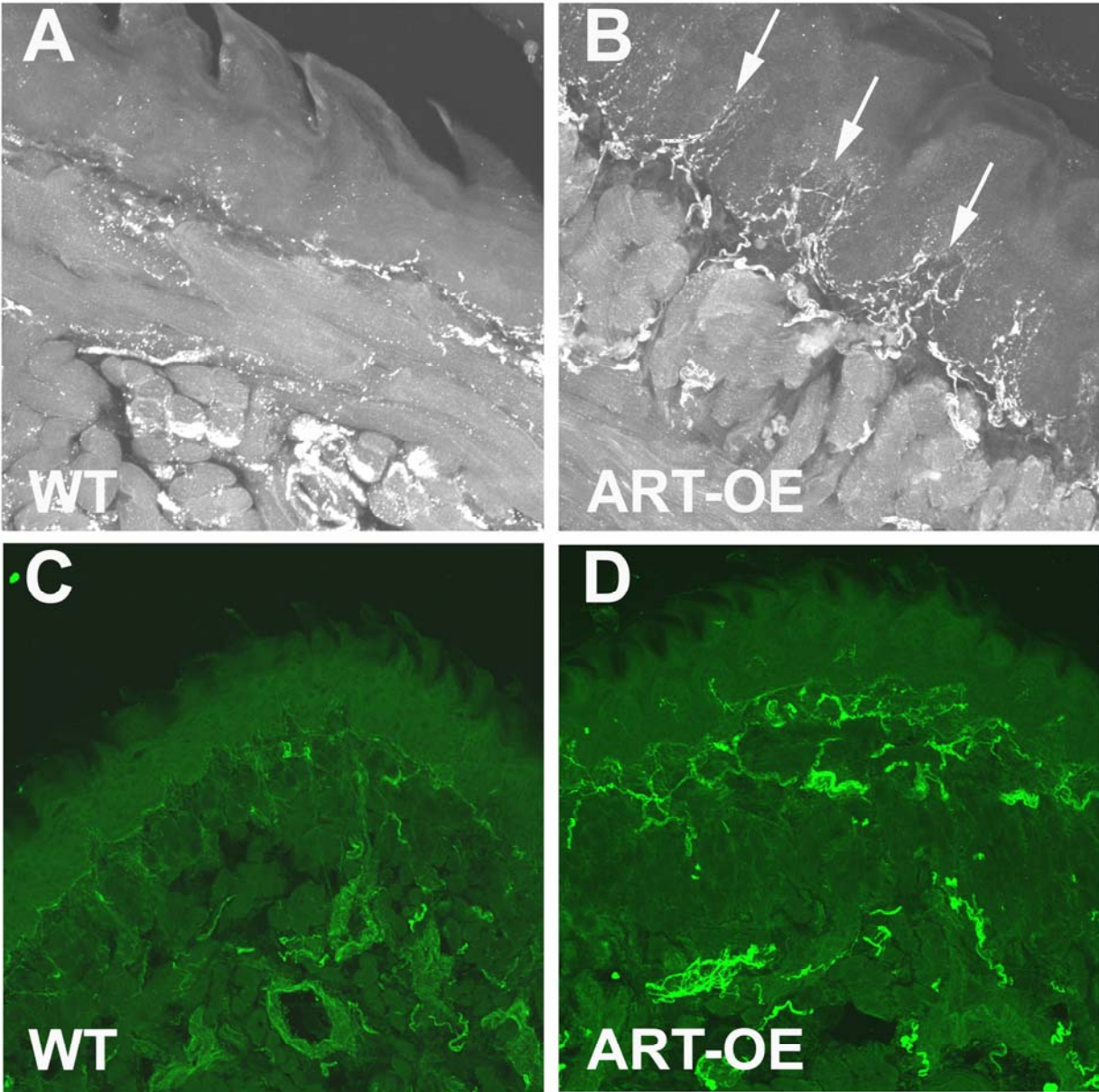


Figure 9. Tongue epithelium from ART-OE mice are hyperinnervated and have increased GFR α 3-positive fibers.

A & B) High magnification view (40X) of immunolabeling for the general neuronal marker PGP9.5. Tongue epithelium from ART-OE mice (B) is hyperinnervated by PGP9.5-positive fibers (arrows) compared to WT (A). C & D) Low magnification view (20X) of GFR α 3 immunolabeling in tongue. Tongue epithelium showed increased GFR α 3 staining in ART-OE (D) compared to WT (C) mice.

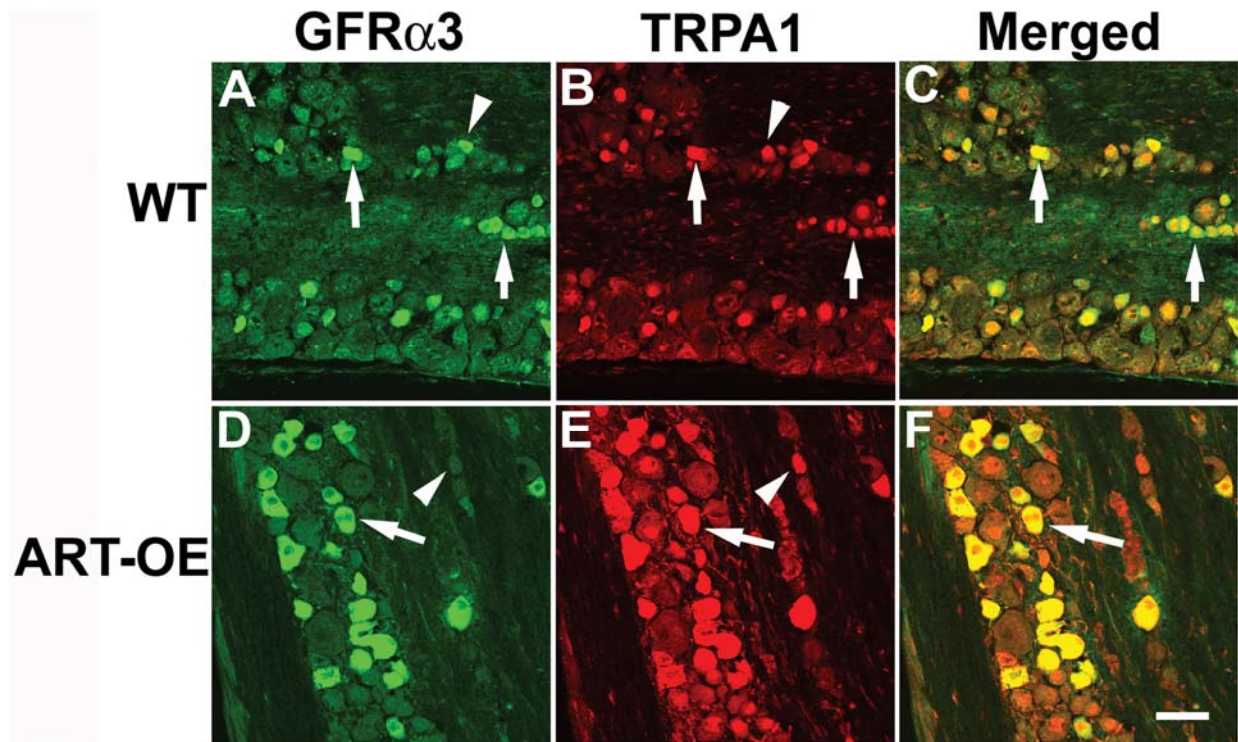


Figure 10. GFR α 3-positive afferents express the TRPA1 channel.

GFR α 3 immunolabeling (green) of WT (A, B, C) and ART-OE (D, E, F) trigeminal ganglia show GFR α 3-labeled neurons exhibit TRPA1 immunoreactivity (red). Complete overlap in labeling occurred in both WT and ART-OE ganglia. Similar overlap in GFR α 3 and TRPA1 labeling was found in the DRG. Bar in F = 70 μ m and applies to all panels.

addition, TRPA1 immunolabeling of neurons in transgenic ganglia appeared more intense, likely reflecting the increase in TRPA1 mRNA shown by RT-PCR assay (Table 2). TRPM8, a TRP channel proposed to detect innocuous cooling (McKemy et al., 2002; Peier et al., 2002), was also assayed and found to be reduced in the TG (-70%) of ART-OE mice ($p \leq 0.005$).

3.7 TONGUES OF ART-OE MICE ARE HYPERINNERVATED BY GFRA3, TRPV1 AND PRESUMPTIVE TRPA1-POSITIVE LINGUAL AFFERENTS.

Since the heavily keratinized tongue is a site that routinely contacts the proposed ligands for TRPV1 (capsaicin, heat, low pH) and TRPA1 (mustard oil, noxious cold), we hypothesized that at least a portion of the changes in TRPV1 and TRPA1 gene expression might occur in afferents innervating the tongue. To test this and to characterize the normal anatomy and neurochemistry of lingual afferents, we retrogradely-labeled the trigeminal neurons that innervate the tongue using WGA and then performed immunohistochemistry for GFR α 3, TRPV1, IB4, and CGRP (Figure 11A). Our results show that approximately 25% of lingual afferents in WT mice contain TRPV1 (Figure 11B), similar to the percentage in cutaneous afferents (Christianson et al., 2006). However, in contrast to cutaneous afferents, where the majority of afferents are IB4-positive, very few (10%) lingual afferents bind IB4 and many (50%) contain CGRP (Figure 11B). Nearly 25% of lingual afferents express GFR α 3 (Figure 11B) and nearly all contain CGRP (GFR α 3/CGRP overlap; WT $96.15 \pm 3.85\%$). These data suggest that lingual afferents may have properties somewhat different from cutaneous afferents.

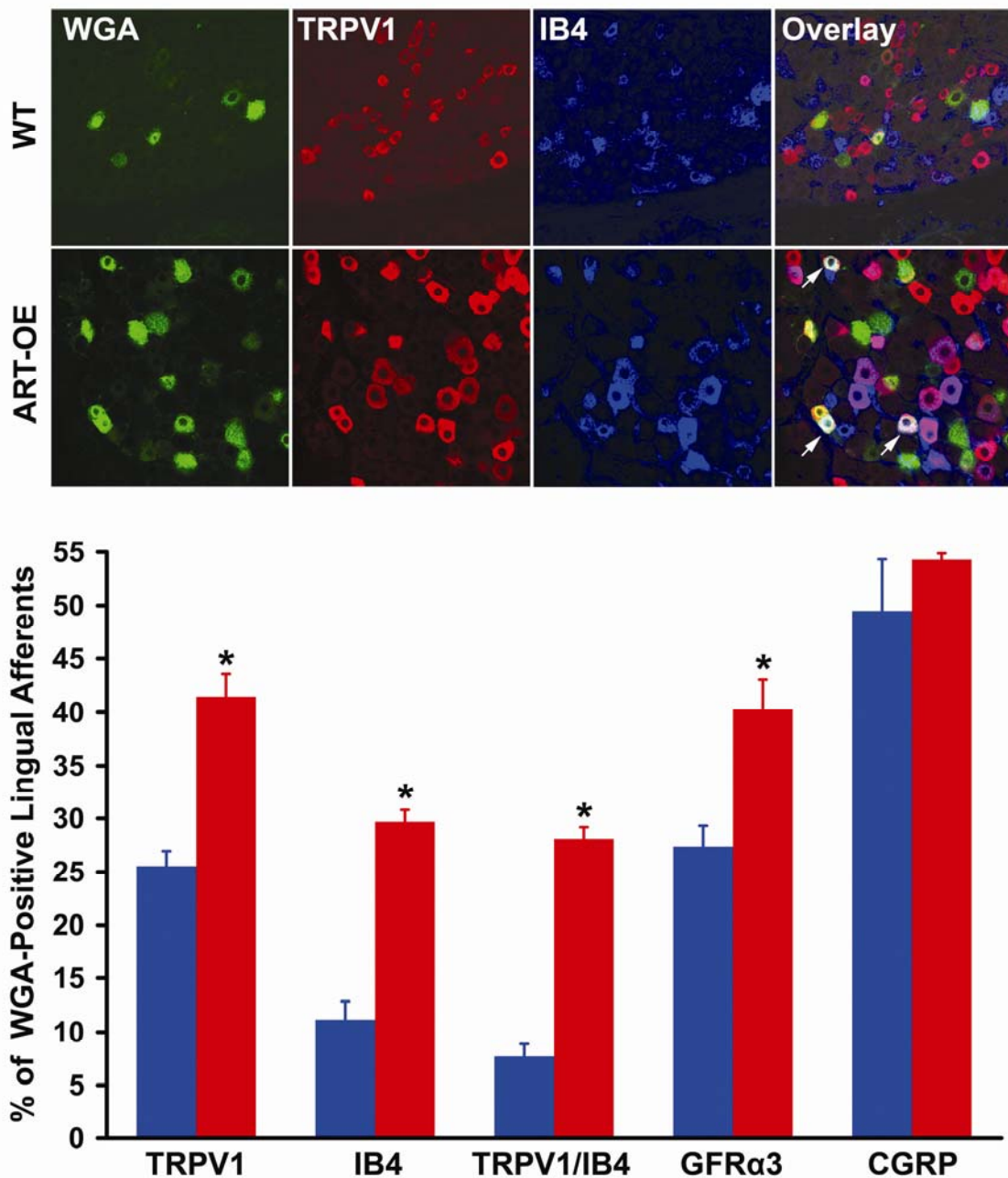


Figure 11. WGA-Positive Lingual Afferents from ART-OE mice have increased GFRα3, TRPV1 and IB4.

Upper Panel) Immunocytochemistry for TRPV1 (red), IB4 (blue) and TRPV1/IB4 overlap (white, merge) in WT and ART-OE mice. Note the increase in number of neurons expressing TRPV1 and IB4 in the ART-OE (arrows, merged panel, white) compared to the WT. Also note the somal hypertrophy in the ART-OE. Lower Panel) Quantification of the percentage of WGA-positive lingual afferents that also express GFRα3 and other neurochemical markers (TRPV1, IB4, CGRP). Note that in ART-OE mice (red bars) there is an increased percentage of WGA-positive neurons that also express GFRα3, TRPV1, IB4, or both TRPV1 and IB4 compared to WT mice (blue bars). However, there was no change in number of WGA-positive neurons that express CGRP in the ART-OE. Mean Percentage ± SEM. Analysis represents at least 4 WT and 4 ART-OE mice for all neurochemical markers, except CGRP where 3 animals from each genotype were quantified. P<0.05 vs. WT.

In the ART-OE mice, there was an increased number of WGA-positive afferents that were also GFR α 3-positive (WT 27.40 \pm 1.92 %; ART-OE 40.32 \pm 2.77 %; $p \leq 0.005$), TRPV1-positive (WT 25.55 \pm 1.42 %; ART-OE 41.49 \pm 2.14 %; $p \leq 0.005$), IB4-positive (WT 11.16 \pm 1.70 %; ART-OE 29.69 \pm 1.13 %; $p \leq 0.005$), or both TRPV1 and IB4-positive (WT 7.70 \pm 1.70 %; ART-OE 28.12 \pm 1.05 %; $p \leq 0.005$) (Figure 11B). There was no change in the number of CGRP-positive (WT 49.48 \pm 4.84 %; ART-OE 54.28 \pm 0.59 %; $p = 0.21$) or CGRP and GFR α 3-positive afferents (WT 96.15 \pm 3.85 %; ART-OE 97.74 \pm 0.37 %; $p = 0.36$) in the ART-OE mice compared to WT mice (Figure 11B). Since most GFR α 3-positive afferents are also TRPA1-positive (Figure 10, above), these results support the hypothesis that the tongue epithelium of ART-OE mice is hyperinnervated by GFR α 3, TRPV1 and presumptive TRPA1-positive lingual nerve fibers.

3.8 LINGUAL NERVES FROM ART-OE MICE ARE HYPERTROPHIED

To examine the fiber diameter and myelination state in lingual afferents, electron microscopy was performed. Low power electron microscopy photomicrographs showed that lingual nerves from ART-OE mice were enlarged (Figure 12A). Lingual nerves from both WT and ART-OE mice contained mostly myelinated fibers and there was not a significant difference in the percentage of myelinated (WT: 70%; ART-OE; 70%) or unmyelinated fibers in WT or ART-OE mice (Figure 12B). However, in the ART-OE mice, both myelinated and unmyelinated fibers were hypertrophied (Figure 12C).

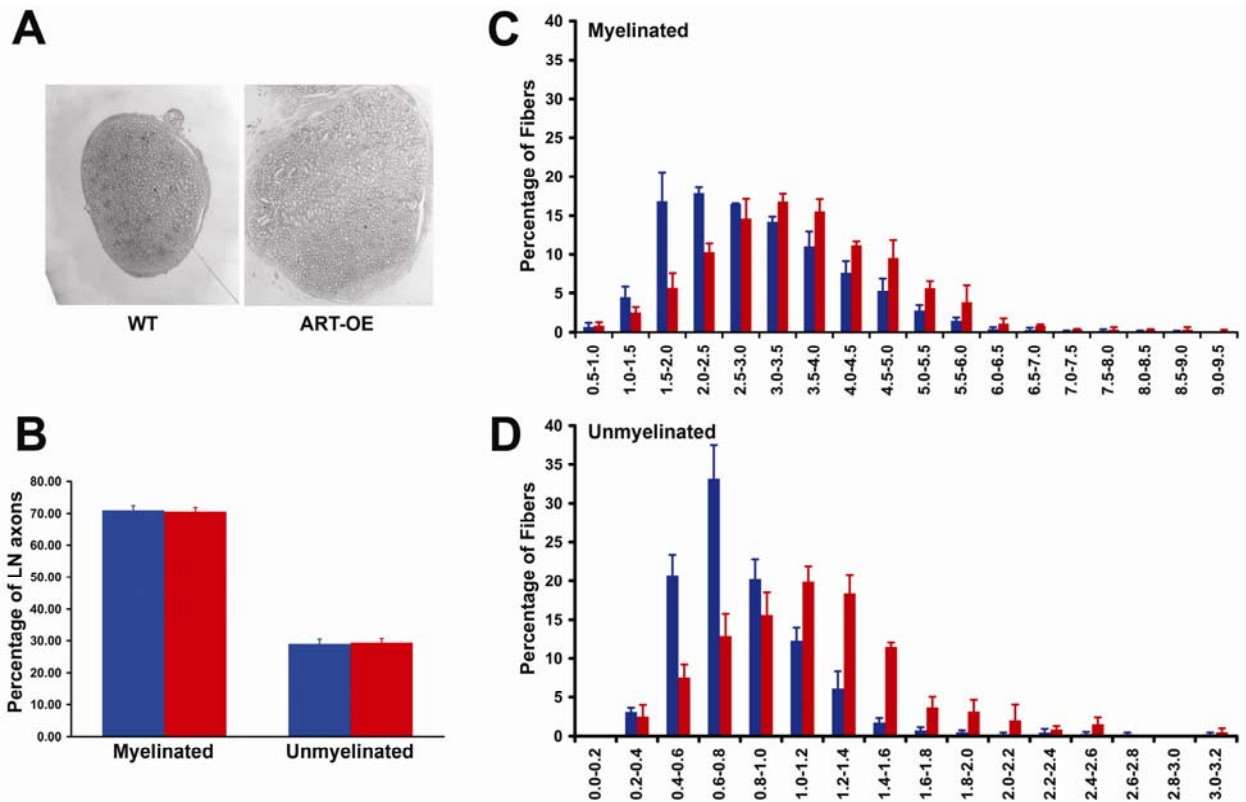


Figure 12. Lingual Nerves from ART-OE mice are hypertrophied.

A) Low magnification electron microscopy images of lingual nerve cross sections from WT (left) and ART-OE (right) mice. Note the overall enlargement in lingual nerve diameter in the ART-OE mouse. B) Quantification of the percentage of myelinated and unmyelinated axons in the lingual nerve of WT (blue) and ART-OE (red) mice. The majority of axons in both genotypes are myelinated and there was no difference in the percentage of myelinated or unmyelinated fibers in WT (n=3) compared to ART-OE mice (n=3). C) Distribution of myelinated axons by size (microns) in WT and ART-OE mice. There was a small amount of hypertrophy in myelinated axons from ART-OE mice (note rightward shift of distribution). D) Size distribution of unmyelinated axons in WT and ART-OE mice. There was a substantial rightward shift in the distribution, indicating that unmyelinated axons from the ART-OE were particularly hypertrophied.

4.0 BEHAVIOR RESULTS

To determine the functional significance of the anatomical, neurochemical and gene expression changes in the ART-OE mice, we performed a battery of behavioral experiments on WT and ART-OE mice. Because of the increased TRPV1 and TRPA1 expression in the DRG, we assessed cutaneous sensitivity to noxious heat using a radiant heat source (Hargreave's) and sensitivity to noxious cold using a cold tail flick assay, a cold ice-block test and a place preference test (where one side was cold). Mechanical sensitivity was also evaluated using von Frey filaments. Since both capsaicin and mustard oil elicit sensations of burning when applied or injected into the skin, we tested nocifensive responses to these chemicals and tested oral aversion to these ligands using a two-bottle drinking choice test. In addition, we tested thermal sensitivity to heat following capsaicin injection. Finally, to test responses to general inflammation, CFA was injected into the hindpaw of WT and ART-OE mice and thermal sensitivity to heat determined 1, 3, 5, and 7 days post-injection.

4.1 ART-OE MICE ARE HYPERSENSITIVE TO NOXIOUS HEAT

Mixed gender mice were tested for sensitivity to noxious heat using the Hargreave's test (Figure 13). ART-OE mice displayed shorter paw withdrawal latencies to radiant heat applied to the plantar surface of the hindpaw compared to WT mice (WT 8.05 ± 0.46 s; ART-OE 6.33 ± 0.27 s; $p \leq 0.005$) (Figure 13A). A separate group of mice divided by gender were also tested prior

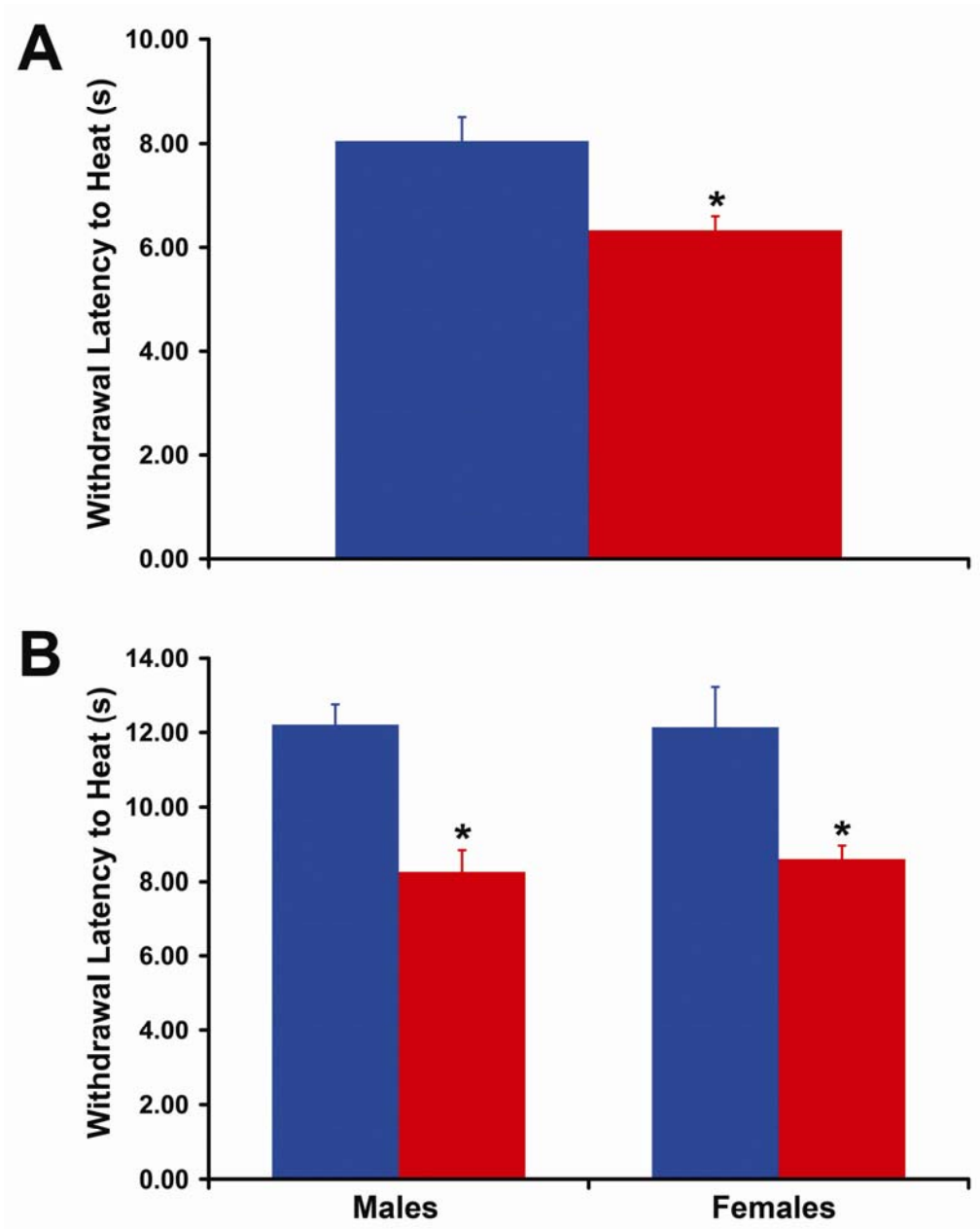


Figure 13. ART-OE mice are hypersensitive to noxious heat.

A) Animals were acclimated to the Hargreave's testing apparatus and a focused radiant heat source was applied to the glabrous skin of the hindpaw. Repeated measures of 8 WT (blue) and 8 ART-OE (red) mice showed faster withdrawal in ART-OE mice. B) In a separate study of 10 WT and 10 ART-OE mice of both genders (40 mice total) for baseline measurement prior to capsaicin injection (see Figure 19, day zero), hypersensitivity to noxious heat was also seen in male and female ART-OE mice compared to WT mice of the same gender. There were no differences in withdrawal threshold to heat between male mice and female mice of either genotype. Mean \pm SEM. * $P < 0.005$ vs WT.

to capsaicin injection (see baseline, Figure 20). A similar hypersensitivity to noxious heat was observed in the ART-OE mice in these experiments (Males: WT 12.21 ± 0.56 s; ART-OE 8.25 ± 0.58 s; $p \leq 0.0005$; Females: WT 12.14 ± 1.1 s; ART-OE 8.59 ± 0.36 s; $p \leq 0.005$) (Figure 13B). These data support an intrinsic role for artemin in regulating sensitivity to noxious heat.

4.2 ART-OE MICE ARE HYPERSENSITIVE TO NOXIOUS COLD STIMULI

Because of the robust increases in transcript levels of TRPA1 and the overlap of GFR α 3 expression with TRPA1 (see Figure 10), we tested sensitivity of WT and ART-OE mice to noxious cold stimuli. Two sets of mixed gender mice were tested for sensitivity to noxious cold by placing their tails in an ethanol bath set to either -15°C or 0°C and measuring latency to tail flick. Testing showed that ART-OE mice had significantly shorter response times compared to WT mice at both -15°C (WT 15.1 ± 2.8 s; ART-OE 5.2 ± 1.0 s; $p \leq 0.005$; $n=20$) and 0°C (WT 10.7 ± 1.7 s; ART-OE 5.2 ± 1.4 s; $p \leq 0.05$; $n=40$) (Figure 14A & 14B).

Sensitivity to noxious cold was also tested by placing mice on a block of ice and measuring the latency to the first nocifensive event and the number of nocifensive events displayed in 1 minute. In these studies mice were separated by gender. This test of noxious cold applied to the plantar surface of the hindpaw also showed that ART-OE mice were hypersensitive to cold (Figure 15). Both male and female ART-OE had shorter latencies to first nocifensive behavior (Males: WT 28.20 ± 2.95 ; ART-OE 16.00 ± 1.25 ; $p \leq 0.005$; Females: WT 20.30 ± 1.47 ; ART-OE 12.30 ± 1.09 ; $p \leq 0.0005$) (Figure 15A). In addition, both male and female ART-OE mice displayed more nocifensive events than WT mice (Males: WT 7 ± 1 ; ART-OE 13 ± 2 ; $p \leq 0.005$; Females: WT 9 ± 1 ; ART-OE 17 ± 1 ; $p \leq 0.0005$) (Figure 15B). Furthermore, the female WT and ART-OE mice displayed shorter latencies to first response compared to WT male and ART-OE male mice, respectively ($p \leq 0.05$). The female ART-OE mice also showed a

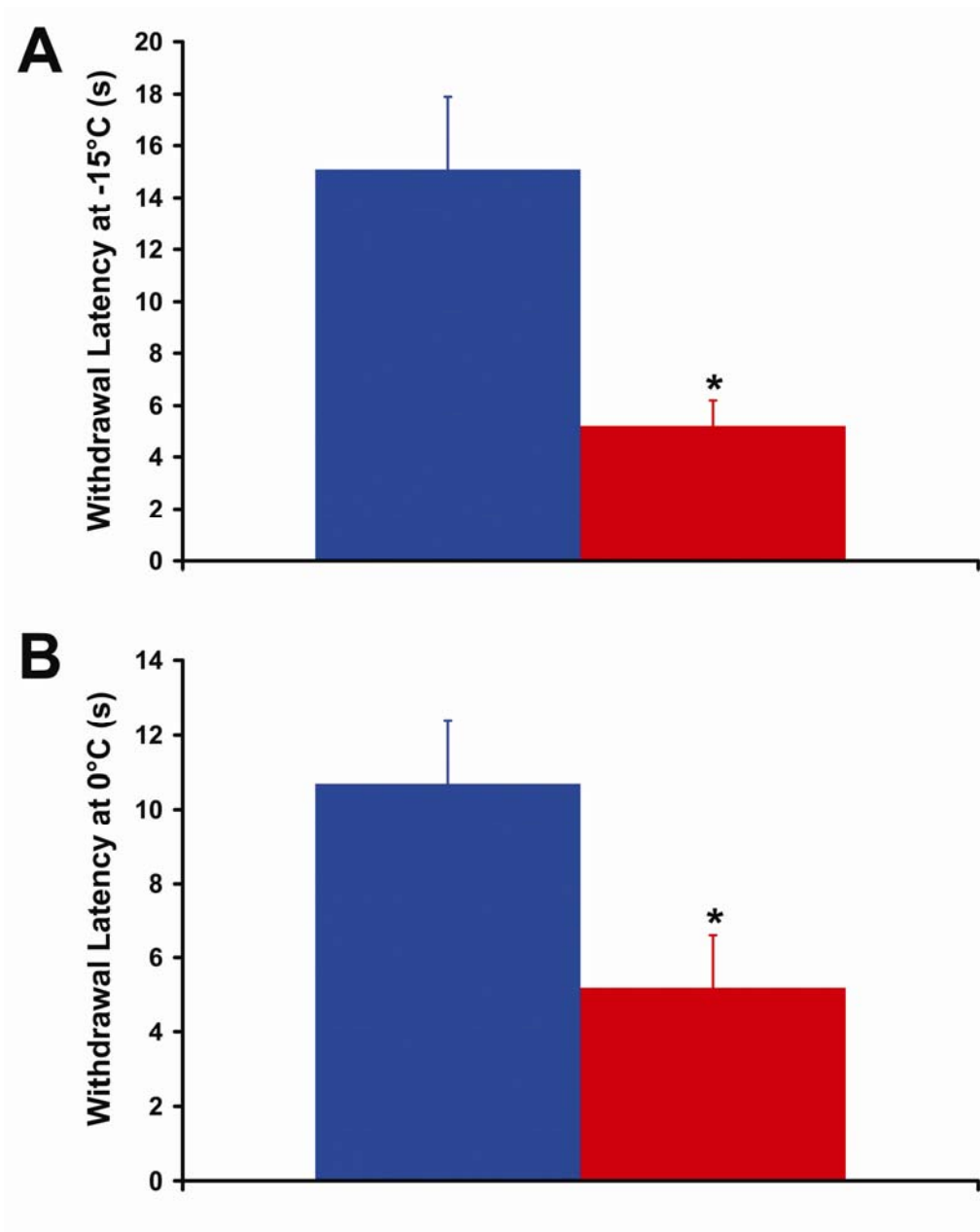


Figure 14. ART-OE mice display hypersensitivity to cold in tail flick assays.

Response to cold was tested by tail immersion in an ethanol bath set to either -15°C (A) or 0°C (B) using two sets of 10 WT (blue) and 10 ART-OE (red) mice of mixed gender (40 mice total). Tail flick response was measured to 0.1 s with a stopwatch. ART-OE mice exhibited lower thresholds than WT mice at both -15°C (A) and 0°C (B). Mean \pm SEM. *P<0.05 vs WT.

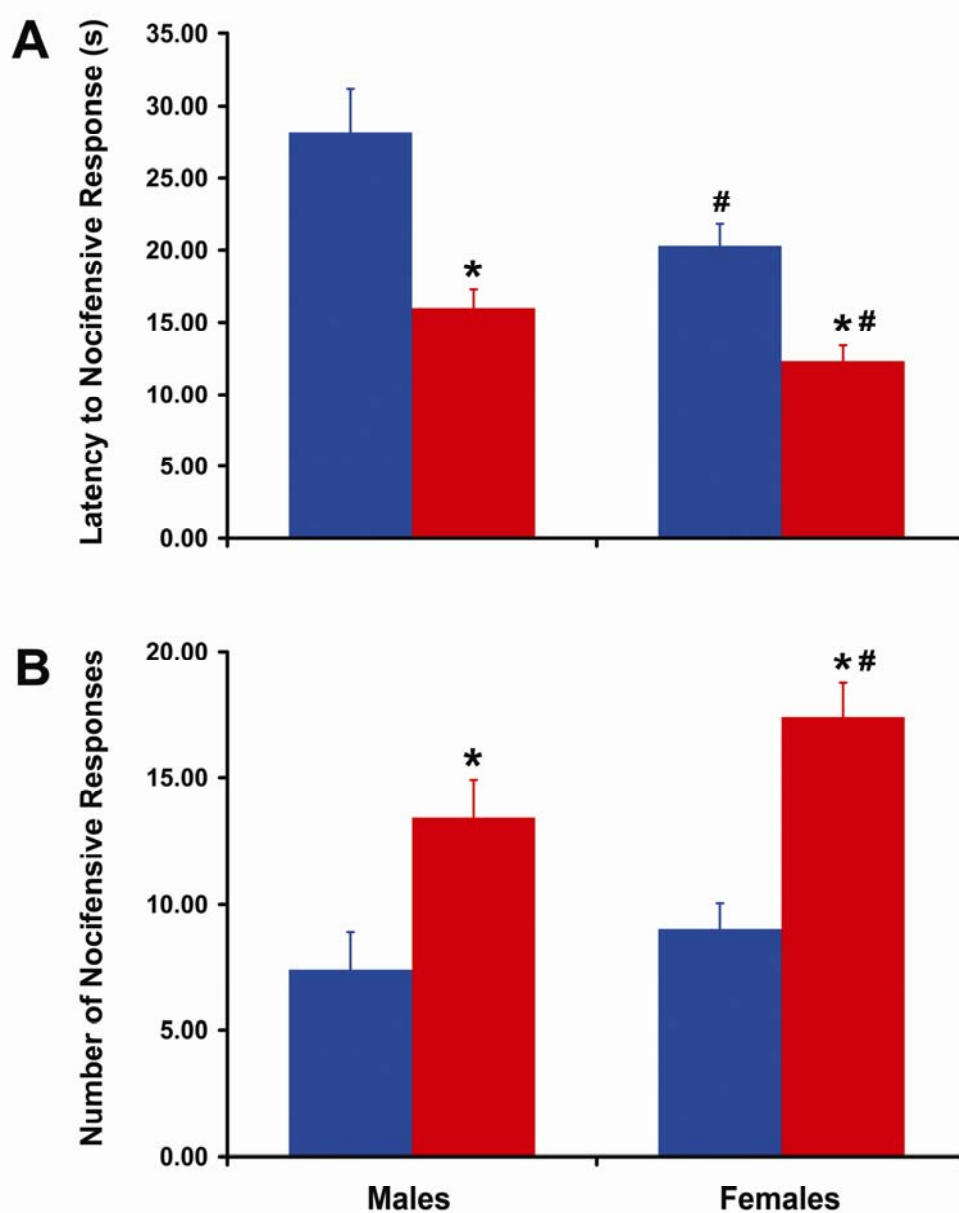


Figure 15. ART-OE mice display behavioral hypersensitivity to noxious cold (-10°C).

Ten WT (blue) and 10 ART-OE mice (red) of both genders (40 mice total) were tested for sensitivity to noxious cold by placing each mouse on a block of ice covered by a plexiglass box for 1 min. A) Latency to first nocifensive response (jumping, paw lifting, paw biting) was recorded to the nearest second using a stopwatch. Both male (left) and female (right) ART-OE mice displayed shorter latencies to first nocifensive response. In addition, female mice of both genotypes displayed shorter latencies to first nocifensive response. B) Number of nocifensive events measured during the 1 min testing period were increased in both male (right) and female (left) ART-OE mice, indicating that the ART-OE mice have increased sensitivity to the detection of noxious cold applied to the plantar hindpaw skin. In addition, female ART-OE mice displayed increased number of events compared to female WT mice. All values mean \pm SEM, * $P < 0.005$ vs WT, # $P < 0.0005$ vs females of same genotype.

greater number of nocifensive responses compared to female WT mice ($p \leq 0.05$). These results indicate that ART-OE mice display increased sensitivity to noxious cold applied to the hindpaw and that female mice are somewhat more sensitive to noxious cold than male mice in either genotype.

Finally, cold responses were evaluated using a place preference test where mice were given a choice between a surface area at room temperature and another surface at 5°C . This test is considerably different than the ice block and tail withdrawal tests as it requires exploration and a conscious decision to avoid the cold side. Both WT and ART-OE mice preferred the room temperature side. However, ART-OE mice of both genders spent even less time on the cold side than WT mice (Males: WT 18.13 ± 1.80 %; ART-OE 10.00 ± 1.58 %; $p \leq 0.005$; Females: WT 25.63 ± 3.56 %; ART-OE 14.07 ± 1.52 %; $p \leq 0.005$) (Figure 16). In addition, in this test both WT and ART-OE male mice spent less time on the cold side than females of the same genotype (Males: $p \leq 0.05$; Females: $p \leq 0.05$). Therefore, in this test male mice of both genotypes are more sensitive to choosing between a room temperature area and an area that is noxiously cold.

Taken together, these three cold behavioral tests indicate that ART-OE mice are hypersensitive to cold and, depending on the type of cold assay, cold responses vary with gender.

4.3 ART-OE MICE ARE NOT SENSITIZED TO MECHANICAL STIMULI

Mixed gender mice were tested for mechanical sensitivity using Von Frey filaments applied to the dorsal surface of the hindpaw. There was no difference in the mechanical thresholds between the WT and ART-OE mice (WT 5.27 ± 0.33 mN; ART-OE 5.14 ± 0.37 mN). In male mice tested for the number of responses to a 4.08 mN von Frey filament on the plantar surface of the hindpaw, there was also no change in mechanical sensitivity (WT 45 ± 6 %; ART-OE 45 ± 7 %; $n=10$).

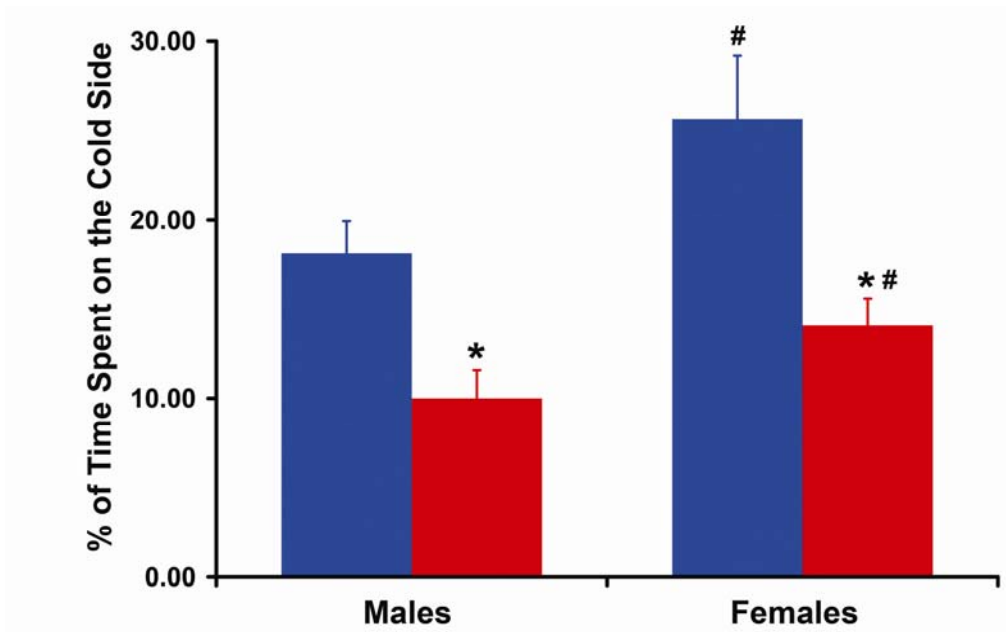


Figure 16. ART-OE mice are hypersensitive to noxious cold (4°C).

Ten WT (blue) and 10 ART-OE mice (red) of both genders (40 mice total) were tested for sensitivity to noxious cold using a place preference test. Mice were permitted to choose between a region where the floor was room temperature (22°C) and another region where the floor was noxiously cold (4°C). Both male (left) and female (right) ART-OE mice spent less time on the cold side than WT mice. In addition, both WT and ART-OE male mice spent less time on the cold side than females of the same genotype. All values mean ± SEM, *P<0.005 vs WT, #P<0.05 vs females of same genotype.

4.4 ART-OE MICE ARE HYPERSENSITIVE TO MUSTARD OIL APPLIED TO THE HINDPAW

Since mustard oil is a ligand for TRPA1, we assayed cutaneous sensitivity to topical application of mustard oil. Following application of mustard oil to the plantar surface of the hindpaw, both male and female ART-OE mice displayed more nocifensive events than WT mice (Males: ART-OE 59 ± 6 ; WT 20 ± 2 ; $p \leq 0.000005$; Females: ART-OE 36 ± 4 ; WT 18 ± 3 ; $p \leq 0.005$) (Figure 17A). In addition, the duration of nocifensive behavior was increased in the ART-OE mice compared to WT mice (Males: ART-OE 270 ± 26 s; WT 97 ± 3 s; $p \leq 0.000005$; Females: ART-OE 147 ± 12 s; WT 78 ± 7 s; $p \leq 0.0005$) (figure 17B). Paw edema (calculated as percentage edema relative to the unpainted paw) was increased in both male and female ART-OE mice compared to WT mice (Males: ART-OE 38 ± 3 %; WT 11 ± 2 %; $p \leq 0.000005$; Females: ART-OE 18 ± 2 %; WT 2 ± 1 %; $p \leq 0.00005$) (Figure 17C). In addition, the duration of nocifensive behavior was increased in male WT and male ART-OE mice compared to females of the same genotype (Males: $p \leq 0.05$; Females: $p \leq 0.0005$), suggesting that male mice are particularly sensitive (or female mice insensitive) to mustard oil application. This gender difference was also reflected in the percentage of edema which was increased in the male compared to female mice in both genotypes (Males: $p \leq 0.005$; Females: $p \leq 0.0005$).

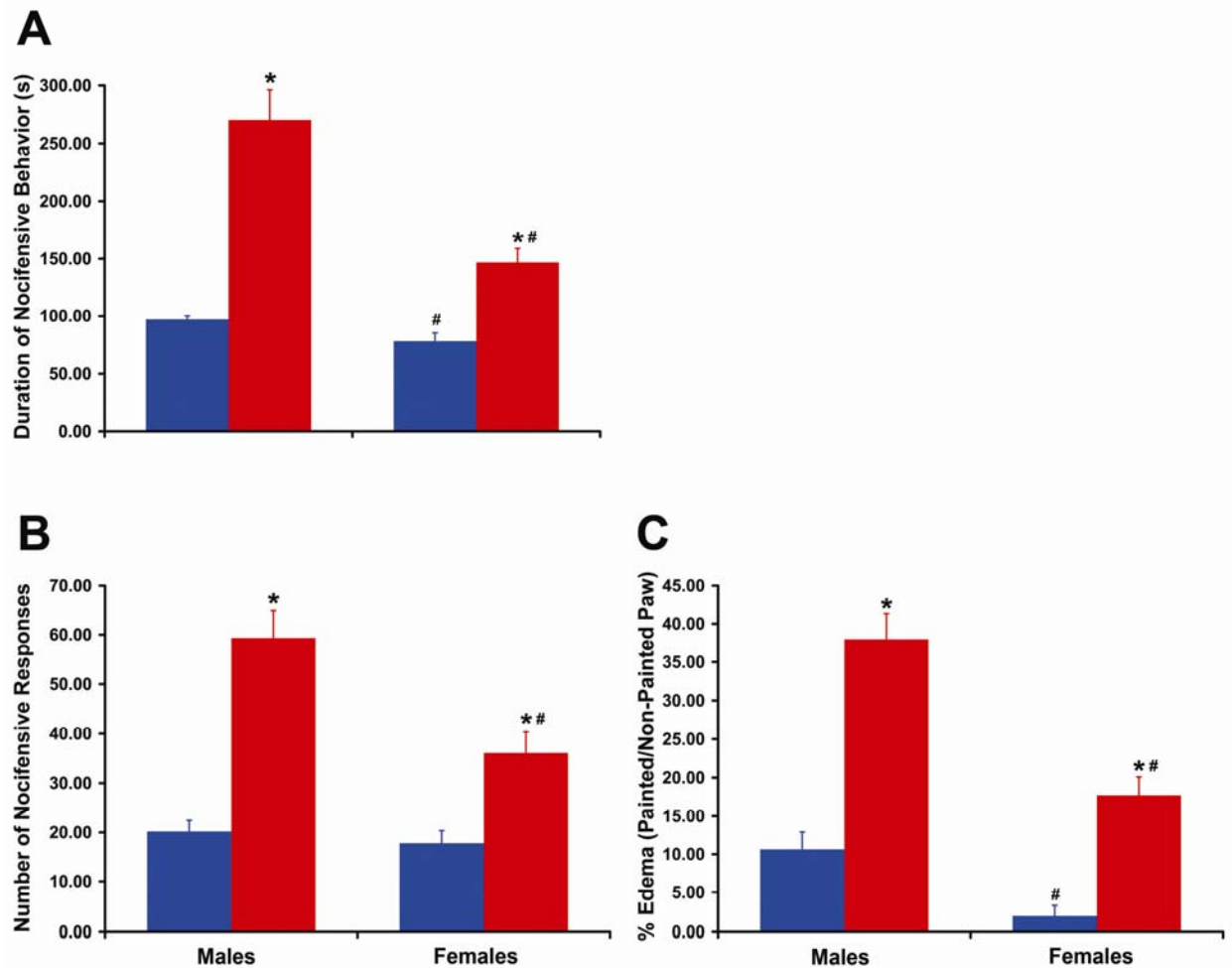


Figure 17. ART-OE mice are hypersensitive to mustard oil.

Ten WT (blue) and 10 ART-OE mice (red) of both genders (40 mice total) were tested for behavioral sensitivity to topical application of 10% mustard oil to the hindpaw. The duration of nocifensive behavior and the number of nocifensive responses in the five minute testing period were recorded. In addition, paw edema was measured at the end of the study in the painted and unpainted paw and percent edema calculated as the ratio of the painted paw/unpainted paw. Both male (left) and female (right) ART-OE mice displayed increased duration of nocifensive behavior (A), increased number of nocifensive responses (B) and increased edema (C) compared to WT mice. In addition male mice of both genotypes displayed increased nocifensive behavior (A) and had increased edema (C) compared to female mice of the same genotype, suggesting that male mice are particularly sensitive to mustard oil application. All values mean \pm SEM, * $P < 0.005$ vs WT, # $P < 0.05$ vs females of same genotype.

4.5 ART-OE MICE ARE HYPERSENSITIVE TO CAPSAICIN INJECTED INTO THE HINDPAW

Nocifensive behavior and thermal sensitivity to noxious heat were assayed following injection of the TRPV1 agonist, capsaicin, into the mouse hindpaw. ART-OE mice of both genders display increased duration of nocifensive behavior (Males: WT 98 ± 20 ; ART-OE 218 ± 25 ; $p \leq 0.005$; Females: WT 98 ± 28 ; ART-OE 254 ± 19 ; $p \leq 0.0005$) (Figure 18A) and the number of nocifensive responses (Males: WT 23 ± 7 ; ART-OE 60 ± 10 ; $p \leq 0.005$; Females: WT 20 ± 7 , ART-OE 61 ± 9 ; $p \leq 0.005$) (Figure 18B). There were no differences between genders of the same genotype.

Mice were also tested for sensitivity to heat following capsaicin injection because TRPV1 also responds to heat, particularly during inflammatory conditions. Compared to baseline thermal sensitivity to noxious heat, both WT and ART-OE became sensitized following capsaicin injection ($P \leq 0.05$). However, both male and female ART-OE mice had decreased withdrawal latencies compared to WT mice of the same gender at 10 min (Males: WT 4.94 ± 0.97 ; ART-OE 2.96 ± 0.39 ; $p \leq 0.05$; Females: WT 4.83 ± 0.83 ; ART-OE 2.82 ± 0.48 ; $p \leq 0.05$), at 30min (Males: WT 7.91 ± 0.99 ; ART-OE 4.98 ± 0.85 ; $p \leq 0.05$; Females: WT 4.22 ± 0.65 ; ART-OE 6.14 ± 0.83 ; $p \leq 0.05$) and at 60 min post capsaicin injection (Males: WT 14.91 ± 1.99 ; ART-OE 6.61 ± 0.63 ; $p \leq 0.0005$; Females: WT 10.47 ± 0.24 ; ART-OE 6.69 ± 0.64 ; $p \leq 0.0005$) (Figure 19). These results suggest that the ART-OE mice were still able to become sensitized to heat despite starting at a sensitized baseline relative to WT mice. Also, note that the slope of the curves is similar for WT and ART-OE male mice except that the ART-OE recovered more slowly than the WT mice (Figure 19A). The ART-OE females also displayed this slower recovery and became transiently hypoalgesic relative to WT mice at 30 min (Figure 19B).

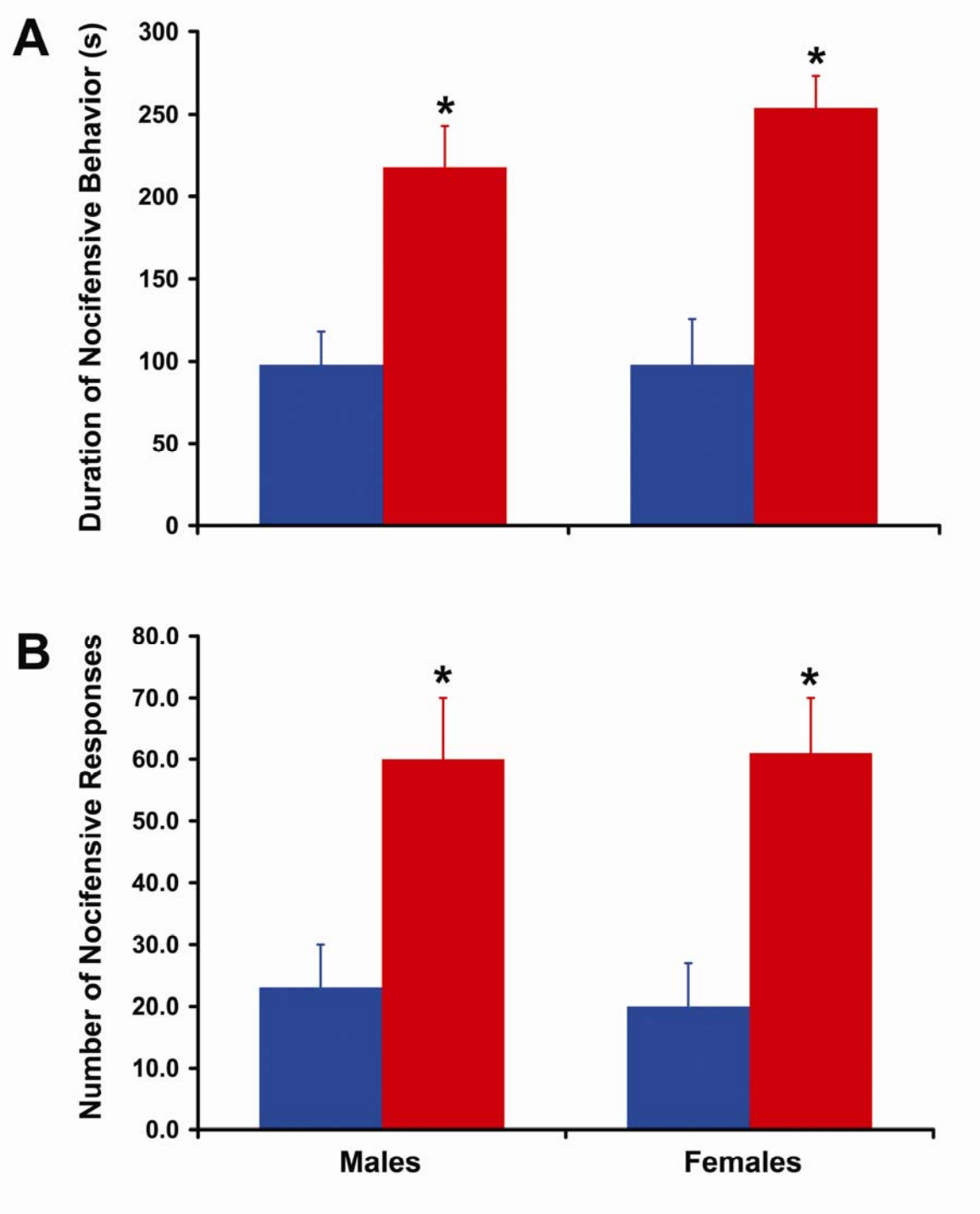


Figure 18. ART-OE mice are hypersensitive to capsaicin injected into the hindpaw.

Ten WT (blue) and 10 ART-OE mice (red) of both genders (40 mice total) were tested for behavioral sensitivity to capsaicin injected into the hindpaw. The duration of nocifensive behavior and the number of nocifensive responses in the five minute testing period were recorded. Both male (left) and female (right) ART-OE mice displayed increased duration of nocifensive behavior (A) and increased number of nocifensive responses (B) compared to WT mice. All values mean \pm SEM, *P<0.005 vs WT.

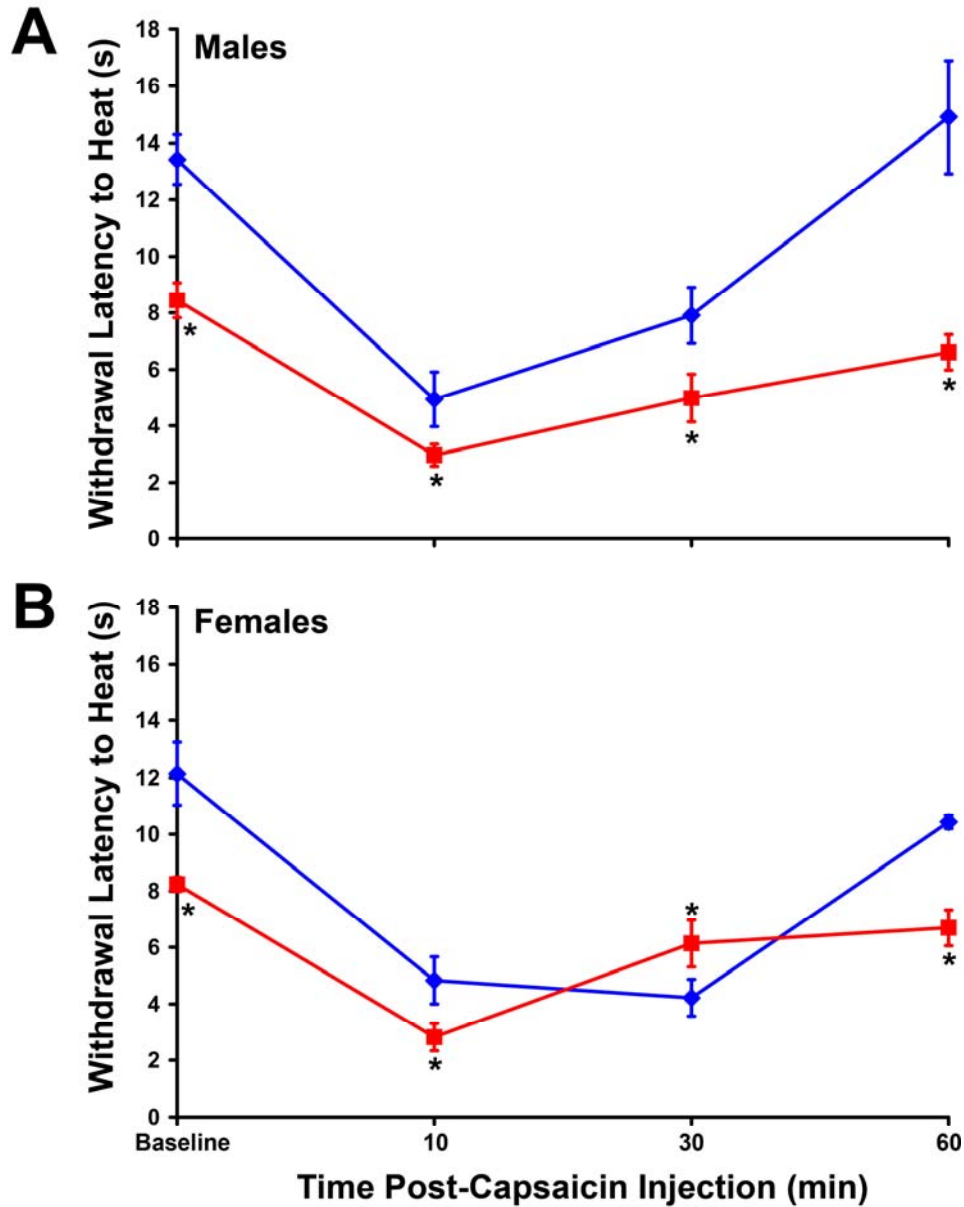


Figure 19. ART-OE mice display sensitivity to heat following capsaicin injection.

Ten WT (blue) and 10 ART-OE mice (red) of both genders (40 mice total) were tested for behavioral sensitivity to capsaicin injected into the hindpaw. Withdrawal response threshold to noxious radiant heat were determined 10, 30 and 60 minutes post-capsaicin injection. A) Both WT and ART-OE male mice displayed shorter withdrawal latencies to heat at 10 min and 30 min after capsaicin injection. However, the percent change from baseline was not different in ART-OE compared to the WT mice, indicating that responses to heat were sensitized in a similar manner in both genotypes. However, at 60 min WT mice had returned to baseline whereas ART-OE were still sensitized indicating that they recover from capsaicin injection more slowly. B) Similar to A), female mice of both genotypes became sensitized to heat following capsaicin injection, but the magnitude of the sensitization from baseline was not different in ART-OE mice compared to WT mice. The female ART-OE mice recovered more slowly than the WT mice, and also became transiently hypoalgesic relative to WT mice at 30 min. Mean \pm SEM. * $P < 0.05$ vs WT.

There was no change in withdrawal latencies of the uninjected foot relative to baseline in either genotype. In addition, injection of vehicle (10% ethanol, 0.5% Tween 20 in saline) did not decrease withdrawal latencies in any of the genotypes at 10, 30, or 60 min post-injection, indicating that capsaicin is required for the development of hypersensitivity. Thus, ART-OE mice of both genders display hypersensitivity to noxious heat following capsaicin injection, but the pattern of responses is similar to that seen in WT mice (percent change from baseline is not different between genotypes).

4.6 IN A MODEL OF INFLAMMATORY PAIN, ART-OE MICE DISPLAY SIMILAR SENSITIVITY TO NOXIOUS HEAT AS WT MICE BUT RECOVER TO THRESHOLDS ABOVE BASELINE

Injection of CFA into the hindpaw is a widely used model of inflammatory pain (Honore et al., 2000). CFA injection causes thermal hyperalgesia with a consistent time course that begins within 1 day and lasts for 7-10 days (Fairbanks et al., 2000; Zwick et al., 2003). Since artemin increases robustly in the hindpaw skin following CFA injection (Malin et al 2006) and ART-OE mice have increased innervation by GFR α 3-positive fibers in the footpad skin, we tested for further sensitization to noxious heat following CFA injection. Both WT and ART-OE male mice had decreased withdrawal latency to noxious heat in the Hargreave's test following induction of inflammation with CFA relative to baseline ($P \leq 0.0005$). ART-OE mice also had significantly shorter withdrawal latencies at day 3 (WT 8.42 ± 0.93 s; ART-OE 6.57 ± 0.33 s; $p \leq 0.05$), day 5 (WT 11.21 ± 0.94 s; ART-OE 9.21 ± 0.25 s; $p \leq 0.05$) and day 7 (WT 12.04 ± 1.10 s; ART-OE 9.44 ± 0.56 s; $p \leq 0.05$) post-CFA compared to WT mice (Figure 20). However, examined on a percentage change from baseline, there was no difference in the ART-OE mice

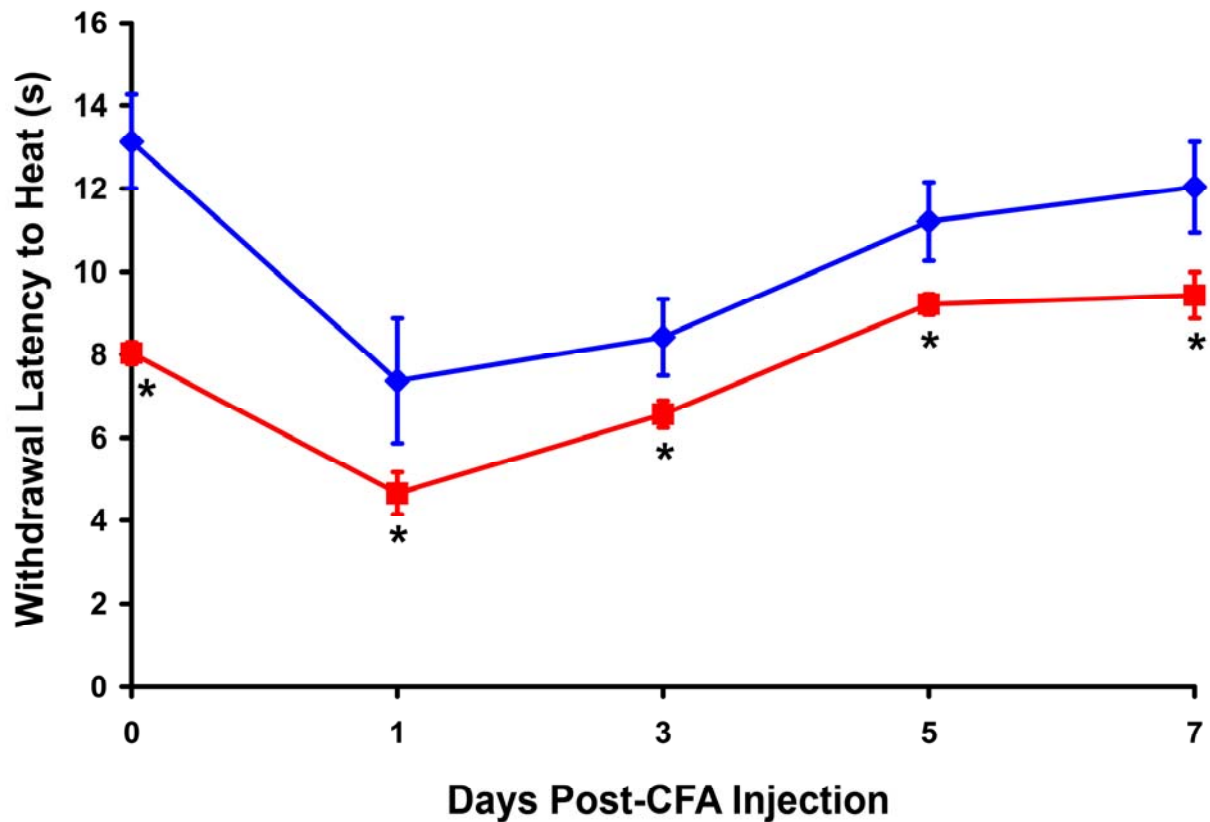


Figure 20. ART-OE mice display similar heat sensitivity to CFA injection

Ten WT (blue) and 10 ART-OE (red) male mice were tested for behavioral sensitivity to noxious heat following CFA induced inflammation. Both WT and ART-OE mice displayed decreased heat thresholds following CFA injection but there was not a difference in the magnitude of the decrease from baseline between the ART-OE and the WT mice. Generally, WT and ART-OE responded with a similar pattern of sensitivity to heat after CFA, although ART-OE became hypoalgesic relative to baseline at day 5 and day 7, suggesting that these mice overcompensate in their recovery. Mean \pm SEM. * $P < 0.05$ vs WT.

compared to WT mice. This suggests that WT and ART-OE mice display similar responses to CFA-induced inflammation and that despite baseline thresholds that are decreased relative to WT mice, ART-OE can still become further sensitized to noxious heat. In addition, when ART-OE mice recover from CFA injection, they display decreased sensitivity (hypoalgesia) at day 5 and day 7 compared to baseline ($p \leq 0.05$), suggesting that they overcompensate for the inflammatory insult. A similar compensatory response was seen in animals overexpressing NGF in the skin (Zwick et al., 2003).

4.7 ART-OE MICE DISPLAY ORAL SENSITIVITY TO CAPSAICIN AND MUSTARD OIL IN THEIR DRINKING WATER

Mice were tested for oral sensitivity to capsaicin or mustard oil using a two bottle drinking test. In this test, one bottle contained water with ligand (capsaicin or mustard oil) and the other bottle contained normal water. Mice were tested over three days and separate groups of male and female WT and ART-OE mice were used for the capsaicin and mustard oil tests (Figure 21). As predicted from the changes in TRPV1 and TRPA1 gene expression, both male and female ART-OE mice drank significantly smaller volumes of capsaicin containing water (Males: WT 1.57 ± 0.09 ml; ART-OE 1.00 ± 0.07 ml; $p \leq 0.005$; Females: WT 1.72 ± 0.11 ml; ART-OE 0.98 ± 0.04 ; $p \leq 0.005$) and mustard oil containing water (Males: WT 1.47 ± 0.14 ml; ART-OE 1.11 ± 0.06 ml; $p \leq 0.05$; Females: WT 1.68 ± 0.10 ml; ART-OE 1.16 ± 0.06 ; $p \leq 0.005$) than WT mice (Figure 21A and C). A similar hypersensitivity was seen when these volumes were calculated as a percentage of total water consumed (Capsaicin: Males: WT 29.08 ± 1.37 %; ART-OE 22.16 ± 1.26 %; $p \leq 0.005$; Females: WT 28.87 ± 19.74 %; ART-OE 19.74 ± 0.79 %; $p \leq 0.005$), (Mustard Oil: Males: WT 26.86 ± 2.09 %; ART-OE 24.10 ± 1.70 %; $p = 0.160$; Females: WT 31.15 ± 2.47 %, ART-OE 22.69 ± 1.58 %; $p \leq 0.005$) (Figure 21 B and D).

However, as a percentage, male ART-OE mice did not drink significantly less mustard oil than WT mice (above, $p=0.160$). This reflects a curious property of the ART-OE male mice that drank significantly less total fluid whenever mustard oil was present (Males: WT: 5.29 ± 0.18 ml, ART-OE: 4.52 ± 0.20 ml; $p \leq 0.005$; Females: WT: 5.47 ± 0.16 ml, ART-OE: 5.19 ± 0.17 ml; $p=0.125$). Thus, male ART-OE mice were hypersensitive to the mustard oil as indicated by the decreased volume of mustard oil. However, because the male ART-OE stopped drinking water altogether, they mask the difference in percentage.

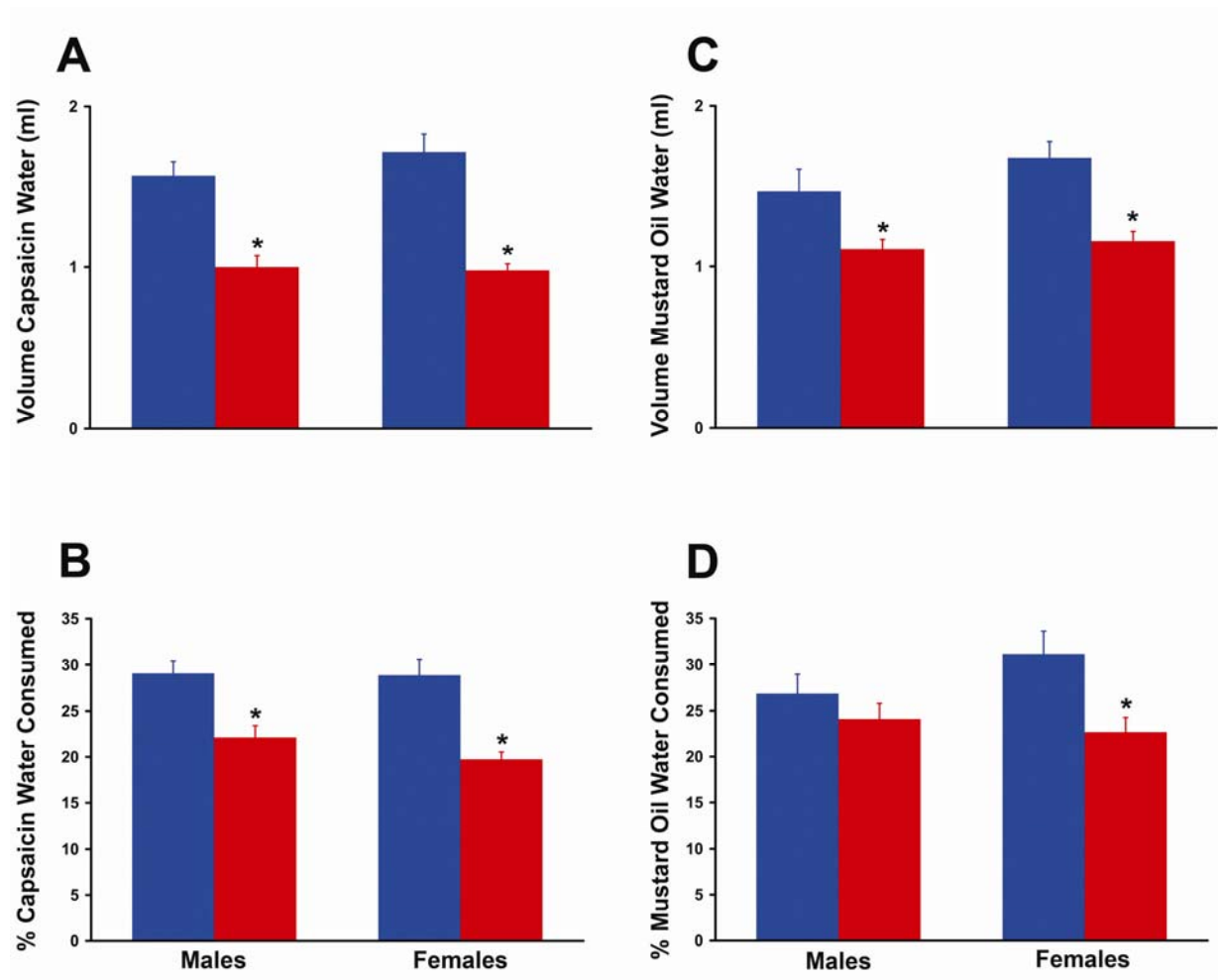


Figure 21. ART-OE mice display oral sensitivity to capsaicin and mustard oil

Ten WT (blue) and 10 ART-OE mice (red) of both genders (40 mice total) were tested for oral sensitivity to the capsaicin and mustard oil using a two bottle drinking aversion test. Mice given free access to the bottles, one of which contained ligand water and the other which contained normal water. A) Both male and female ART-OE drank a decreased volume of capsaicin containing water than WT mice. B) Same as A but calculated as a percentage of total water consumed. C) Both male and female ART-OE drank a decreased volume of mustard oil containing water than WT mice. D) Calculated as a percentage, female ART-OE mice drank less mustard oil containing water, but male ART-OE mice did not drink significantly less as a percentage of total water. Mean \pm SEM. * $P < 0.05$ vs WT.

5.0 CALCIUM IMAGING RESULTS

To determine if individual sensory neurons from the ART-OE mice were functionally sensitized to the ligands for TRPV1 and TRPA1, as suggested in the drinking behavioral experiments, calcium imaging studies of dissociated trigeminal neurons that were back-labeled from the tongue were performed. In these experiments, the number and magnitude of responses to 1 μ M capsaicin and 100 μ M mustard oil were determined in trigeminal and backlabeled lingual afferents.

5.1 MUSTARD OIL RESPONSES IN TRIGEMINAL NEURONS (NON-BACK-LABELED NEURONS)

In response to application of mustard oil, ART-OE mice had more mustard oil responsive trigeminal neurons than WT mice (WT 28% \pm 8; ART-OE 42 \pm 2; $p \leq 0.05$; WT n=5; ART-OE n=6; WT m.o. responsive cells 31; ART m.o. responsive cells 53) (Figure 22A). In addition, in response to mustard oil, trigeminal neurons from the ART-OE mice had calcium transients of larger magnitude (F_{area}) than WT mice (WT 12.24 \pm 2.06, ART-OE 32.67 \pm 6.01; $P=0.007$) (Figure 23A). These results suggest that trigeminal neurons from ART-OE mice have more mustard oil responsive cells and the responses are larger as indicated by the increased area of the calcium transients.

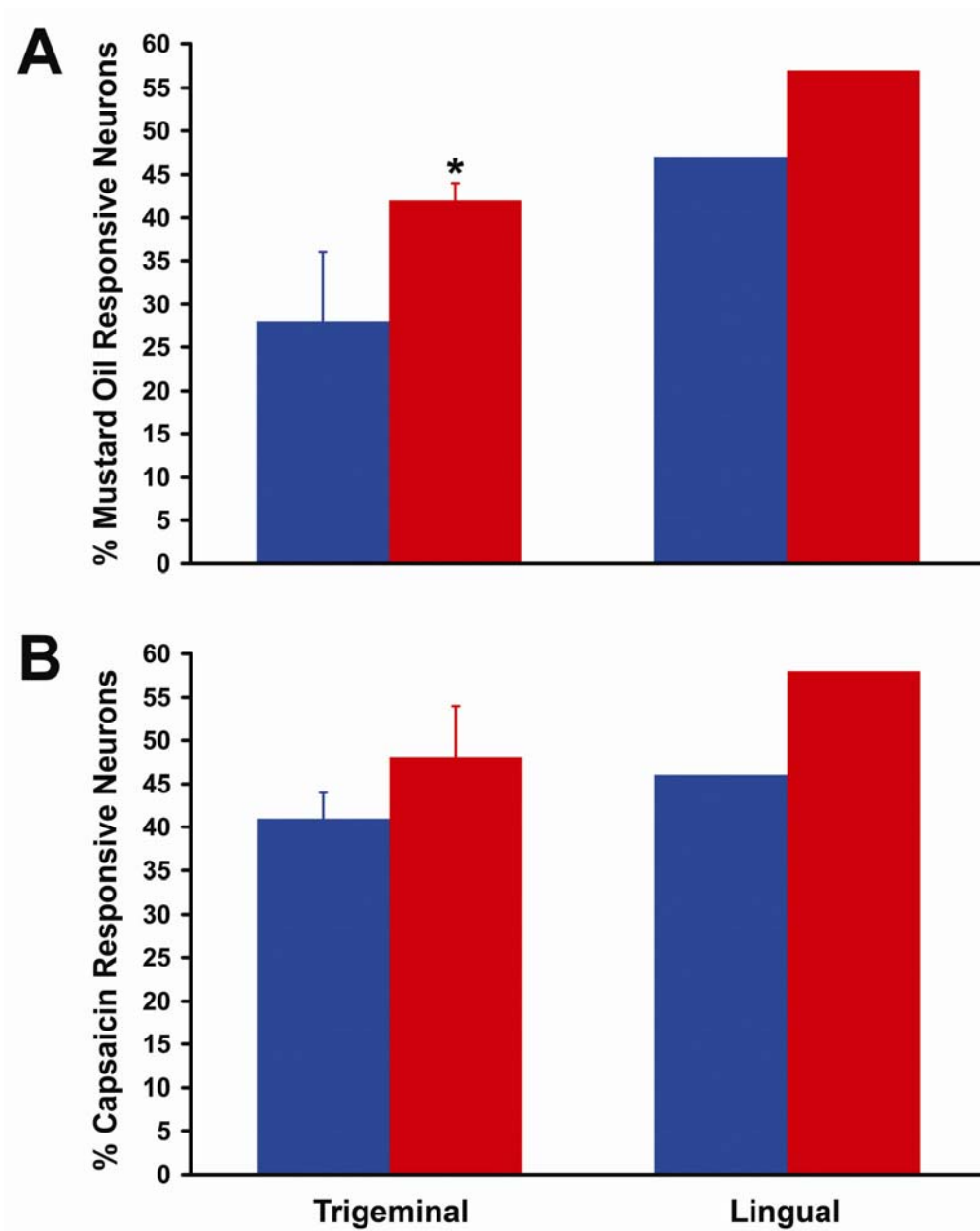


Figure 22. Trigeminal and Lingual Afferent Calcium Responses to Mustard Oil and Capsaicin

A) Percentage of trigeminal neurons (left) and WGA-backlabeled lingual neurons (right) that responded to application of 100 μ M mustard oil. ART-OE mice (red) had a larger percentage of trigeminal neurons that responded to mustard oil (53 responsive cells of 126 total cells, n=6) compared to WT mice (blue) (31 responsive cells of 109 total cells, n=5). A similar trend towards increased percentage of mustard oil-responsive neurons was seen in lingual afferents from the ART-OE mouse (WT: 8 of 17, n=5; ART-OE: 12 of 21, n=6). B) Percentage of trigeminal neurons and WGA-backlabeled lingual neurons that responded to application of 1 μ M capsaicin. There was no difference in the percentage of trigeminal neurons that responded to capsaicin oil between WT and ART-OE mice (WT: 65 responsive cells of 152 total cells, n=10; ART-OE: 85 responsive cells of 196 total cells, n=11). However in the lingual afferents from ART-OE mice, there was a trend towards an increased percentage of capsaicin-responsive neurons (WT: 12 of 26, n=9; ART-OE: 23 of 40, n=12). Mean \pm SEM. *P<0.05 vs WT.

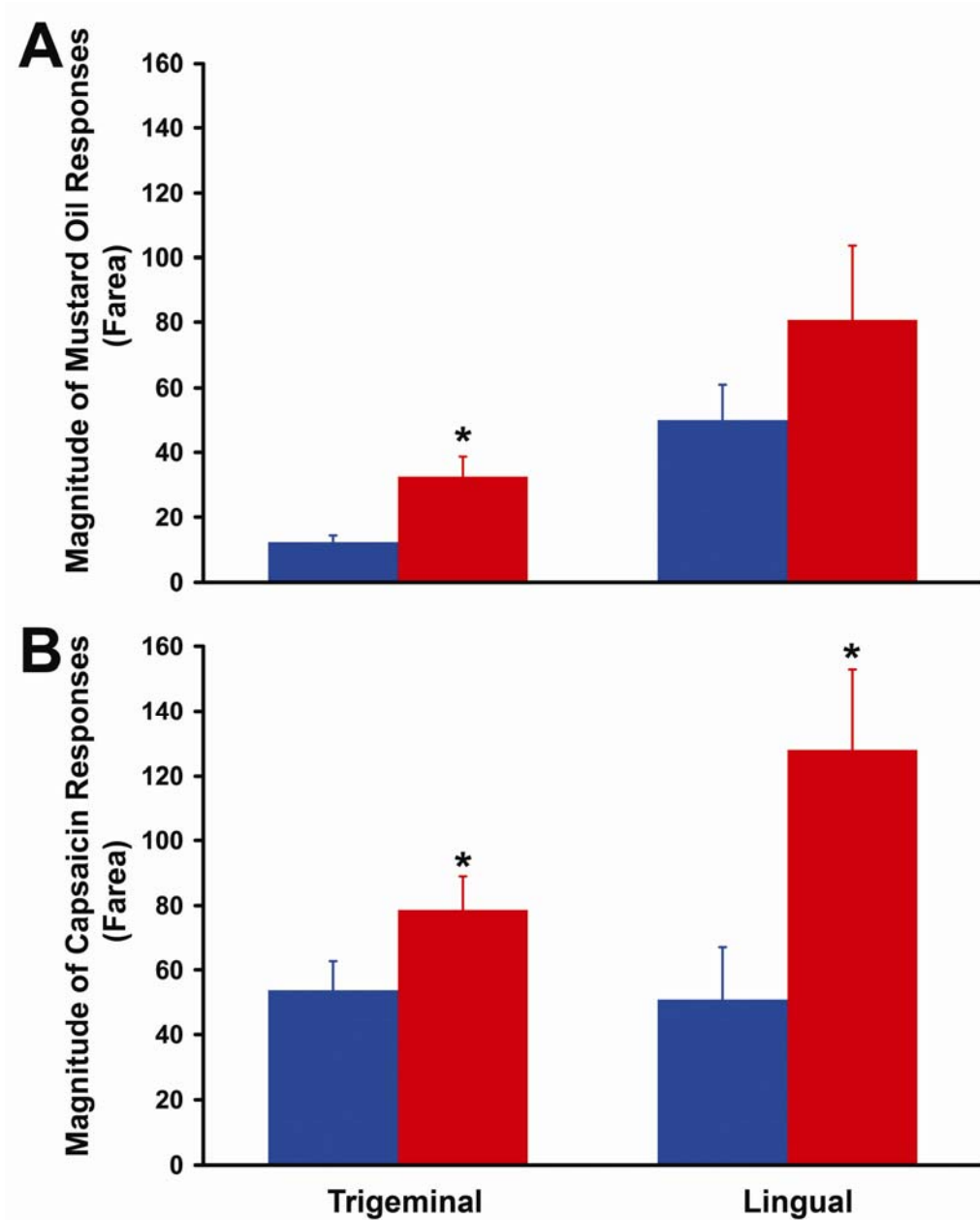


Figure 23. Magnitude of Calcium Responses to Mustard Oil and Capsaicin in Trigeminal and Lingual Afferents

A) Magnitude of response (F_{area}) of trigeminal neurons (left) and WGA-backlabeled lingual neurons (right) that responded to application of 100 μ M mustard oil. Trigeminal neurons from ART-OE mice (red) had larger responses to mustard oil (n=46) compared to WT mice (blue) (n=27). A similar trend towards increased magnitude of mustard oil response was seen in lingual afferents from the ART-OE mouse (WT: n=8; ART-OE: n=9; p=0.13). B) Magnitude of response (F_{area}) of trigeminal neurons and WGA-backlabeled lingual neurons to application of 1 μ M capsaicin. Trigeminal neurons from ART-OE mice had a larger response to capsaicin (n=64) compared to WT mice (blue) (n=46). In addition, lingual afferents from ART-OE mice had a larger calcium response to capsaicin (n=11) compared to WT mice (n=7). Mean \pm SEM. *P<0.05 vs WT.

5.2 CAPSAICIN RESPONSES IN TRIGEMINAL NEURONS (NON-BACK-LABELED NEURONS)

In contrast to mustard oil, the number of responsive trigeminal neurons to application of capsaicin was not different in the ART-OE mice compared to the WT mice (WT 41 ± 3 ; ART-OE 48 ± 6 ; $p=0.17$; WT $n=10$; ART-OE $n=11$; WT cap responsive cells 65; ART cap responsive cells 85) (Figure 22B). However, trigeminal neurons that responded to capsaicin in the ART-OE mice had larger F_{area} than WT mice (WT 54 ± 9 ; ART-OE 79 ± 10 ; $P=0.04$) (Figure 23B). These results suggest that trigeminal ganglia from ART-OE mice do not have more capsaicin responsive neurons but that the capsaicin responsive neurons present exhibit larger calcium transients. This functional result may reflect the increase in TRPV1 mRNA but not an increase in percentage of TRPV1-positive neurons seen in the ART-OE.

5.3 LINGUAL AFFERENTS FROM ART-OE MICE APPEAR TO BE SENSITIZED TO CAPSAICIN AND MUSTARD OIL

Calcium imaging from WGA-backlabeled lingual afferents showed that there were trends towards increased percentages of capsaicin (WT 46%; ART-OE 58%) and mustard oil responsive cells (WT 47%; ART-OE 57%) in the ART-OE mice. In addition, the magnitude of response in lingual afferents to capsaicin was increased (Area: WT 51 ± 16 ; ART-OE 128 ± 25 ; $p=0.02$) (Figure 23B). Application of mustard oil also produced a trend toward increased calcium flux in lingual afferents from the ART-OE animals (Area: WT 50 ± 11 ; ART-OE 81 ± 23 ; $p=0.13$) (Figure 23A). In addition, compared to the general trigeminal afferents, there were a greater number of lingual afferents that responded to capsaicin or mustard in both genotypes, indicating that the tongue is uniquely designed to detect these noxious chemicals. Taken

together, these imaging results support our hypothesis that lingual afferents in the ART-OE mouse are hypersensitive to capsaicin and mustard oil and convey at least a portion of the behavioral sensitivity observed in the drinking tests.

6.0 DISCUSSION

6.1 ANATOMY: SURVIVAL EFFECTS OF ARTEMIN

Our results indicate that transgene-driven overexpression of artemin in skin and tongue keratinocytes enhances developmental survival and functional properties of a unique subpopulation of sensory neurons that are GFR α 3-, TRPV1-, and TRPA1-positive. The in vivo survival effect seen in the ART-OE mice is consistent with in vitro studies showing increased survival of postnatal sensory neurons cultured with artemin (Baloh et al., 1998b; Baudet et al., 2000). It is somewhat surprising, then, that adult GFR α 3^{-/-} mice have normal numbers of DRG and TG neurons and adult ART^{-/-} mice have no apparent differences in density of CGRP-positive or IB4-binding DRG neurons and have normal GFR α 3-positive fiber innervation patterns in whole mount E14.5 embryos (Nishino et al., 1999; Honma et al., 2002). The artemin independent survival of GFR α 3-positive afferents seen in the mice lacking artemin and the apparent GFR α 3-independent survival of sensory neurons in the GFR α 3^{-/-} may reflect overlapping GFL dependencies during development. GDNF or neurturin may support survival of these neurons by binding GFR α 3, GFR α 1 or GFR α 2 since there may be overlapping GFR α receptor expression early in development (Baudet et al., 2000) and there is some evidence that GDNF family ligands may be promiscuous in their receptor selectivities (Baloh et al., 1998b). NGF signaling through TrkA, which is also expressed in GFR α 3 neurons (Orozco et al., 2001), may also have promoted survival. However, in the ART^{-/-} studies, actual counts of sensory neurons were not reported and sensory projections in postnatal mice were not examined, so there

still could be small losses in sensory neuron numbers or defects in sensory innervation patterns in these mice.

6.2 ANATOMY: GFRA3 AND TRPV1 IMMUNOLABELING

In newborn mice, GFR α 3 mRNA is expressed robustly in 20-34% of sensory ganglia neurons, mostly in small and intermediate diameter neurons (Naveilhan et al., 1998; Baudet et al., 2000). In adult mouse, 19-20% of DRG neurons express GFR α 3 (Orozco et al., 2001), supporting a role for artemin in adult systems and during development. In our study, overexpression of artemin in the skin caused a 20.5% increase in neuron number in the DRG of adult mice. Based on immunolabeling studies, a portion of this increase likely reflects addition of small to intermediate diameter GFR α 3-positive neurons that project to dermal and epidermal compartments of skin. However, while there was clearly an increase in total number of GFR α 3-positive neurons, no difference in percentage was detected between the WT and ART-OE mice in GFR α 3 total cell counts. An increase in percentage of GFR α 3-positive neurons would be expected if all of the increase in cell number in the ART-OE mouse (20.5%) was from GFR α 3-positive neurons. This raises a number of possibilities. First, artemin may be promoting the survival of neurturin or GDNF-responsive neurons that express GFR α 3 early in development. Second, some artemin responsive cells may downregulate expression of GFR α 3 in the adult to concentrations below the detection level of our GFR α 3 antibody.

Our studies also show that both the skin and the tongue are hyperinnervated by GFR α 3-positive fibers and that the somal size of GFR α 3-positive afferents is increased nearly 30% in the ART-OE. Thus, in addition to an increased number of GFR α 3-positive afferents innervating the skin and tongue, increased branching causing hypertrophy of the neuronal soma may also contribute to the functional results observed in our study.

Since a previous report indicated that nearly all GFR α 3-positive neurons were also TRPV1-positive, we confirmed this result in our study. In the DRG, over 95% of neurons that were GFR α 3-positive were also TRPV1-positive in both WT and ART-OE mice. However, immunolabeling in the skin showed that in WT mice TRPV1 was only detected at low levels in a few of the GFR α 3-positive *fibers*. However, in the ART-OE skin nearly all GFR α 3-positive fibers displayed high intensity TRPV1 labeling. This increase in GFR α 3/TRPV1-afferent colabeling likely reflects enhanced expression of TRPV1 protein and is consistent with the elevation of TRPV1 mRNA and somal hypertrophy of TRPV1-positive neurons in the ART-OE.

6.3 ANATOMY: LINGUAL AFFERENTS

One concern with these anatomical results is that DRG and TG are heterogenous populations of afferents that project to many target tissues. To confirm that the changes in gene expression and immunolabeling for GFR α 3 and TRPV1 occurred in keratinized tissues, we performed retrograde labeling from the tongue, a site of transgene expression. These studies showed that there were a larger percentage of TRPV1 and GFR α 3-positive afferents innervating target tissues overexpressing artemin. Furthermore, electron microscopy of lingual nerve segments showed that nerves from ART-OE mice were enlarged and contained hypertrophied unmyelinated and myelinated fibers (although hypertrophy was less pronounced in the myelinated fibers). Thus, the increase in size of lingual nerve segments likely resulted from a combination of fiber hypertrophy and increased number of GFR α 3-positive fibers, further confirming that afferents innervating the tongue were responsive to artemin.

In addition, our results from WT mice in the backlabeling studies suggests that lingual afferents are similar to cutaneous afferents in TRPV1 expression, but dissimilar in that most

lingual afferents are IB4-negative and many are CGRP-positive (Christianson et al., 2006). Interestingly, IB4-binding and overlap between TRPV1 and IB4 was increased in the ART-OE, suggesting that artemin may promote the survival of TRPV1/IB4-positive afferents or upregulate the sugar residues that IB4 binds. We have previously found that IB4 binding increases following CFA injection (C.M Elitt, unpublished observations) and nerve injury (H.R. Koerber, unpublished observations). Since artemin is upregulated following inflammation and injury (Baloh et al., 1998b; Malin et al., 2006), it is possible that the increase in IB4-binding in the back-labeled lingual afferents in the ART-OE mice result from the increased concentration of artemin in the tongue.

6.4 ANATOMY: ARTEMIN REGULATION OF TRPA1

One of the most striking findings of our anatomical characterization of the ART-OE mice was the robust increase in expression of TRPA1 mRNA in both the DRG and TG. Immunolabeling showed that many of the TRPA1-positive neurons were also GFR α 3-positive. TRPA1 mRNA has previously been shown to be present in a subpopulation of TRPV1-positive neurons (Story et al., 2003), and since TRPV1 is present in nearly all GFR α 3-positive afferents, it is not surprising that nearly all of the GFR α 3-positive afferents in our study were TRPA1-positive. TRPA1 protein and mRNA expression was present in a large number of neurons in both DRG and TG as evidenced by a large number of TRPA1-immunolabeled neurons and low Ct values (similar to TRPV1 Ct values) in our RT-PCR assays. There is widespread disagreement about the number of TRPA1-positive afferents in the literature ranging from very small percentages (4%) (Story et al., 2003) in mouse to much larger distributions in rat (32-38%) (Obata et al., 2005; Katsura et al., 2006c) and mouse (20-57%) (Jordt et al., 2004; Nagata et al.,

2005). Our results agree with a wider distribution and suggest that neurons expressing low levels of TRPA1 may dramatically increase their expression in response to artemin.

It is highly significant that all GFR α 3-positive neurons also express TRPV1 and TRPA1 because it suggests that artemin supports nociceptor neurons that respond to various stimuli such as heat, cold, capsaicin and mustard oil. Behavioral studies and calcium imaging experiments support this functional role of artemin.

6.5 BEHAVIORAL RESPONSES TO HEAT

Previous studies have shown that TRPV1 is required for heat hypersensitivity during inflammation (Caterina et al., 2000; Davis et al., 2000). NGF upregulates TRPV1 mRNA and protein expression during inflammation (Ji et al., 2002; Amaya et al., 2003) and blocking increases in NGF expression with anti-NGF antibodies alleviates the hypersensitivity to noxious heat in inflammatory pain models (Ji et al., 2002). Our behavioral studies show that overexpression of artemin produces hypersensitivity to noxious heat applied to the skin, supporting the hypothesis that, like NGF, artemin regulates TRPV1 expression and function. The role of artemin in promoting sensitivity to noxious heat is further strengthened by intracellular recording data in an ex vivo preparation showing that C-fibers from ART-OE mice have reduced heat thresholds and increased firing frequencies in response to a heat ramp applied to the skin (Elitt et al., 2006). Interestingly, C-fiber afferents in mice that overexpress NGF in the skin exhibited increased firing frequencies but had unchanged heat thresholds and did not have increases in TRPV1 mRNA (Stucky et al., 1999; Molliver et al., 2005), suggesting that findings in the ART-OE mice are unique. Furthermore, artemin mRNA increases dramatically in the skin during inflammation, even more than NGF (Malin et al., 2006). Therefore, the increased expression and/or sensitization of TRPV1 in GFR α 3-positive neurons observed in the ART-OE

mouse suggests that artemin may play a key role in modulating afferent thermal sensitivity to heat during inflammation.

Behavioral responses to injection of the TRPV1 agonist, capsaicin, in the ART-OE mouse further support the role of artemin in modulating TRPV1 expression and function. Both WT and ART-OE mice displayed increased sensitivity to heat following capsaicin injection and percentage decrease in withdrawal latencies from baseline were similar in both genotypes. This observation that ART-OE mice, despite already being sensitized to heat relative to WT mice at baseline, were still able to become further sensitized to heat following capsaicin injection suggests that sensitization of TRPV1 was not maximal in the ART-OE. (A similar result was observed when a more general inflammant, CFA, was injected into the hindpaw). In addition, application of the TRPV1 agonist, capsaicin, to dissociated DRG neurons from ART-OE mice showed that the number of responsive cells and the magnitude of responses were increased in ART-OE animals (Elitt et al., 2006). Given that acute artemin can also potentiate capsaicin responses in dissociated WT neurons (Malin et al., 2006), our behavioral sensitivity to capsaicin and heat likely reflect a combination of increased number of TRPV1-positive afferents, increased expression of TRPV1 in individual afferents and increased sensitivity of the TRPV1 channel.

6.6 MUSTARD OIL BEHAVIOR

Our behavioral studies also suggest that artemin upregulation of TRPA1 leads to behavioral sensitivity to mustard oil applied topically to the mouse hindpaw. The two studies of mice with disruption in the pore region of TRPA1 suggest that TRPA1 is certainly one of, if not the only, mustard oil receptor (Bautista et al., 2006; Kwan et al., 2006). Kwan et al. showed a substantially reduced number of mustard oil-responsive cells and reduced behavioral sensitivity to oral or injected mustard oil, whereas Bautista et al. show the complete absence of mustard oil

responses behaviorally or in dissociated cells. Of note is that the binding site for mustard oil is still present in the knockout construct and presumably expressed in the TRPA1^{-/-} mice, raising the possibility that mustard oil binding alone may transduce a portion of the mustard oil response in the Kwan TRPA1 ^{-/-} mice. Regardless, the majority of the mustard oil response is conveyed via TRPA1, suggesting that TRPA1 mediates the increased sensitivity to mustard oil seen in our study.

These studies also showed dramatic differences in nocifensive responses and resulting edema in male versus female mice. Male mice of both genotypes displayed much more edema and lengthier and more abundant nocifensive behavior. There was no difference in TRPA1 mRNA expression between male and female mice of either genotype (data not shown), suggesting that the abundance of TRPA1 is unlikely to account for this difference (although protein expression could still be different). Other endogenous inflammatory mediators that are known to sensitize TRPA1, such as bradykinin (Bandell et al., 2004) may be differentially regulated in female and male mice during inflammation and could account for this behavioral difference. Estrogen and androgen receptors are present on small diameter DRG neurons (Sohrabji et al., 1994; Papka et al., 1997; Keast and Gleason, 1998) and therefore sex hormones may modulate the response of TRPA1 to mustard oil. While the exact mechanism is unknown at this point, there is a clear gender difference in the response to topical application of mustard oil.

6.7 ROLE OF TRPA1 IN COLD BEHAVIOR

In addition to hypersensitivity to mustard oil, ART-OE mice also display hypersensitivity to noxious cold applied to the hindpaw. The role of TRPA1 in cold detection remains highly controversial. Our results suggest that TRPA1 is present in most GFR α 3-positive neurons and therefore increases in TRPA1 protein expression or function could mediate the hypersensitivity

to noxious cold seen in these studies. In heterologous systems, TRPA1 is directly activated by noxious cold stimuli (Story et al., 2003; Bandell et al., 2004), but in dissociated neurons activation of TRPA1 by noxious cold is more difficult. Responses in dissociated DRG neurons can be delayed for up to a 1 min following application of noxious (12°C) cold (Reid, 2005), suggesting the possibility that cold activation of TRPA1 in native neurons is actively inhibited and may require a lengthy stimulus for activation. It is not surprising then that response latencies to noxious cold applied to the hindpaw in the ice block test were delayed, taking nearly 30 seconds in WT mice and 16 seconds in ART-OE mice for the first response. Thus, cold responses may be very different than heat responses and require stimuli of longer and more intense duration.

In an attempt to clarify the role of TRPA1 in cold detection, two groups disrupted the TRPA1 gene (Bautista et al., 2006; Kwan et al., 2006). Bautista et al. found no difference in latency to hindpaw lift on a cold plate (0°C) and no difference in flinches/min in the acetone test between wildtype and TRPA1^{-/-} mice. However, Kwan et al found decreases in the number of hindpaw lifts over five minutes in the cold plate test (0°C) (particularly in female mice) and decreased duration of paw shake in the acetone test. These studies suggest that the method of measuring responses and the gender of the mice used may also be critical in testing noxious cold behavior. Our results from three different types of cold tests in mice of both genders indicate that the ART-OE mice are sensitized to noxious cold supporting a role for TRPA1 in detecting noxious cold stimuli.

Few studies have examined the electrophysiological properties of nociceptors that respond to noxious cold. The limited studies have used widely varying applications of noxious cold stimuli and therefore produced varying results. For example, in monkey, 78% of A δ and C-

nociceptors were excited by ice applied to their receptive fields (LaMotte and Thalhammer, 1982). In the rat hindpaw, 10% of A δ and 8% of C-nociceptors were excited by cold stimuli at 12°C (Leem et al., 1993). A more comprehensive study examining stimulus response functions for cutaneous nociceptors (saphenous nerve) over a wide range of controlled cold stimulus temperatures, found that all A δ nociceptors were sensitive to noxious cold applied with a Peltier device (2°C steps, 10 second application) with response thresholds that varied from 14 to -18°C (mean -4.6°C) (Simone and Kajander, 1997). The same group examined C-fibers and found that all responded to noxious cold (range 12°C to -6°C, mean 3°C) (Simone and Kajander, 1996). These studies suggest that there are many noxious cold cutaneous nociceptors but temperature and duration of stimulation are critical for their detection. While the temperature of the hindpaw skin in our behavioral tests was not directly measured, it was likely near 0°C, as there was little melting of the ice block and hindpaws maintained nearly constant contact with the ice. Thus, our results may be explained by activation of cutaneous nociceptors.

Some evidence suggests that responses to noxious cold applied to the skin may be due to nociceptors innervating veins (Fruhstorfer and Lindblom, 1983; Klement and Arndt, 1992). We cannot rule this out as a possible mechanism for the behavioral sensitivity to cold observed in our studies. It is also possible that a combination of both nociceptors innervating skin and those innervating deeper structures could mediate the responses to noxious cold.

6.8 ORAL BEHAVIOR

Drinking aversion testing in the ART-OE mice also confirmed that these mice were hypersensitive to mustard oil and capsaicin, the ligands for TRPA1 and TRPV1. The role of lingual afferents in pain detection has not been extensively studied despite the prevalence of chronic oral pain conditions. Interestingly, one treatment that is effective for oral pain (Burning

Mouth Pain, in particular) is a capsaicin containing oral rinse (Epstein and Marcoe, 1994). Our results suggest that artemin responsive, TRPA1-, TRPV1-positive afferents may mediate some of the hypersensitivities seen in oral pain disorders. It would be extremely interesting to measure artemin concentrations from tongue biopsies of patients with burning mouth syndrome.

One concern with our drinking experiments is that geniculate neurons in taste cells of the tongue might be contributing to the hypersensitivity seen in the ART-OE mouse. A very recent report demonstrates that TRPV1 mRNA and TRPA1 mRNA are expressed by geniculate ganglion neurons in rats (Katsura et al., 2006a), contradicting an earlier study in mouse that showed TRPV1 mRNA was not expressed in geniculate neurons (Matsumoto et al., 2001). It is unknown if GFR α 3 is expressed in geniculate neurons so it is difficult to know if geniculate neurons are contributing to a portion of our findings of hypersensitivity in the ART-OE animals. Future experiments examining GFR α 3 and TRPV1 immunolabeling of geniculate ganglia from WT and ART-OE mice will likely provide some clues about the contribution of geniculate neurons to our findings.

6.9 CALCIUM IMAGING STUDIES

Calcium imaging studies of both trigeminal and lingual afferents generally support our cutaneous and lingual behavioral and anatomical results. Although our cell numbers are relatively small, there were trends that indicated more lingual afferents responded to mustard oil and capsaicin and increases in the magnitudes of the responses to these ligands. The apparent increase in number of responses further support the hypothesis that artemin increases the number of TRPV1/TRPA1-positive afferents innervating the tongue, as observed for TRPV1 in our back-labeling anatomical studies. The increased magnitude of response to capsaicin and mustard oil suggests that artemin increases expression or sensitivity of these channels in individual neurons.

In addition, the percentage of lingual afferents that responded to capsaicin in the calcium imaging studies was also greater than the TRPV1-immunolabeled percentage in our backlabeling experiments (WT immunolabeling for TRPV1=25%, calcium imaging=47% of cells were capsaicin responsive; ART-OE immunolabeling TRPV1=42%, calcium imaging=58%). This likely reflects increased sensitivity of functional assays such as Ca^{++} imaging compared to immunocytochemical detection of protein by antibody visualization (Breese et al., 2005; Malin et al., 2006). Finally, in general, there were also more capsaicin and mustard oil sensitive lingual afferents than trigeminal afferents that responded to these chemicals in both WT and ART-OE mice. This suggests that lingual afferents may be uniquely designed to sense noxious thermal and chemical stimuli.

Findings in non-lingual trigeminal afferents for mustard oil were similar to findings in the lingual afferent population, except that the number of responses and magnitude of responses were generally smaller in a given genotype. These mustard oil responses support a functional role for the increase in TRPA1 mRNA in the trigeminal ganglia and complement findings in DRG neurons where both the number and magnitude of mustard oil responses were increased in ART-OE neurons (S.A. Malin, unpublished observations). In contrast to findings in lingual afferents and DRG neurons, the number of capsaicin responsive trigeminal neurons was not different in the ART-OE. However, the magnitude of response in capsaicin sensitive neurons appeared to be larger in trigeminal neurons. This suggests that trigeminal neurons were sensitized by artemin but differences in number of responses were not readily apparent. Therefore, increases in TRPV1-positive neurons in the trigeminal ganglia may be in select populations of afferents, such as the lingual population, that are hidden in the overall trigeminal population.

6.10 BROADER ISSUES AND FUTURE EXPERIMENTS

Since artemin is expressed beginning in early development (E11) and maintained throughout adulthood, one concern with experiments in the ART-OE mouse (and transgenic animals in general) is that compensation for chronically increased artemin may occur, thereby calling into question the biological relevance of these mice. While there is some validity to this argument, these mice have provided information critical about artemin regulation of TRPA1 and TRPV1 expression and function that would otherwise have been missed. In addition, parallel work in our laboratory studying the acute effects of artemin has complemented the findings in the ART-OE mouse. For example, a single injection of artemin into the mouse hindpaw produces thermal hyperalgesia lasting for hours and in combination with NGF lasting for 7 days (Malin et al., 2006), supporting the idea that artemin can robustly sensitize nociceptors as seen in the ART-OE mouse. In addition, application of artemin to dissociated DRG neurons potentiates capsaicin responses and the potentiation is larger than that seen with other GDNF family members or NGF (Malin et al., 2006), further supporting our findings that artemin can regulate TRPV1 function. Future experiments will also address whether application of artemin to dissociated sensory neurons leads to upregulation of TRPV1 mRNA and TRPA1 mRNA as seen in the ART-OE mouse and if mustard oil or cold responses can be potentiated by acute application of artemin to dissociated neurons.

As discussed earlier, artemin increases dramatically following CFA-induced inflammation (5-fold more than NGF) (Malin et al., 2006) and is also upregulated in the distal nerve segment following sciatic nerve transaction (Baloh et al., 1998b). TRPA1 also increases following CFA-induced inflammation in rats (Obata et al., 2005) and the same is true in mouse where TRPA1 increases nearly 4 fold in lumbar DRGs following CFA injection (unpublished

observations, S.A. Malin). Given our findings in the ART-OE mouse (increased TRPA1, cold hypersensitivity), it is intriguing to speculate that artemin may mediate a large portion of the increase in TRPA1 seen during injury or inflammation, thereby contributing to cold hyperalgesia seen in these models. Future experiments using TRPA1 siRNA in the ART-OE mouse or crossing in TRPA1 KO mice with the ART-OE mice will provide critical insights into the validity of this conjecture.

In summary, our results demonstrate that artemin promotes survival and modulates functional properties of a select population of TRPV1- and TRPA1-positive nociceptors critical for the detection of noxious thermal and chemical stimuli. Increases in artemin concentrations in the skin or tongue during inflammatory or neuropathic pain conditions may play a role in initiating the hypersensitivities to heat and cold observed in these types of chronic pain. Based on our studies, targeted interventions to minimize increases in artemin or the channels it upregulates, TRPV1 and TRPA1, may produce novel therapeutics for patients with chronic pain.

BIBLIOGRAPHY

- Airaksinen MS, Saarma M (2002) The GDNF family: signalling, biological functions and therapeutic value. *Nat Rev Neurosci* 3:383-394.
- Al-Anzi B, Tracey WD, Jr., Benzer S (2006) Response of *Drosophila* to wasabi is mediated by painless, the fly homolog of mammalian TRPA1/ANKTM1. *Curr Biol* 16:1034-1040.
- Albers KM, Wright DE, Davis BM (1994) Overexpression of nerve growth factor in epidermis of transgenic mice causes hypertrophy of the peripheral nervous system. *J Neurosci* 14:1422-1432.
- Albers KM, Woodbury CJ, Ritter AM, Davis BM, Koerber HR (2006) Glial cell-line-derived neurotrophic factor expression in skin alters the mechanical sensitivity of cutaneous nociceptors. *J Neurosci* 26:2981-2990.
- Albers KM, Perrone TN, Goodness TP, Jones ME, Green MA, Davis BM (1996) Cutaneous overexpression of NT-3 increases sensory and sympathetic neuron number and enhances touch dome and hair follicle innervation. *J Cell Biol* 134:487-497.
- Amaya F, Oh-hashi K, Naruse Y, Iijima N, Ueda M, Shimosato G, Tominaga M, Tanaka Y, Tanaka M (2003) Local inflammation increases vanilloid receptor 1 expression within distinct subgroups of DRG neurons. *Brain Res* 963:190-196.
- Babes A, Zorzon D, Reid G (2004) Two populations of cold-sensitive neurons in rat dorsal root ganglia and their modulation by nerve growth factor. *Eur J Neurosci* 20:2276-2282.
- Baloh RH, Gorodinsky A, Golden JP, Tansey MG, Keck CL, Popescu NC, Johnson EM, Jr., Milbrandt J (1998a) GFRalpha3 is an orphan member of the GDNF/neurturin/persephin receptor family. *Proc Natl Acad Sci U S A* 95:5801-5806.

- Baloh RH, Tansey MG, Golden JP, Creedon DJ, Heuckeroth RO, Keck CL, Zimonjic DB, Popescu NC, Johnson EM, Jr., Milbrandt J (1997) TrnR2, a novel receptor that mediates neurturin and GDNF signaling through Ret. *Neuron* 18:793-802.
- Baloh RH, Tansey MG, Lampe PA, Fahrner TJ, Enomoto H, Simburger KS, Leitner ML, Araki T, Johnson EM, Jr., Milbrandt J (1998b) Artemin, a novel member of the GDNF ligand family, supports peripheral and central neurons and signals through the GFRalpha3-RET receptor complex. *Neuron* 21:1291-1302.
- Bandell M, Story GM, Hwang SW, Viswanath V, Eid SR, Petrus MJ, Earley TJ, Patapoutian A (2004) Noxious cold ion channel TRPA1 is activated by pungent compounds and bradykinin. *Neuron* 41:849-857.
- Baudet C, Mikaelis A, Westphal H, Johansen J, Johansen TE, Ernfors P (2000) Positive and negative interactions of GDNF, NTN and ART in developing sensory neuron subpopulations, and their collaboration with neurotrophins. *Development* 127:4335-4344.
- Bautista DM, Jordt SE, Nikai T, Tsuruda PR, Read AJ, Poblete J, Yamoah EN, Basbaum AI, Julius D (2006) TRPA1 mediates the inflammatory actions of environmental irritants and proalgesic agents. *Cell* 124:1269-1282.
- Bennett DL, Michael GJ, Ramachandran N, Munson JB, Averill S, Yan Q, McMahon SB, Priestley JV (1998) A distinct subgroup of small DRG cells express GDNF receptor components and GDNF is protective for these neurons after nerve injury. *J Neurosci* 18:3059-3072.
- Breese NM, George AC, Pauers LE, Stucky CL (2005) Peripheral inflammation selectively increases TRPV1 function in IB4-positive sensory neurons from adult mouse. *Pain* 115:37-49.

- Carstens E, Saxe I, Ralph R (1995) Brainstem neurons expressing c-Fos immunoreactivity following irritant chemical stimulation of the rat's tongue. *Neuroscience* 69:939-953.
- Caterina MJ, Julius D (2001) The vanilloid receptor: a molecular gateway to the pain pathway. *Annu Rev Neurosci* 24:487-517.
- Caterina MJ, Schumacher MA, Tominaga M, Rosen TA, Levine JD, Julius D (1997) The capsaicin receptor: a heat-activated ion channel in the pain pathway. *Nature* 389:816-824.
- Caterina MJ, Leffler A, Malmberg AB, Martin WJ, Trafton J, Petersen-Zeitz KR, Koltzenburg M, Basbaum AI, Julius D (2000) Impaired nociception and pain sensation in mice lacking the capsaicin receptor. *Science* 288:306-313.
- Christianson JA, McIlwrath SL, Koerber HR, Davis BM (2006) Transient receptor potential vanilloid 1-immunopositive neurons in the mouse are more prevalent within colon afferents compared to skin and muscle afferents. *Neuroscience* 140:247-257.
- Chuang HH, Prescott ED, Kong H, Shields S, Jordt SE, Basbaum AI, Chao MV, Julius D (2001) Bradykinin and nerve growth factor release the capsaicin receptor from PtdIns(4,5)P₂-mediated inhibition. *Nature* 411:957-962.
- Corey DP, Garcia-Anoveros J, Holt JR, Kwan KY, Lin SY, Vollrath MA, Amalfitano A, Cheung EL, Derfler BH, Duggan A, Geleoc GS, Gray PA, Hoffman MP, Rehm HL, Tamasauskas D, Zhang DS (2004) TRPA1 is a candidate for the mechanosensitive transduction channel of vertebrate hair cells. *Nature* 432:723-730.
- Crowley C, Spencer SD, Nishimura MC, Chen KS, Pitts-Meek S, Armanini MP, Ling LH, McMahon SB, Shelton DL, Levinson AD, et al. (1994) Mice lacking nerve growth factor display perinatal loss of sensory and sympathetic neurons yet develop basal forebrain cholinergic neurons. *Cell* 76:1001-1011.

- Davies AM (1996) The neurotrophic hypothesis: where does it stand? *Philos Trans R Soc Lond B Biol Sci* 351:389-394.
- Davis JB, Gray J, Gunthorpe MJ, Hatcher JP, Davey PT, Overend P, Harries MH, Latcham J, Clapham C, Atkinson K, Hughes SA, Rance K, Grau E, Harper AJ, Pugh PL, Rogers DC, Bingham S, Randall A, Sheardown SA (2000) Vanilloid receptor-1 is essential for inflammatory thermal hyperalgesia. *Nature* 405:183-187.
- Dhaka A, Viswanath V, Patapoutian A (2006) Trp ion channels and temperature sensation. *Annu Rev Neurosci* 29:135-161.
- Djouhri L, Lawson SN (2004) A-beta-fiber nociceptive primary afferent neurons: a review of incidence and properties in relation to other afferent A-fiber neurons in mammals. *Brain Res Brain Res Rev* 46:131-145.
- Donnerer J, Schuligoi R, Stein C (1992) Increased content and transport of substance P and calcitonin gene-related peptide in sensory nerves innervating inflamed tissue: evidence for a regulatory function of nerve growth factor in vivo. *Neuroscience* 49:693-698.
- Elitt CM, McIlwrath SL, Lawson JJ, Malin SA, Molliver DC, Cornuet P, Koerber HR, Davis BM, Albers KM (2006) Artemin overexpression in skin enhances expression of TRPV1 and TRPA1 in cutaneous sensory neurons and leads to behavioral sensitivity to heat and cold. *Journal of Neuroscience*.
- Epstein JB, Marcoe JH (1994) Topical application of capsaicin for treatment of oral neuropathic pain and trigeminal neuralgia. *Oral Surg Oral Med Oral Pathol* 77:135-140.
- Fairbanks CA, Schreiber KL, Brewer KL, Yu CG, Stone LS, Kitto KF, Nguyen HO, Grocholski BM, Shoeman DW, Kehl LJ, Regunathan S, Reis DJ, Yeziarski RP, Wilcox GL (2000)

- Agmatine reverses pain induced by inflammation, neuropathy, and spinal cord injury. Proc Natl Acad Sci U S A 97:10584-10589.
- Fruhstorfer H, Lindblom U (1983) Vascular participation in deep cold pain. Pain 17:235-241.
- Furuse T, Blizard DA, Moriwaki K, Miura Y, Yagasaki K, Shiroishi T, Koide T (2002) Genetic diversity underlying capsaicin intake in the Mishima battery of mouse strains. Brain Res Bull 57:49-55.
- Galoyan SM, Petruska JC, Mendell LM (2003) Mechanisms of sensitization of the response of single dorsal root ganglion cells from adult rat to noxious heat. Eur J Neurosci 18:535-541.
- Heuckeroth RO, Enomoto H, Grider JR, Golden JP, Hanke JA, Jackman A, Molliver DC, Bardgett ME, Snider WD, Johnson EM, Jr., Milbrandt J (1999) Gene targeting reveals a critical role for neurturin in the development and maintenance of enteric, sensory, and parasympathetic neurons. Neuron 22:253-263.
- Holland GR, Robinson PP (1992) Axon populations in cat lingual and chorda tympani nerves. J Dent Res 71:1468-1472.
- Honma Y, Araki T, Gianino S, Bruce A, Heuckeroth R, Johnson E, Milbrandt J (2002) Artemin is a vascular-derived neurotropic factor for developing sympathetic neurons. Neuron 35:267-282.
- Honore P, Rogers SD, Schwei MJ, Salak-Johnson JL, Luger NM, Sabino MC, Clohisy DR, Mantyh PW (2000) Murine models of inflammatory, neuropathic and cancer pain each generates a unique set of neurochemical changes in the spinal cord and sensory neurons. Neuroscience 98:585-598.

- Jancso G (1992) Pathobiological reactions of C-fibre primary sensory neurones to peripheral nerve injury. *Exp Physiol* 77:405-431.
- Jancso G, Kiraly E, Jancso-Gabor A (1977) Pharmacologically induced selective degeneration of chemosensitive primary sensory neurones. *Nature* 270:741-743.
- Jancso N, Jancso-Gabor A, Szolcsanyi J (1967) Direct evidence for neurogenic inflammation and its prevention by denervation and by pretreatment with capsaicin. *Br J Pharmacol Chemother* 31:138-151.
- Ji RR, Samad TA, Jin SX, Schmoll R, Woolf CJ (2002) p38 MAPK activation by NGF in primary sensory neurons after inflammation increases TRPV1 levels and maintains heat hyperalgesia. *Neuron* 36:57-68.
- Jing S, Yu Y, Fang M, Hu Z, Holst PL, Boone T, Delaney J, Schultz H, Zhou R, Fox GM (1997) GFRalpha-2 and GFRalpha-3 are two new receptors for ligands of the GDNF family. *J Biol Chem* 272:33111-33117.
- Jordt SE, McKemy DD, Julius D (2003) Lessons from peppers and peppermint: the molecular logic of thermosensation. *Curr Opin Neurobiol* 13:487-492.
- Jordt SE, Bautista DM, Chuang HH, McKemy DD, Zygmunt PM, Hogestatt ED, Meng ID, Julius D (2004) Mustard oils and cannabinoids excite sensory nerve fibres through the TRP channel ANKTM1. *Nature* 427:260-265.
- Katsura H, Tsuzuki K, Noguchi K, Sakagami M (2006a) Differential Expression of Capsaicin-, Menthol-, and Mustard Oil-Sensitive Receptors in Naive Rat Geniculate Ganglion Neurons. *Chem Senses*.

- Katsura H, Obata K, Mizushima T, Yamanaka H, Kobayashi K, Dai Y, Fukuoka T, Tokunaga A, Sakagami M, Noguchi K (2006b) Antisense knock down of TRPA1, but not TRPM8, alleviates cold hyperalgesia after spinal nerve ligation in rats. *Exp Neurol* 200:112-123.
- Katsura H, Obata K, Mizushima T, Yamanaka H, Kobayashi K, Dai Y, Fukuoka T, Tokunaga A, Sakagami M, Noguchi K (2006c) Antisense knock down of TRPA1, but not TRPM8, alleviates cold hyperalgesia after spinal nerve ligation in rats. *Exp Neurol*.
- Keast JR, Gleeson RJ (1998) Androgen receptor immunoreactivity is present in primary sensory neurons of male rats. *Neuroreport* 9:4137-4140.
- Klement W, Arndt JO (1992) The role of nociceptors of cutaneous veins in the mediation of cold pain in man. *J Physiol* 449:73-83.
- Kotzbauer PT, Lampe PA, Heuckeroth RO, Golden JP, Creedon DJ, Johnson EM, Jr., Milbrandt J (1996) Neurturin, a relative of glial-cell-line-derived neurotrophic factor. *Nature* 384:467-470.
- Krimm RF, Miller KK, Kitzman PH, Davis BM, Albers KM (2001) Epithelial overexpression of BDNF or NT4 disrupts targeting of taste neurons that innervate the anterior tongue. *Dev Biol* 232:508-521.
- Kwan KY, Allchorne AJ, Vollrath MA, Christensen AP, Zhang DS, Woolf CJ, Corey DP (2006) TRPA1 contributes to cold, mechanical, and chemical nociception but is not essential for hair-cell transduction. *Neuron* 50:277-289.
- LaMotte RH, Thalhammer JG (1982) Response properties of high-threshold cutaneous cold receptors in the primate. *Brain Res* 244:279-287.
- LaMotte RH, Shain CN, Simone DA, Tsai EF (1991) Neurogenic hyperalgesia: psychophysical studies of underlying mechanisms. *J Neurophysiol* 66:190-211.

- Lauria G, Majorana A, Borgna M, Lombardi R, Penza P, Padovani A, Sapelli P (2005) Trigeminal small-fiber sensory neuropathy causes burning mouth syndrome. *Pain* 115:332-337.
- Leem JW, Willis WD, Chung JM (1993) Cutaneous sensory receptors in the rat foot. *J Neurophysiol* 69:1684-1699.
- Leitner ML, Wang LH, Osborne PA, Golden JP, Milbrandt J, Johnson EM, Jr. (2005) Expression and function of GDNF family ligands and receptors in the carotid body. *Exp Neurol* 191 Suppl 1:S68-79.
- Lin LF, Doherty DH, Lile JD, Bektesh S, Collins F (1993) GDNF: a glial cell line-derived neurotrophic factor for midbrain dopaminergic neurons. *Science* 260:1130-1132.
- Lindfors PH, Voikar V, Rossi J, Airaksinen MS (2006) Deficient nonpeptidergic epidermis innervation and reduced inflammatory pain in glial cell line-derived neurotrophic factor family receptor alpha2 knock-out mice. *J Neurosci* 26:1953-1960.
- Lucini C, Maruccio L, Tafuri S, Bevaqua M, Staiano N, Castaldo L (2005) GDNF family ligand immunoreactivity in the gut of teleostean fish. *Anat Embryol (Berl)* 210:265-274.
- Lundy RF, Jr., Contreras RJ (1995) Tongue adaptation temperature influences lingual nerve responses to thermal and menthol stimulation. *Brain Res* 676:169-177.
- Macpherson LJ, Hwang SW, Miyamoto T, Dubin AE, Patapoutian A, Story GM (2006) More than cool: Promiscuous relationships of menthol and other sensory compounds. *Mol Cell Neurosci*.
- Malin SA, Molliver DC, Koerber HR, Cornett P, Frye R, Albers KM, Davis BM (2006) GDNF Family Members Sensitize Nociceptors in vitro and Produce Thermal Hyperalgesia in vivo. *Journal of Neuroscience*.

- Masure S, Geerts H, Cik M, Hoefnagel E, Van Den Kieboom G, Tuytelaars A, Harris S, Lesage AS, Leysen JE, Van Der Helm L, Verhasselt P, Yon J, Gordon RD (1999) Enovin, a member of the glial cell-line-derived neurotrophic factor (GDNF) family with growth promoting activity on neuronal cells. Existence and tissue-specific expression of different splice variants. *Eur J Biochem* 266:892-902.
- Matsumoto I, Emori Y, Ninomiya Y, Abe K (2001) A comparative study of three cranial sensory ganglia projecting into the oral cavity: in situ hybridization analyses of neurotrophin receptors and thermosensitive cation channels. *Brain Res Mol Brain Res* 93:105-112.
- McKemy DD, Neuhauser WM, Julius D (2002) Identification of a cold receptor reveals a general role for TRP channels in thermosensation. *Nature* 416:52-58.
- Milbrandt J, de Sauvage FJ, Fahrner TJ, Baloh RH, Leitner ML, Tansey MG, Lampe PA, Heuckeroth RO, Kotzbauer PT, Simburger KS, Golden JP, Davies JA, Vejsada R, Kato AC, Hynes M, Sherman D, Nishimura M, Wang LC, Vandlen R, Moffat B, Klein RD, Poulsen K, Gray C, Garces A, Johnson EM, Jr., et al. (1998) Persephin, a novel neurotrophic factor related to GDNF and neurturin. *Neuron* 20:245-253.
- Molliver DC, Snider WD (1997) Nerve growth factor receptor TrkA is down-regulated during postnatal development by a subset of dorsal root ganglion neurons. *J Comp Neurol* 381:428-438.
- Molliver DC, Lindsay J, Albers KM, Davis BM (2005) Overexpression of NGF or GDNF alters transcriptional plasticity evoked by inflammation. *Pain* 113:277-284.
- Montell C, Rubin GM (1989) Molecular characterization of the *Drosophila* trp locus: a putative integral membrane protein required for phototransduction. *Neuron* 2:1313-1323.

- Moore MW, Klein RD, Farinas I, Sauer H, Armanini M, Phillips H, Reichardt LF, Ryan AM, Carver-Moore K, Rosenthal A (1996) Renal and neuronal abnormalities in mice lacking GDNF. *Nature* 382:76-79.
- Moriyama T, Iida T, Kobayashi K, Higashi T, Fukuoka T, Tsumura H, Leon C, Suzuki N, Inoue K, Gachet C, Noguchi K, Tominaga M (2003) Possible involvement of P2Y2 metabotropic receptors in ATP-induced transient receptor potential vanilloid receptor 1-mediated thermal hypersensitivity. *J Neurosci* 23:6058-6062.
- Nagata K, Duggan A, Kumar G, Garcia-Anoveros J (2005) Nociceptor and hair cell transducer properties of TRPA1, a channel for pain and hearing. *J Neurosci* 25:4052-4061.
- Naveilhan P, Baudet C, Mikaelis A, Shen L, Westphal H, Ernfor P (1998) Expression and regulation of GFRalpha3, a glial cell line-derived neurotrophic factor family receptor. *Proc Natl Acad Sci U S A* 95:1295-1300.
- Nishino J, Mochida K, Ohfuji Y, Shimazaki T, Meno C, Ohishi S, Matsuda Y, Fujii H, Saijoh Y, Hamada H (1999) GFR alpha3, a component of the artemin receptor, is required for migration and survival of the superior cervical ganglion. *Neuron* 23:725-736.
- Obata K, Katsura H, Mizushima T, Yamanaka H, Kobayashi K, Dai Y, Fukuoka T, Tokunaga A, Tominaga M, Noguchi K (2005) TRPA1 induced in sensory neurons contributes to cold hyperalgesia after inflammation and nerve injury. *J Clin Invest* 115:2393-2401.
- Orozco OE, Walus L, Sah DW, Pepinsky RB, Sanicola M (2001) GFRalpha3 is expressed predominantly in nociceptive sensory neurons. *Eur J Neurosci* 13:2177-2182.
- Papka RE, Srinivasan B, Miller KE, Hayashi S (1997) Localization of estrogen receptor protein and estrogen receptor messenger RNA in peripheral autonomic and sensory neurons. *Neuroscience* 79:1153-1163.

- Peier AM, Moqrich A, Hergarden AC, Reeve AJ, Andersson DA, Story GM, Earley TJ, Dragoni I, McIntyre P, Bevan S, Patapoutian A (2002) A TRP channel that senses cold stimuli and menthol. *Cell* 108:705-715.
- Petruzzi M, Lauritano D, De Benedittis M, Baldoni M, Serpico R (2004) Systemic capsaicin for burning mouth syndrome: short-term results of a pilot study. *J Oral Pathol Med* 33:111-114.
- Pittman DW, Contreras RJ (1998) Responses of single lingual nerve fibers to thermal and chemical stimulation. *Brain Res* 790:224-235.
- Porreca F, Ossipov MH, Gebhart GF (2002) Chronic pain and medullary descending facilitation. *Trends Neurosci* 25:319-325.
- Quartu M, Serra MP, Manca A, Mascia F, Follesa P, Del Fiacco M (2005) Neurturin, persephin, and artemin in the human pre- and full-term newborn and adult hippocampus and fascia dentata. *Brain Res* 1041:157-166.
- Reid G (2005) ThermoTRP channels and cold sensing: what are they really up to? *Pflugers Arch* 451:250-263.
- Rossi J, Luukko K, Poteryaev D, Laurikainen A, Sun YF, Laakso T, Eerikainen S, Tuominen R, Lakso M, Rauvala H, Arumae U, Pasternack M, Saarna M, Airaksinen MS (1999) Retarded growth and deficits in the enteric and parasympathetic nervous system in mice lacking GFR alpha2, a functional neurturin receptor. *Neuron* 22:243-252.
- Silos-Santiago I, Molliver DC, Ozaki S, Smeyne RJ, Fagan AM, Barbacid M, Snider WD (1995) Non-TrkA-expressing small DRG neurons are lost in TrkA deficient mice. *J Neurosci* 15:5929-5942.

- Silverman JD, Kruger L (1988) Lectin and neuropeptide labeling of separate populations of dorsal root ganglion neurons and associated "nociceptor" thin axons in rat testis and cornea whole-mount preparations. *Somatosens Res* 5:259-267.
- Simone DA, Kajander KC (1996) Excitation of rat cutaneous nociceptors by noxious cold. *Neurosci Lett* 213:53-56.
- Simone DA, Kajander KC (1997) Responses of cutaneous A-fiber nociceptors to noxious cold. *J Neurophysiol* 77:2049-2060.
- Simons CT, Carstens MI, Carstens E (2003) Oral irritation by mustard oil: self-desensitization and cross-desensitization with capsaicin. *Chem Senses* 28:459-465.
- Simons CT, Dessirier JM, Jinks SL, Carstens E (2001) An animal model to assess aversion to intra-oral capsaicin: increased threshold in mice lacking substance p. *Chem Senses* 26:491-497.
- Smeyne RJ, Klein R, Schnapp A, Long LK, Bryant S, Lewin A, Lira SA, Barbacid M (1994) Severe sensory and sympathetic neuropathies in mice carrying a disrupted Trk/NGF receptor gene. *Nature* 368:246-249.
- Sohrabji F, Miranda RC, Toran-Allerand CD (1994) Estrogen differentially regulates estrogen and nerve growth factor receptor mRNAs in adult sensory neurons. *J Neurosci* 14:459-471.
- Story GM, Peier AM, Reeve AJ, Eid SR, Mosbacher J, Hricik TR, Earley TJ, Hergarden AC, Andersson DA, Hwang SW, McIntyre P, Jegla T, Bevan S, Patapoutian A (2003) ANKTM1, a TRP-like channel expressed in nociceptive neurons, is activated by cold temperatures. *Cell* 112:819-829.

- Stucky CL, Rossi J, Airaksinen MS, Lewin GR (2002) GFR alpha2/neurturin signalling regulates noxious heat transduction in isolectin B4-binding mouse sensory neurons. *J Physiol* 545:43-50.
- Stucky CL, Koltzenburg M, Schneider M, Engle MG, Albers KM, Davis BM (1999) Overexpression of nerve growth factor in skin selectively affects the survival and functional properties of nociceptors. *J Neurosci* 19:8509-8516.
- Sugiura T, Tominaga M, Katsuya H, Mizumura K (2002) Bradykinin lowers the threshold temperature for heat activation of vanilloid receptor 1. *J Neurophysiol* 88:544-548.
- Takahashi M (2001) The GDNF/RET signaling pathway and human diseases. *Cytokine Growth Factor Rev* 12:361-373.
- Tansey MG, Baloh RH, Milbrandt J, Johnson EM, Jr. (2000) GFRalpha-mediated localization of RET to lipid rafts is required for effective downstream signaling, differentiation, and neuronal survival. *Neuron* 25:611-623.
- Tohda C, Sasaki M, Konemura T, Sasamura T, Itoh M, Kuraishi Y (2001) Axonal transport of VR1 capsaicin receptor mRNA in primary afferents and its participation in inflammation-induced increase in capsaicin sensitivity. *J Neurochem* 76:1628-1635.
- Wang Y, Erickson RP, Simon SA (1993) Selectivity of lingual nerve fibers to chemical stimuli. *J Gen Physiol* 101:843-866.
- Widenfalk J, Tomac A, Lindqvist E, Hoffer B, Olson L (1998) GFRalpha-3, a protein related to GFRalpha-1, is expressed in developing peripheral neurons and ensheathing cells. *Eur J Neurosci* 10:1508-1517.

- Woodbury CJ, Zwick M, Wang S, Lawson JJ, Caterina MJ, Koltzenburg M, Albers KM, Koerber HR, Davis BM (2004) Nociceptors lacking TRPV1 and TRPV2 have normal heat responses. *J Neurosci* 24:6410-6415.
- Worby CA, Vega QC, Chao HH, Seasholtz AF, Thompson RC, Dixon JE (1998) Identification and characterization of GFRalpha-3, a novel Co-receptor belonging to the glial cell line-derived neurotrophic receptor family. *J Biol Chem* 273:3502-3508.
- Zwick M, Davis BM, Woodbury CJ, Burkett JN, Koerber HR, Simpson JF, Albers KM (2002) Glial cell line-derived neurotrophic factor is a survival factor for isolectin B4-positive, but not vanilloid receptor 1-positive, neurons in the mouse. *J Neurosci* 22:4057-4065.
- Zwick M, Molliver DC, Lindsay J, Fairbanks CA, Sengoku T, Albers KM, Davis BM (2003) Transgenic mice possessing increased numbers of nociceptors do not exhibit increased behavioral sensitivity in models of inflammatory and neuropathic pain. *Pain* 106:491-500.